Advanced Drug Delivery Reviews 216 (2025) 115476

Contents lists available at ScienceDirect

Advanced Drug Delivery Reviews

journal homepage: www.elsevier.com/locate/adr

Integrated modeling of biomarkers, survival and safety in clinical oncology drug development

Han Liu [a,1], Eman I.K. Ibrahim [a,1], Maddalena Centanni [a], Céline Sarr [b], Karthik Venkatakrishnan [c], Lena E. Friberg [a,*]

[a] Department of Pharmacy, Uppsala University, Box 580, 75123, Uppsala, Sweden
[b] Pharmetheus AB, Dragarbrunnsgatan 77, 753 19, Uppsala, Sweden
[c] EMD Serono Research and Development Institute, Inc., Billerica, MA, USA

GRAPHICAL ABSTRACT

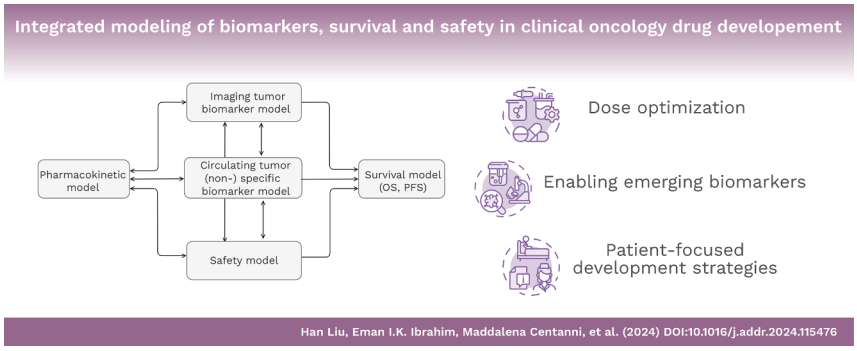

ARTICLE INFO

Keywords:
Anticancer drugs
Pharmacokinetic
Pharmacodynamic
Pharmacometrics
Joint models
Model-informed drug development
Dose optimization

ABSTRACT

Model-based approaches, including population pharmacokinetic-pharmacodynamic modeling, have become an essential component in the clinical phases of oncology drug development. Over the past two decades, models have evolved to describe the temporal dynamics of biomarkers and tumor size, treatment-related adverse events, and their links to survival. Integrated models, defined here as models that incorporate at least two pharmacodynamic/ outcome variables, are applied to answer drug development questions through simulations, e.g., to support the exploration of alternative dosing strategies and study designs in subgroups of patients or other tumor indications. It is expected that these pharmacometric approaches will be expanded as regulatory authorities place further emphasis on early and individualized dosage optimization and inclusive patient-focused development

Abbreviations: ADC, antibody-drug conjugate; CAR-T, Chimeric antigen receptor; CLL, chronic lymphocytic leukemia; CTC, circulating tumor cells; CTCAE, common terminology criteria for adverse events; ctDNA, circulating tumor DNA; IIV, inter-individual variability; IOV, inter-occasion variability; IPP, individual pharmacokinetics (pharmacodynamics) parameters; K-M, Kaplan-Meier; K-PD, kinetic-pharmacodynamics; MIDD, model-informed drug development; ML, machine-learning; NHL, non-Hodgkin lymphoma; NLME, nonlinear mixed-effect; PD, pharmacodynamic; PFS, progression-free survival; PPP&D, population pharmacokinetics (pharmacodynamics) parameters and data; PRO, patient-reported outcomes; RECIST, response evaluation criteria in solid tumors; SLD, sum of the longest diameters; TGI, tumor growth inhibition; TSR, tumor size ratio; VPC, visual predictive check.

* Corresponding author at: Dept of Pharmacy, Box 580, Uppsala University, SE-75123, Uppsala, Sweden.
E-mail address: lena.friberg@farmaci.uu.se (L.E. Friberg).

[1] shared first authorship.

https://doi.org/10.1016/j.addr.2024.115476
Received 31 May 2024; Received in revised form 12 September 2024; Accepted 15 November 2024
Available online 20 November 2024

Dose individualization
Tumor growth inhibition model

strategies. This review provides an overview of integrated models in the literature, examples of the considerations that need to be made when applying these advanced pharmacometric approaches, and an outlook on the expected further expansion of model-informed drug development of anticancer drugs.

1. Introduction

Cancer remains a leading cause of mortality worldwide, accounting for nearly 10 million deaths and 20 million newly diagnosed cases in 2022 alone [1]. The development and approval of novel anti-cancer treatments have significantly improved patients' life expectancy and quality of life in the past decades. Nevertheless, bringing a new oncology drug to the market is a lengthy, complex, and expensive process [2]. Oncology drug discovery and development face numerous challenges due to the complexity of cancer biology, the heterogeneity of cancer among and within patients, and the development of treatment resistance due to epigenetic, genetic, and microenvironmental factors [3–5]. Consequently, the failure rate of pivotal phase III trials and the average costs for developing new oncology drugs are higher than other therapeutic areas [6,7].

The shift from chemotherapy to molecularly targeted agents and immuno-oncology therapy has added complexity to oncology drug development in finding a dose with a balanced benefit-risk profile [8]. This is evident in the high burden of post-marketing requirements to evaluate alternative doses or dosing frequencies for approved anticancer drugs [9]. Historically, chemotherapy dose-finding has relied on determining a maximally tolerated dose (MTD) in phase I trials, which is then used in phase II and III trials under the premise that 'more is better' [10]. However, higher dose levels do not always result in increased antitumor effects for new cancer treatment modalities. This is because target saturation can occur below the MTD, and the exposure–response can be less pronounced or even flat [11]. In addition, these treatments often require prolonged use, raising the potential for tolerability issues, which can lead to dose reductions, interruptions, or even treatment discontinuation, ultimately diminishing the potential therapeutic benefits [12]. From the perspectives of patients and healthcare providers, pharmacoeconomic considerations are important, as reducing excessive doses can help alleviate the substantial costs associated with many new treatments, including costs and healthcare resources that may be incurred for the management of adverse effects secondary to suboptimal dosage [13–15]. Therefore, dose optimization for oncology drugs remains a multi-dimensional problem that provides opportunities for innovative integrative approaches [16].

To improve evidence generation and decision-making in the clinical development of oncology drugs, drug developers have been using modeling and simulation to integrate and leverage data accumulated from preclinical and clinical studies [17]. This approach is now known as model-informed drug development (MIDD) [18–20]. In 1994, the International Conference on Harmonization (ICH) laid the groundwork for MIDD with its guidelines, emphasizing the need for studies that characterize the links between drug dose, its concentrations, and clinical response using statistical and pharmacometric techniques [21]. Subsequent Food and Drug Administration (FDA) guidelines have further supported and detailed MIDD practices [22]. For this review, we will focus on clinical drug development, however, it is important to note that MIDD efforts begin before human studies are conducted. While statistical methodologies are essential for MIDD, addressing clinical drug development challenges often requires additional approaches to account for the physiological mechanisms of disease progression and drug effects [23]. Pharmacometrics is a field that integrates mathematical-statistical models with biological, pathophysiological, and pharmacological principles to characterize the interactions between xenobiotics and patients, including both beneficial and adverse effects [24]. Pharmacometrics has become widely recognized as a tool in drug development and plays an integral role in the MIDD framework, as well as in the oncology area [25–27].

Within pharmacometrics, nonlinear mixed-effect (NLME) modeling techniques play a pivotal role in quantifying the relationship between drug dose and its concentrations in pharmacokinetic (PK) analysis (i.e., what the body does to the drug), and the relationship between drug exposure and its response in pharmacodynamic (PD) analysis (i.e., what the drug does to the body) [28,29]. These models are commonly referred to as the population PK and population PD models. Population models handle longitudinal data of individual patients and thus have the capacity to

i) Describe the temporal change in drug exposure, account for dosing history and changes in clearance.
ii) Characterize the disease progression and dynamics of efficacy or safety biomarkers based on the mechanistic understanding of the underlying biology and pharmacology.
iii) Quantify the onset, duration, persistence, and severity of adverse events (AEs), which are factors of vital considerations for patient tolerance and overall quality of life.
iv) Quantify the magnitude and identify the sources of population heterogeneity in drug exposure and clinical response.
v) Identify subgroups of patients who may benefit from different dosing strategies compared to the general population.

Pharmacometric analysis can also include survival models, which analyze and predict the time until an event of interest occurs, such as progression-free survival (PFS) and overall survival (OS) [30].

Different variables or predictors can be integrated to form model-based frameworks that are constructed to provide a comprehensive understanding of drug behavior and disease progression, as illustrated in Fig. 1. These frameworks combine the relationships between patient characteristics, dosing history, drug exposure, disease progression, efficacy and safety outcomes, and survival, offering a holistic view of the evidence gathered from multiple studies. A crucial aspect of utilizing these frameworks is to simulate outcomes under various unstudied scenarios, such as different treatment combinations, dosing strategies, patient populations, or study designs [31]. Additionally, models for study execution and patient behavior, including drop-out and compliance, can be incorporated to explore their impact on study outcomes [32]. The integrated model can be continuously updated to include new information as it is acquired. Simulations can then be performed before each decision point, ensuring the most current data is utilized to inform subsequent decisions [33]. This iterative process allows for dynamic adjustments and refinements, enhancing the accuracy and relevance of the model predictions throughout the phases of drug development.

The applications and value proposition for iteratively integrating pharmacometric modeling and simulation throughout the oncology drug development lifecycle are manifold. The envisioned benefits include but are not limited to the following contexts of use:

- Enable optimization of dosage (i.e., dose and dosing schedule), including response-adaptive dosing strategies to maximize benefit versus risk.
- Inform and increase confidence in patient selection and enrichment hypotheses.
- Inform patient-focused safety monitoring and risk management/ mitigation.
- Enable early development go/ no-go decision-making.
- Bolster evidence to advance research in new endpoints (e.g., molecular response metrics).

- Predict and increase the probability of success via model-based clinical trial simulations through *in-silico* trial design optimization.
- Increase rigor in disease understanding enabling cross-population bridging and extrapolation (e.g., pediatrics, global development).
- Enable efficient evidence generation for new routes of administration and less frequent posology aimed at improving convenience for patients and healthcare providers.

This review aims to comprehensively explore the integrated modeling approaches applied in the clinical development of oncology drugs. Here, we focus on the integrated model frameworks incorporating longitudinal information on two or more PD variables, including biomarkers, safety outcomes, and survival. Relevant literature was reviewed to identify existing integrated models within the oncology field and offer a comprehensive overview. The specific sections encompass:

- Introduction to NLME modeling and survival analysis (Section 2).
- Common sub-models for the integrated frameworks, including PK, biomarkers, safety, survival outcomes, and covariates (Section 3).
- Methodology for integrated model development (Section 4).
- A review of published integrated models in oncology (Section 5).
- Value of integrated models in oncology drug dose optimization (Section 6).
- Value of integrated models in patient-focused drug development strategies (Section 7).
- Value of integrated models in enabling emerging biomarkers (Section 8).

Drawing from this overview, the review aspires to articulate a forward-looking perspective on the trajectory of this rapidly evolving discipline to engage researchers and stakeholders within the pharmaceutical, regulatory, and clinical sectors of practice.

2. Pharmacometric modeling

2.1. NLME models for repeated measurements

The NLME concept was initially introduced to the field of pharmacometrics by Sheiner et al. [34]. These models are suitable to characterize data collected over time from multiple individuals, with different study designs (e.g., dosing regimens, sampling frequency, etc.) and to quantitatively separate and explain different types of variability. A basic NLME model integrates i) a nonlinear structural model (i.e., fixed effect) that describes how the population curve changes over time, ii) a stochastic model (i.e., random effect) that describes how individual curves deviate from the population curve, and how individual observations deviate from the individual curve (i.e., residual unexplained variability, RUV), and iii) a covariate model that describes how individual characteristics or external factors affect deviations of individual responses from the population average. The mixed term refers to the combination of both fixed and random effects. The model can be written as:

$$y_{ij} = f(t_{ij}, \theta_i) + h(\varepsilon_{ij})$$

$$\theta_i = g(\theta, X_{1,i}, X_{2,i}, \cdots, X_{n,i}, \eta_i) \quad (1)$$

Here, $\boldsymbol{f}(.)$ defines the individual curve of the dependent variable (e.g., drug concentration, biomarkers, or AEs), depending on the structural model, over time $\boldsymbol{j}$ and based on the individual parameter $\boldsymbol{\theta_i}$. $\boldsymbol{g}(.)$ introduces covariates $\boldsymbol{X_{n,i}}$ and the random variable $\boldsymbol{\eta_i}$ to characterize the inter-individual variability (IIV) around the typical parameter $\boldsymbol{\theta}$. $\boldsymbol{h}(.)$ includes the random variable $\boldsymbol{\varepsilon_{ij}}$ to describe RUV between model

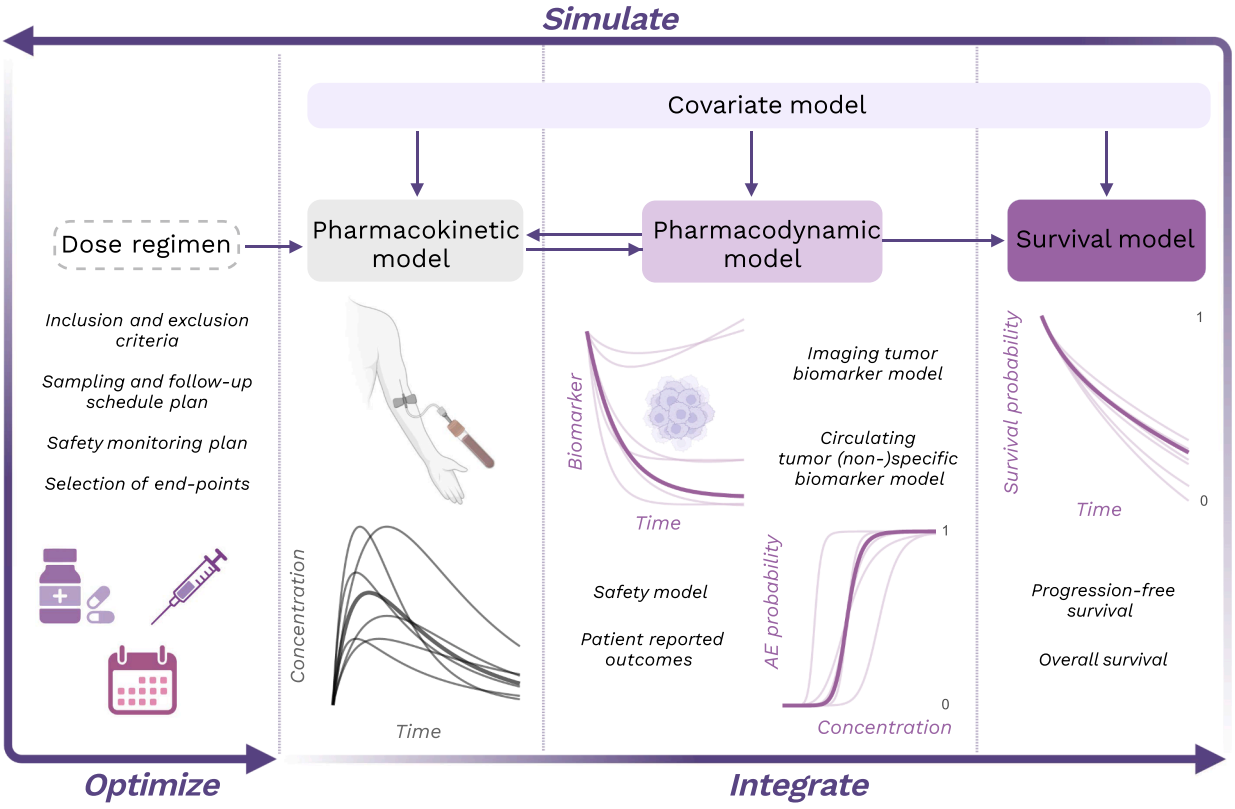

Fig. 1. Illustration outlining the components of the integrated modeling framework, encompassing sub-models. This framework facilitates the integration of covariates, pharmacokinetic, pharmacodynamic, and survival data. Serving as a simulation engine in model-informed drug development (MIDD), it enables optimization of clinical trial design across multiple dimensions, such as inclusion and exclusion criteria, dosing regimen, sampling and follow-up schedule, safety monitoring plan, and the selection of endpoints. Illustrations were created by BioRender.com.

predictions and observations. Random variables η_i and ε_{ij} are assumed to follow a normal distribution with mean 0 and their respective variances, ω^2 and σ^2, respectively. For a more detailed introduction to population modeling, the reader is referred to earlier literature [28,35].

2.2. Survival analysis for time-to-event data

Time-to-event (TTE) data, often used in the context of clinical studies and medical research, refers to information about the duration until a specific event of interest occurs. This event is typically an outcome like death or disease recurrence. Survival analysis, which is frequently employed in pharmacometrics, involves various statistical methods, such as Kaplan-Meier (K-M) survival curves, Cox proportional hazards regression, and parametric survival models.

The K-M method is a non-parametric approach for estimating the survival probability over time. The Log-rank test can be used to compare the K-M curves, which requires categorizing continuous covariates. For example, in an exposure-PFS analysis, subjects might be divided into exposure quantiles instead of fully utilizing the continuous information provided by the exposure data. The Cox proportional hazard analysis is a semi-parametric method that analyzes the relationship between the patient's survival time and one or more predictors. K-M and Cox models are widely used for quantifying the impact of multiple baseline covariates on survival but are generally unsuitable for simulation.

Parametric survival analysis involves fitting a specific parametric distribution, such as exponential, Weibull, or log-normal, to TTE data to describe the baseline hazard. Such models are often favored by pharmacometricians due to their capacity to conduct simulations of hypothetical scenarios, such as alternative dose regimens [30].

Non-parametric cumulative incidence functions have been suggested for handling competing risks in oncology trials with composite endpoints [36]. The corresponding parametric method for competing risk analysis includes multistate models [37]. Multistate models can also account for the impact of intermediate events (e.g., second-line treatment) on the risk of primary events (e.g., death). A multistate survival model (Fig. 2) extends traditional survival analysis by splitting the transition from treatment initiation to death into distinct stages, such as response, progression, and second-line treatment [38]. As a result, multistate survival models can naturally integrate multiple clinical endpoints (e.g., objective response rate (ORR), time to response, duration in response, time to progression (TTP), PFS, OS) and have been proposed as a platform model for describing TTE endpoints in oncology trials [38,39].

To date, within the context of pharmacometrics applied to oncology drug development, multistate models have been applied to 1) integrate with a population tumor size model to enhance predictions of survival [40], 2) facilitate decision-making, including estimating the effect of investigated treatment on OS while accounting for the confounding effect of second-line therapy [41], and informing dose selection of anticancer treatments [42].

3. Components of an integrated modeling framework

3.1. Pharmacokinetic metrics

PK involves the absorption, distribution, metabolism, and excretion (ADME) of drugs within the body. In this review, we primarily focus on systemic drug exposures, such as plasma drug concentrations, even though target-site exposure (e.g., intra-tumoral concentrations) is more directly related to drug effect. This is due to the difficulties to measure concentrations in tumor [43]. NLME PK models are commonly developed to characterize the ADME properties of drugs in a target population using observed PK data. This type of analysis is also known as population PK analysis and can help to identify sources of individual variability in drug exposure [28].

Identifying a PK determinant for the PD response is crucial for enhancing clinical trial outcomes by enabling the optimal selection of dose regimen and patient population. Individual PK parameters and exposure metrics computed from a population PK model can be tested as 'drivers' of the PD response. These metrics include time-point drivers (e.g., C_{max}, C_{trough}) and summaries of exposure measurements (e.g., the area under the curve to the end of the dosing period at a steady state ($AUC_{0\text{-}tau,ss}$) or average concentration at steady state ($C_{avg,ss}$)). They can be applied as constant or time-varying PK metrics, in addition to the model-predicted drug concentration–time (t) (C(t)) curve [29]. PK metrics are often highly correlated and thus multiple metrics could perform equally well in predicting the response. The selection of PK metrics to test should be carefully considered and guided by biological

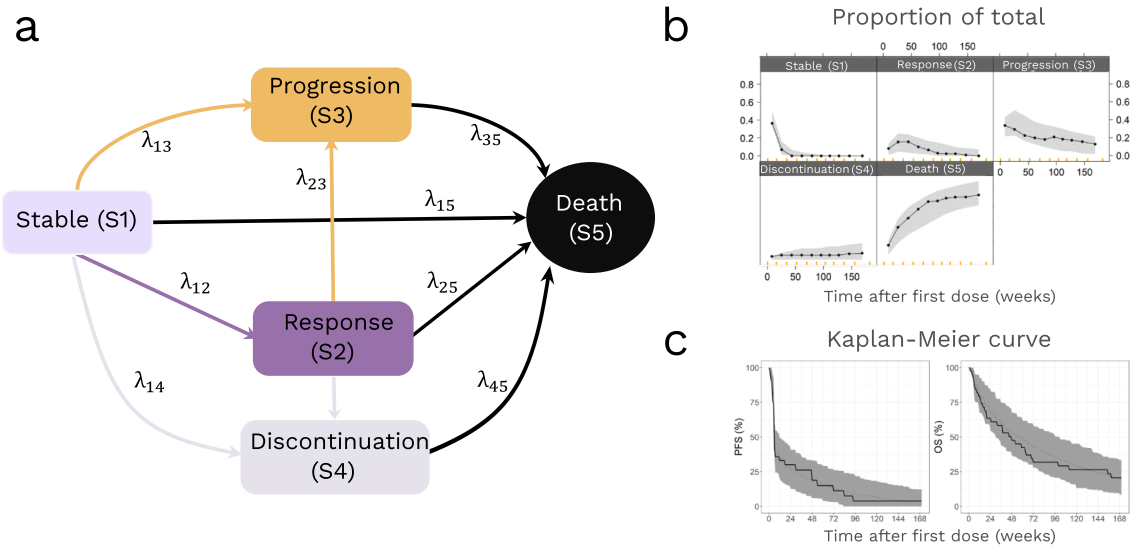

Fig. 2. State and transition diagram of an example multistate model (a). Each compartment represents one state and the arrows represent transitions of patients between states. λ_{ij} denotes the transition hazard from state i to state j. Example of observed and predicted proportions of patients in each state over time after the first dose (b). The black lines represent the observed data and the shaded gray areas are 95% confidence intervals from simulations based on a developed model. Example of a Kaplan-Meier curve of progression-free survival (PFS) and overall survival (OS) (c). The black lines represent the observed data and the shaded gray areas are 95% CI based on simulations. A PFS event is defined as a transition to the state of progression/death from stable or response states, and events are censored if patients transit to the discontinuation state. An OS event is defined as a transition to the state of death.

plausibility and clinical significance to mitigate the risk of inflated type I errors.

While the evaluation of C(t) is possible, the PD turnover in oncology is typically slow, which minimizes the advantage of using C(t) over summary metrics. Alternatively, time-varying PK summary metrics can be used to reflect the change in exposure over time. For example, Lu et al. [44] evaluated dose, C(t), and AUC_{ss} in a pharmacokinetic-pharmacodynamic (PKPD) analysis of tumor response in patients with thyroid cancer. C(t) and AUC_{ss} outperformed the dose and demonstrated similar performance in predicting the time course of tumor response.

In situations where no PK observations are available, the typical PK parameters corrected for previously identified covariates, based on an established PK model, can be used to predict the individual exposure metrics to drive the PD response [45]. Alternatively, a kinetic-PD (K-PD) model can be fitted to the PD data while the drug's kinetics are inferred based on recorded dose intensity and schedule, as well as the PD dynamics [46–48]. This approach has been applied to connect dose and biomarker kinetics for predictive simulations in oncology drug development [49,50].

In emerging modalities such as monoclonal antibodies, bispecific antibodies, and antibody-drug conjugate (ADC), intricate mechanisms like target-mediated drug disposition (TMDD) and other system-based conditions, such as cachexia, can result in complex interplay between PK and PD [51]. As a result, a time-varying clearance is often observed. In such a case, clearance may predict response in exposure–response analysis [52] and bidirectional models between PK and PD may be preferred [53].

3.2. Pharmacodynamic biomarker models

Biomarkers are characteristics that are objectively measured and evaluated as indicators of biological processes, pathological conditions, or pharmacologic responses to therapeutic interventions. They can be categorized into different types based on their specific context of use [54]: *surrogate endpoints* are used in clinical trials as a substitute for direct measuring of how a patient feels, functions, or survives; *predictive biomarkers* can be used to help identify individuals who are likely to show either beneficial or adverse effects following exposure to a medical product or environmental factor, and *prognostic biomarkers* can be incorporated to predict the likelihood of a clinical event, disease recurrence, or progression. PD biomarkers are a class of biomarkers that quantitatively characterize processes on the causal path between drug administration and effect [55]. These include i) target engagement, ii) drug-induced physiological or pathophysiological change such as tumor shrinkage, and iii) clinical response. It is common for PD biomarkers to have predictive and prognostic value, and they may be used as surrogate endpoints in clinical trials.

In oncology settings, PD biomarkers can be categorized into imaging biomarkers and biomarkers of disease biology that are measured in circulation, tumor, or surrogate tissues. Since it is often not feasible to characterize tumor and tissue-based biomarkers longitudinally, this review will primarily focus on imaging and circulating biomarkers.

3.2.1. Imaging biomarkers

Imaging biomarkers include size-based measurements, such as unidimensional or volumetric anatomical assessment of tumor burden, based on computed tomography (CT) or magnetic resonance imaging (MRI) scans, as well as functional assessment with positron emission tomography (PET) or MRI [56]. Assessment of the changes in the disease burden through imaging techniques plays an important role in the clinical evaluation of cancer therapeutics. The most widely used imaging biomarker is the sum of the longest diameters (SLD) of target lesions, in addition to assessments of non-target lesions and identification of new lesions from the scans. For solid tumors, these measurements form the basis of response evaluation criteria in solid tumors (RECIST) endpoints (e.g., ORR and PFS), which are pivotal for early clinical decision-making in both drug development and clinical practice [57].

Emerging imaging biomarkers hold promise for detecting disease progression earlier than the conventional CT. One example is tumor metabolic activity measured using Fluorodeoxyglucose (FDG)-PET/CT scans [58]. FDG is a radio-labeled glucose analogue that accumulates in cells with high glycolytic activity, and the accumulation can be quantified by maximum standardized uptake value (SUV_{max}) [59]. FDG-PET can differentiate viable tumor tissue from fibrotic ones and detect changes in metabolic activity, which may precede changes in tumor size [60]. In some cases, PET response criteria in solid tumors (PETCIST) based on FDG-PET scans have been shown to better correlate with patient outcomes and thus better predict the effectiveness of new anticancer therapies compared to RECIST [61].

3.2.2. Circulating biomarkers

Circulating biomarkers in oncology refer to substances that can be detected in blood or other biofluids and provide valuable information about the cancer's presence, characteristics, or progression. As exemplified in a recent review [62], circulating biomarkers include a diverse array of analytes of proven value in monitoring cancer progression and treatment efficacy. They can be further divided into tumor-specific or non-tumor-specific biomarkers, including 1) non-specific markers of disease burden such as lactate dehydrogenase (LDH) and neutrophil-to-lymphocyte ratio (NIR), 2) tumor-specific markers like prostate-specific antigen (PSA) in prostate cancer, cancer antigen 125 (CA-125) in ovarian cancer, circulating tumor cells (CTC), and circulating nucleic acids (i.e., circulating tumor DNA (ctDNA) and RNA (ctRNA)).

3.2.3. NLME models of longitudinal biomarkers and tumor kinetics

Population PD models, ranging from empirical to mechanistic, are implemented to describe the drug effects and their relation to the PD biomarker dynamics. Exposure-effect relationships are an important part of PD models. Commonly used exposure-effect relationships include linear, log-linear, E_{max}, or sigmoidal E_{max} functions [61]. These relationships link PK metrics to PD parameters [63]. The development and evaluation workflows for PD models have been well-presented in a previously published tutorial [63]. In this section, we highlight some basic concepts of PD modeling and discuss a few of the most commonly used models.

In oncology, PD biomarkers typically exhibit a slow turnover rate, resulting in gradual changes in their levels over time. Therefore, continuous monitoring and long-term assessments are crucial for accurately understanding these dynamics. Turnover, or indirect response, models are widely used to describe longitudinal observations (*Equation (2)*).

$$dR/dt = k_{in} - k_{out}{}^{*}R(t) \tag{2}$$

Where R represents the PD biomarker measured to evaluate response, k_{in} represents the zero-order rate constant for production of response, and k_{out} represents the first-order rate constant for loss of response. To introduce longer delays between drug administration and effect, a transit compartment model can be used [64].

Ordinary differential and algebraic equations have been used to characterize the tumor dynamics [65–68]. Two reviews have summarized these approaches and offer insights into selecting appropriate modeling strategies [69,70]. The model commonly used, in the form of ordinary differential equations, is the tumor growth inhibition (TGI) model proposed by Claret et al. (*Equation (3),* Fig. 3*A*) [71]. This model was originally developed based on tumor size data from colorectal cancer patients receiving capecitabine or 5-fluorouracil and has since then been applied in various cancer types and drugs. The model characterizes tumor size (i.e., SLD) as a function of time and drug exposure. It includes the natural growth rate of the tumor (k_G) and the drug-induced killing effect (k_D). Additionally, a function describing the development of drug resistance (λ) can be introduced to describe observed tumor regrowth.

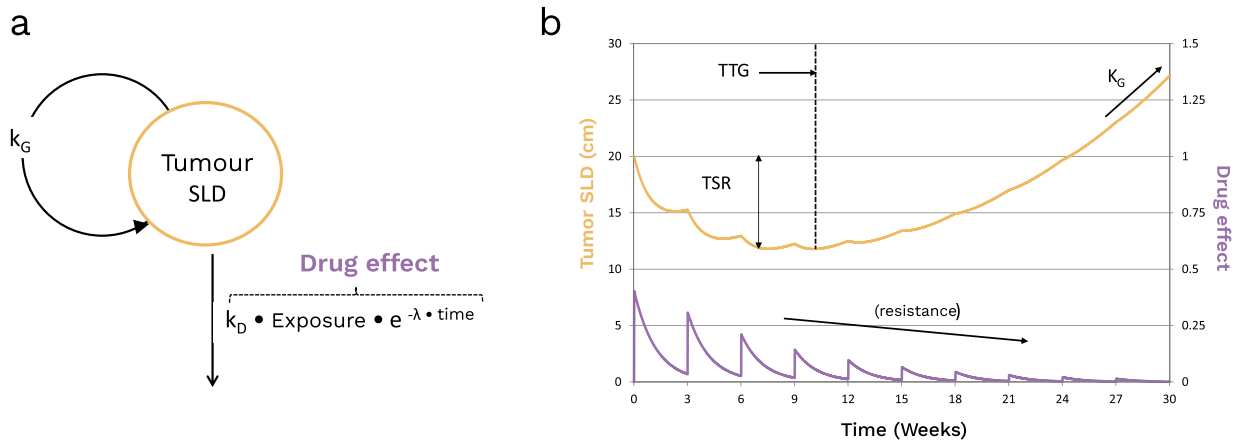

Fig. 3. (A) Tumor growth inhibition (TGI) model structure diagram. k_G, the tumor growth rate constant; k_D, the tumor decay rate constant; Exposure, drug exposure; λ, exponential decay constant of drug effect over time. (B) The sum of the longest diameters (SLD) predictions based on the TGI model illustrating the model-derived tumor size metrics. The solid line represents the absolute SLD (yellow) or drug effect (purple) over time. The tumor size ratio (TSR) is the ratio between the model-predicted SLD and the baseline SLD at a specific time point. Time to tumor growth (TTG) is the duration from time 0 to the time of tumor regrowth. Figure reprinted with permission (Bender et al. Population pharmacokinetic-pharmacodynamic modeling in oncology: a tool for predicting clinical response, Br J Clin Pharmacol 2015; copyright John Wiley and Sons).

$$dSLD/dt = k_G - k_D{*}Exposure{*}e^{-\lambda{*}t}{*}SLD(t) \quad (3)$$

From a TGI model, several metrics can be derived to evaluate tumor response to therapy, including tumor size ratio (TSR), the model-predicted tumor size time-course (absolute TS(t) or relative change from baseline or nadir), time-to-tumor growth (TTG), and k_G [67]. The derivation of these metrics is summarized in Fig. 3B. These metrics are frequently evaluated as individual predictors for the hazard related to survival.

An alternative model structure divides the baseline tumor size into drug-sensitive and drug-resistant parts by separating tumor mass into two subpopulations. This approach was applied to describe the SLD kinetics characterized in HER2-negative metastatic breast cancer in patients receiving docetaxel or paclitaxel [72], metastatic colorectal cancer (mCRC) patients treated with cetuximab [73], and advanced melanoma patients treated with pembrolizumab [74]. In these cases, the drug-resistant tumor cells were hypothesized to transfer from an initial quiescent state to a proliferative state using a set of transit compartment models. These subpopulation models enabled the characterization of tumor kinetics when dealing with cancers having molecular variation in the oncogenic drivers leading to the evolution of resistance and/ or differential sensitivity to drug effect (e.g., T315I mutation in *BCR-ABL* in chronic myeloid leukemia) [75].

Alternatively, algebraic equations have been employed to characterize the dynamics of tumor size. One commonly used model has been proposed by Stein et al. [76] (*Equation (4)*) to describe the change in PSA measurements following an experimental vaccine in metastatic prostate cancer patients. This model structure was later applied to characterize the dose–response relationship of everolimus in metastatic renal cell carcinoma (mRCC) [47]. The model assumes that the changes in tumor size during the treatment are due to two independent elements proportional to baseline (y_o): an exponential tumor growth (g) and a tumor regression (d). The term "-1" ensures tumor size is $y(0) = y_o$ at time 0 (*Equation (4)*).

$$y(t) = y_o{*}(e^{-d{*}t} + e^{g{*}t} - 1) \quad (4)$$

Oncology treatments, such as chemotherapies, can directly kill or inhibit the growth of tumor cells. Alternatively, the drug may affect one or more precursors that impact PD variables, such as tumor size. This is common with targeted therapies, where the drug affects receptor-mediated pathways and signaling cascades, or with immunotherapies, where the drug enhances the immune system's ability to identify and destroy cancer cells. In cases where precursor measurements aren't available, a theoretical compartment representing its turnover can be used to characterize the time delay in PD response [77]. When longitudinal data on mediator biomarkers are available, they can be incorporated into a comprehensive PD modeling framework to connect PK exposure with downstream PD measures [78].

3.3. Safety models

The safety of anti-cancer treatments can be assessed by continuous measurements of biomarkers. For example, the severity of neutropenia is determined by the level of absolute neutrophil count (ANC), which can be categorized into different grades following the Common Terminology Criteria for Adverse Events (CTCAE). In some cases, when the intensity of a safety outcome is not directly or easily quantifiable, ordinal variables are collected. For instance, Grade 1 mild fatigue is characterized as 'relieved by rest', Grade 2 moderate fatigue is 'not relieved by rest and limiting instrumental activities of daily living', and Grade 3 for severe fatigue that 'limit self-care activities of daily living'. To capture the development and the duration of ordered categorical AEs, pharmacometric Markov models could be utilized, with examples of the application of both discrete-time and continuous-time Markov models [79–87]. For AEs that are measured as continuous data and later on categorized in CTCAE, an alternative and better approach is to describe the longitudinal data with models containing mechanistic components, such as the myelosuppression model used for describing neutropenia [88] and the semi-mechanistic models for transaminitis [89]. Safety outcomes are sometimes analyzed as TTE data using survival models. One example is the time to the occurrence of febrile neutropenia in cancer patients receiving chemotherapy [90]. Since many anticancer drugs share the same toxicities, the same structural models for safety may be applicable across drugs and indications.

3.4. PFS and OS models

In cancer clinical trials, the most common endpoints to measure efficacy are OS and PFS, i.e., TTE data. OS is defined as the time from the start of the treatment or diagnosis/ randomization to the event of death. For OS data, the exact time of death is known, otherwise the data is censored if a patient drops out from survival follow-up or if the study follow-up ends (i.e., right censored). Despite being considered the gold standard endpoint in oncology trials, the utility of OS for decision-making in early to mid-stage drug development is limited. Observing a

sufficient number of events can take years, depending on the indication, so OS is generally used only as the primary outcome in phase III trials. Additionally, OS can be influenced by confounding factors as patients may switch to new lines of therapy after disease progression [41]. Therefore, surrogate endpoints are considered to inform decision-making in early-phase trials. For solid tumors, PFS is among the most commonly assessed surrogate endpoints.

According to RECIST 1.1, PFS is an intermediate endpoint defined as the earliest occurrence of death or disease progression. Disease progression includes target lesion progression, non-target lesion progression, and the appearance of new lesions. PFS is interval-censored (except for when death occurs), as tumor assessments are scheduled at specific intervals, i.e., the exact time of progression is unknown but a time interval in which it happens is observed. PFS and OS can be analyzed separately using traditional survival models, such as the Cox proportional hazard model or the parametric TTE model. They can also be integrated through multistate survival models [42]. Alternatively, PFS can be described by developing separate models for different types of progression events. Typically, progression in target lesions is captured using longitudinal SLD models, while non-target lesion progression and the emergence of new lesions are characterized through TTE models with interval censoring [91–93].

3.5. Dropout model for longitudinal measurements

In oncology trials, patients typically drop out of repeated measurements (e.g., SLD measured during tumor assessment) when treatment is discontinued upon disease progression as specified in the treatment protocol (e.g., per RECIST criteria) or due to various reasons before disease progression (e.g., intolerable AEs). Note that patients who discontinue treatment and measurements are still often followed up for survival; that is, patients may drop out from longitudinal measurements but not necessarily from OS follow-up.

The dropout mechanism can be categorized into three types: 1) completely random dropout (CRD): dropout is not correlated with observed/ unobserved data and can be ignored in model development for the longitudinal data; 2) random dropout (RD): the probability of dropout is dependent on observed data and/ or covariates, but is not dependent on missing data, and 3) not at random dropout (NRD): the probability of dropout is dependent on unobserved data and/ or covariates. The dropout model for RD is essential for adequate simulations from the response/safety model but can be developed independently. On the other hand, the dropout model for NRD needs to be fitted together with the model for longitudinal measurements, e.g., the disease progression or the AE model [94,95].

In oncology settings evaluating the drug effect on the disease, the dropout mechanism is often RD or NRD. Dropout models are primarily developed to make simulations from a tumor size model mimic observed data [73 53,96]. Predictors identified for dropout include tumor-related metrics such as progressive disease (i.e., 20 % increase from baseline), and appearance of new lesions. Not accounting for dropout in simulations may undermine the reliability of simulation-based model evaluation or result in faulty predictions when answering 'what if' questions [97]. Additionally, ignoring patient dropout may introduce bias into parameter estimates of the NLME model, albeit the number of dropout events generally needs to be high to be influential [98].

Hazard models can be used to describe dropouts that are observed at an exact time or are interval-censored [94]. Zheng et al. developed a tumor size-dropout model, which identified model-based predictors including absolute tumor size, tumor size percent change from baseline, disease progression status, and time since progression [99]. If dropout is interval censored (e.g., for SLD measurements that can only occur at the time of tumor assessment), logistic regression offers a more straightforward implementation and, most often, equally good performance in comparison to hazard models [78].

3.6. Covariate model

Covariate analysis is an integral aspect of pharmacometric model development, aiming to identify and describe relations between covariates (i.e., predictor observed variables) and model parameters, including PKPD parameters in NLME models and event hazards in survival models. The best practices for planning, conducting, reporting, and interpreting covariate analyses to guide decision-making have been detailed in a recent review [100]. This analysis can help to 1) identify the presence or confirm the absence of specific patient subgroups at potential risk of over/under exposure in PK, excessive toxicity, or suboptimal efficacy, 2) enhance the predictive performance of the model, and 3) deepen the understanding of predictable sources of variability or system mechanism. The information obtained from the covariate analysis can inform decisions regarding dose selection, dose individualization, or the design of clinical trials across various patient subgroups. In most cases, covariates are observed at baseline and treated as time-invariant during model development. However, if the covariate is observed at multiple time points, considering them as time-varying can enhance model fit and provide further insights, especially regarding disease evolution and resistance to treatment response [101].

Common covariates of interest include demographics (e.g., race, age, and weight), laboratory values (e.g., creatinine, albumin, and pheno/genotype), disease factors (e.g., etiology, time since diagnosis), therapy factors (e.g., co-medication, pre-medication), habit/environmental factors (e.g., smoking, drug administration with/without food, diet), or trial factors (e.g., study site).

4. Methodology for integrating models

4.1. Simultaneous and joint modeling

In this approach, model parameters for two or more dependent variables are estimated simultaneously. For example, the parameters of a PK model and a biomarker PD model can be estimated simultaneously, assuming that both PK and PD data inform each other. This allows parameters and their uncertainties to be determined by all the data. However, this method may be computationally expensive and time-consuming, and it may be challenging to achieve a stable overall model for different variables included [40,102]. Generally, the PD contribution to the PK model can be assumed negligible, except in the case of biologics, where the PD impact on drug clearance is significant, making simultaneous modeling beneficial to characterize the bidirectional interplay between their PK and PD [53].

The simultaneous approach was initially considered for analyses with two (or more) types of continuous data. Hu and Sale expanded this approach to be applicable also for continuous type data estimated with TTE data using the NONMEM software [94]. In the statistical literature, the simultaneous estimation of continuous and TTE data, such as death, using mixed-effects models and a parametric survival function, respectively, has been referred to as joint modeling. This modeling approach allows for the integration of dynamic changes in biomarkers and disease status with the survival function (Equation (5)).

$$h_i(t) = h_0(t) \bullet e^{(\alpha \bullet X_i + \beta \bullet Y_i(t))} \quad (5)$$

here, $h_0(t)$ is the baseline hazard function, X_i represents the covariates and $Y_i(t)$ represents the longitudinal model-predicted predictors for individual *i*. α and β are the estimated coefficients related to the corresponding predictors.

The workflow of joint modeling of the NLME and survival models has been detailed in a recent tutorial [103], which can also be applied to scenarios where the event of interest occurs more than once (i.e., recurrent TTE data) or when multiple competing risk events co-exist [40,104].

4.2. Sequential modeling

Sequential modeling is an alternative to simultaneous modeling and is most commonly selected for practical reasons such as shorter estimation times and more stable parameter estimation. Zhang et al. introduced the naming of two different sequential approaches: (i) the "individual PK parameters'' (IPP) approach, where individual parameters from a PK analysis are used to inform on the individual drug concentration-time profile in a PKPD model, and (ii) the "population PK parameters and data" (PPP&D) approach, where the population PK parameters are fixed, but both the PK and PD data inform on the individual PK parameter estimates during the estimation of PD parameters [105]. The same concepts can be applied to scenarios where individual PD parameters or PD model-derived time-varying metrics are tested as predictors of another PD variable or a TTE hazard.

It is assumed that the individual parameters in the IPP approach have been estimated without error. Therefore, the parameter uncertainty can be underestimated in the second step of the estimation. In addition, bias may be introduced during the estimation of the parameters of the second dependent variable, especially for individuals with sparse data contributing to the first-step model. In this case, the individual parameter estimate may shrink towards the population parameter estimate in the case of η-shrinkage or their model predictions may shrink towards the observed data in the case of ε-shrinkage [102,106]. With increased shrinkage, there is a corresponding increase in the standard error of posterior individual parameter estimates [107]. To address this concern, the individual PK parameters with standard error (IPPSE) method was introduced, resembling IPP but taking into consideration the standard errors associated with individual parameter estimates [102,106].

For the evaluation of the performance of modeling approaches to describe the association between tumor kinetics and OS, Krishnan and Friberg evaluated the performance of the different sequential approaches in comparison to the simultaneous approach [108]. The PPP&D approach provided similar or better accuracy and precision of the parameter estimates of a tumor size model and hazard of death as the simultaneous method, while the IPP approach was not as good. Chen et al. subsequently confirmed that joint modeling more accurately predicts OS than IPP based on the concordance index and Brier score [109]. PPP&D was, however, not explored. On the other hand, results by Gonçalves et al. showed that the IPP approach could offer comparable prediction of OS hazard ratio to joint modeling despite the bias in the k_G parameter estimate, based on a large dataset including one phase II and five phase III clinical trials [110]. Further investigation is required to confirm these results in phase Ib or phase II clinical trials, where there are constraints on the number of patients and measurements, as well as in different cancer indications.

4.3. Considerations in the selection of tumor kinetic metrics

In standard tumor size-OS analyses, tumor size metrics such as TSR, TTG, and k_G are typically treated as baseline variables, assumed to be known at the beginning of the study, preceding tumor size follow-ups. Consequently, the future observed data is used to predict the present death hazard, potentially introducing immortal time bias and an inflated Type I error when identifying a statistically significant predictive relationship to survival [111,112]. For TS(t) and dTS(t)/dt that are incorporated as time-varying predictors, the risk of immortal time bias cannot be fully mitigated, as the individual tumor size parameters utilized for metric derivation are estimated based on all available tumor size data including future observations [113]. To prevent future observations from being used to predict current outcomes, tumor size metrics can be assessed prospectively by continuously updating them as new data becomes available [40,42]. Alternatively, the landmark approach can be used to reduce immortal time bias by selecting a landmark time t during the study and including only patients who have survived until t in survival predictions based on tumor size metrics calculated at t [114].

As mentioned above, shrinkage towards the typical value may bias the estimated individual parameters in case of limited individual tumor-size data. Consequently, the actual difference in response between individuals may be obscured. A simulation study demonstrated that the accuracy (defined as falling within 80– 125 % of the simulated "true" value) of the model-derived TSR metric at week 6 was adequate for 91 % of patients based on tumor size data up to 12 weeks [108]. However, the accuracy observed for TTG and k_G metrics was lower (43 and 77 % of patients, respectively) and occurred in the later stages of follow-up (42 and 60 weeks, respectively), as they require information on tumor growth compared to TSR. Both TSR at week 6 and the model-predicted time course of tumor size, whether an absolute or relative change, demonstrated superior forecasting capabilities of survival compared to TTG or k_G. These simulation results highlight the impact of tumor imaging follow-up data on the unbiased estimation of tumor size metrics and the predicted hazard of death for individual patients. As such, it is recommended to evaluate only tumor size metrics with high estimation accuracy as predictors in survival analysis.

4.4. Model evaluation

Different approaches to model evaluation could be used to assess the ability of a model to describe the data and evaluate the predictability of the model [115,116]. The goodness of fit plots are the basic prediction-based tools for evaluating how well an NLME model describes the data by detecting potential misspecifications in the structural model and/or the random effects models [115].

Simulation-based tools are considered the gold standard for assessing the model's predictive performance [116]. They rely on a large number of simulation replicates based on the assessed model and the study design. A comparison between a statistical summary computed from the observed data and corresponding summaries computed from the simulated data replicates is performed and illustrated visually in visual predictive check (VPC) plots. VPCs of NLME models are obtained by plotting the observed percentiles together with the predicted percentiles of the dependent variable against the independent variable (e.g., time, dose, or other covariates of interest), with a confidence interval for each predicted percentile computed based on the simulated datasets [116]. The parametric models implemented in TTE analyses are typically evaluated by K-M VPCs, where the confidence interval based on simulated survival curves is computed and compared with the observed data [78,81]. For simulation-based evaluation, it is crucial to reproduce specific design and data features, such as adaptive designs, response-guided treatments, changes in dosing regimens, therapeutic drug monitoring, missing data, and dropouts. Ignoring these features might lead to misleading trends in simulation-based graphs, despite the model being adequate [116].

In the context of individualized medicine, Desmee et al. [117] introduced the theory of individual dynamic prediction (IDP) to the integrated NLME and survival models, aiming to evaluate the model's performance in forecasting individual survival probability based on available biomarker observations. The concept is to utilize the biomarker values of an individual i until a landmark time s to forecast the biomarker dynamics and risk of death between s and the prediction horizon $s + t$, where t is the time since landmark for individual i. The estimated population parameters were implemented as prior distribution to derive individual parameters and survival probability, and the uncertainty in IDP is accounted for by sampling from the individual parameter conditional distribution. To evaluate IDP performance across models, two scoring methods are employed: the area under the receiver operating characteristic curve (ROC AUC) and the Brier score [118]. These scores quantify the model's capacity for discrimination (i.e., the model's ability to differentiate patients of low and high risk of survival) and the calibration (i.e., the model's ability to predict TTE observations). The IDP methodology can be applied to all types of integrated NLME and survival models, such as the tumor size-multistate model

[40].

The predictive ability of NLME population and survival models can also be assessed via external validation, where the model's ability to predict data on which it was not trained is investigated. Claret et al. [119] developed a TGI-OS model using data from the phase II study POPLAR (atezolizumab versus docetaxel), which was successfully validated with data from a phase II study BIRCH (atezolizumab) and a phase III study OAK (atezolizumab versus docetaxel). Nevertheless, a drawback of the external validation approach is that if the predictive performance fails, it will be challenging to discern whether the cause lies in inaccurate model parameters or disparities between the patient populations [120]. Therefore, depending on the purpose of the model, it may be preferred to use all available data for model development. This may especially be preferable in situations where the patient population is sparsely represented, such as in rare cancers, pediatrics cohorts, or among patients with specific molecular profiles or covariates that reflect unique clinical usage and dosing context.

5. Integrated models

The review of integrated models focused on publications from January 2013 till December 2023. The models were identified through a comprehensive literature review and classified into distinct types as shown in Fig. 4 and below:

- models integrating imaging biomarkers with a survival model (Section 5.1).
- models integrating circulating biomarkers with/without a survival model (Section 5.2).
- models integrating imaging and circulating biomarkers with a survival model (Section 5.3).
- models integrating safety biomarkers with/without a survival model (Section 5.4).
- models integrating efficacy and safety biomarkers (Section 5.5).

This classification facilitates a more nuanced understanding and organized presentation of their diverse attributes and functionalities within the field of oncology. Table 1 provides additional details of all identified research articles on integrated models that are discussed in this section. Fig. 5 provides an overview of the integrated models reviewed, focusing on the methods used to link NLME models with survival models and the publication timeline of these models.

5.1. Models integrating imaging biomarkers with a survival model

This section reviews illustrative examples where models for imaging biomarkers are integrated with survival data, illustrated by integrated models showcased in the orange box in Fig. 4.

5.1.1. SLD models

NLME modeling has been used to describe the longitudinal SLD of various solid tumors. The most common method to link SLD dynamics to OS is through using tumor size model-predicted metrics as predictors of the hazard of death. The 'best' identified metric seen includes TSR [50,91,121,122], TTG [123–126], k_G [119,127], TS(t) [128,129], first derivative of tumor size (dTS(t)/dt) [130,131], or a combination of TS(t) and percent change from baseline [99,109], or TTG and dTS(t)/dt [132].

Mechanism-based tumor size models may increase the predictive accuracy for survival outcomes by incorporating parameters describing underlying tumor heterogeneity and associated variability in drug effect, resistance mechanisms, and evolutionary dynamics [133]. Zhou et al. [134] developed an evolutionary dynamic model describing tumor cell numbers derived from one-dimensional measurements of liver metastatic lesions in patients with mCRC, assuming the ellipsoidal shape of lesions. The developed model aimed to describe different cell populations (sensitive and resistant cells) and their change in composition throughout the pre-diagnostic, treatment, and post-treatment follow-up process. The model estimated the killing rate for sensitive cells, the natural death rate, the transition rate from sensitive to resistant cells, the resistant subclones regrowth rate, and the number of resistant subclones. The inclusion of evolutionary parameters significantly improved the prediction accuracy of the Cox proportional hazard model for both PFS and OS as compared to a model based solely on baseline characteristics.

Model development for OS may benefit from Machine Learning (ML) methods. Chan et al. [135] derived individual SLD metrics based on a TGI model in 668 patients with non-small cell lung cancer (NSCLC) receiving atezolizumab or docetaxel in a phase III trial [119]. Various ML techniques were used to identify SLD metrics and other covariates as predictors of OS, including linear ML methods such as Lasso and boosting, as well as nonlinear ML methods such as random forest and kernel machine. The prediction performance of OS was similar between the traditional approach and ML methods based on evaluating the Brier score, although the linear ML boosting method performed marginally better. However, the authors hypothesized that nonlinear ML methods

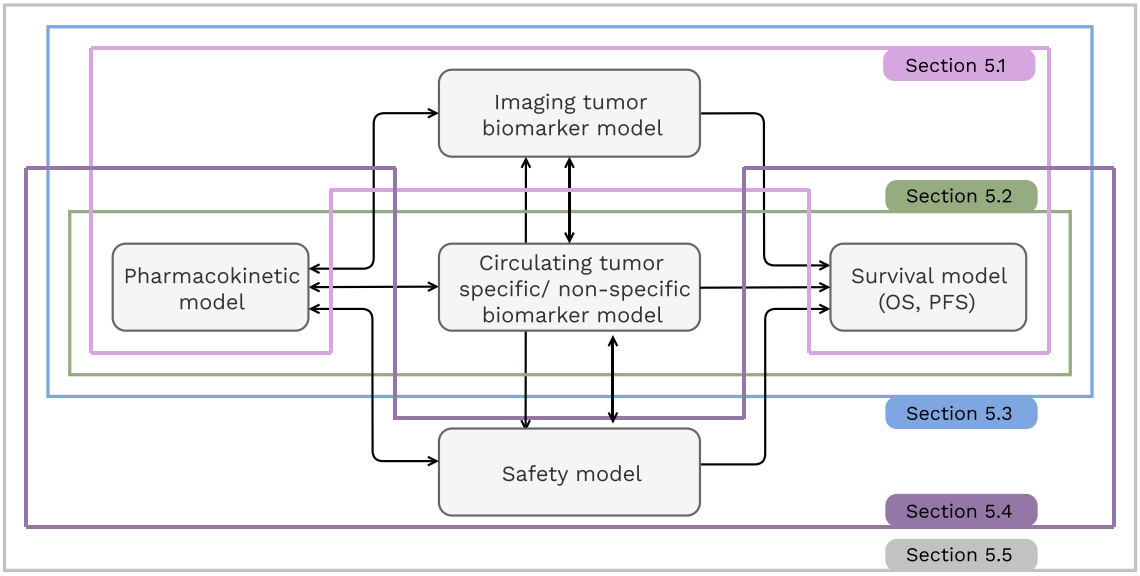

Fig. 4. Illustration of the components of the integrated modeling framework.

Table 1
List of integrated models reviewed in section 5 (January 2013 till December 2023).

Tumor	Treatment	Phase	NLME model		Survival model				Ref.
			Biomarkers	Predictors	Outcome	Model type	Predictors	Method *	
Section 5.1.1 SLD-based models									
RCC	Temsirolimua, interferon, sunitinib, sorafenib, axitinib	II/III	SLD	–	OS	Parametric TTE (log-normal)	TSR at week 8	IPP	[121]
Ovarian cancer	Carboplatin with or without gemcitabine	III	SLD	–	Time to appearance of new lesion	Parametric TTE (Weibull)	TSR (t) if t < week 12, TSR at week 12 if t ≥ week 12	IPP	[91]
					OS	Parametric TTE (Weibull)	TSR (t) if t < week 12, TSR at week 12 if t ≥ week 12, new lesion, SLD_{BL}		
Ovarian cancer	Chemotherapy with or without bevacizumab	III	SLD	–	OS	Landmark cox proportional hazard model	TSR at week 8, SLD_{BL}	IPP	[122]
mCRC	Chemotherapy with or without panitumumab	III	Tumor cell number derived from liver metastatic lesion	–	PFS, OS	Cox proportional hazards models	Response to treatment, malignant cell natural death, resistant subclones regrowth rates, parameters regroup, cell subclones, transition rate to resistance	IPP	[134]
HER2-negative breast cancer	Docetaxel with or without bevacizumab	III	SLD	K-PD	OS	Multistate model	Past change in SLD from baseline, time to progression, past change in SLD between previous two measurements	IPP	[40]
NSCLC	Atezolizumab, docetaxel	III	SLD	–	OS	Parametric TTE (log-normal), ML models	Log-normal (log k_G), lasso/boosting (log k_G, TTG), random forest (log k_G, TTG), kernel machine (log k_G, TTG, Log k_S)	IPP	[135]
mCRC	Chemotherapy with or without cetuximab	I/II/III	SLD	K-PD	OS	Parametric TTE (Weibull)	TSR at week 8, SLD_{BL}	IPP	[50]
					DO	Parametric TTE (log-logistic)	–	Joint	
mCRC	Chemotherapy with or without bevacizumab	III	SLD	–	OS	Parametric TTE (Weibull)	TTG	IPP	[123]
NSCLC	Motesanib	III	SLD	–	OS	Parametric TTE (log-normal)	Log (TTG), SLD_{BL}	IPP	[124]
NSCLC	Maintenance treatment: erlotinib, bevacizumab with or without pemetrexed	III	SLD	–	OS	Parametric TTE (log-normal)	TTG, SLD_{BL}	IPP	[125]
Gastric cancer	Chemotherapy with or without bevacizumab	III	SLD	–	OS	Parametric TTE (log-normal)	Log (TTG)	IPP	[126]
NSCLC	Atezolizumab, chemotherapies	II/III	SLD	–	OS	Parametric TTE (log-normal)	Log (k_G)	IPP	[119]
SCLC, NSCLC, UC, TNBC, RCC	Atezolizumab with or without chemotherapies and/or targeted therapies	II/III	SLD	–	OS	Parametric TTE (log-normal)	Log (k_G)	IPP	[127]
Squamous NSCLC	Gemcitabine and cisplatin with or without necitumumab	III	SLD	Necitumumab $C_{avg,ss}$	OS	Parametric TTE (Weibull and Gompertz)	TS (t), necitumumab $C_{ss,avg}$	Joint	[128]
Pancreatic cancer	Gemcitabine	II/III	SLD	AUC_{weekly}	OS	Parametric TTE (Weibull)	Log (TS(t))	Joint	[129]
Melanoma	Ipilimumab	III	SLD	$C_{ave,firstdose}$	OS	Cox proportional hazard model	dTS(t)/dt at week 8	IPP	[130]
Bladder cancer	Atezolizumab	II	SLD	–	OS	Parametric TTE (Weibull)	dTS(t)/dt	Joint	[131]

(*continued on next page*)

Table 1 (*continued*)

Tumor	Treatment	Phase	NLME model		Survival model				Ref.
			Biomarkers	Predictors	Outcome	Model type	Predictors	Method *	
Urothelial bladder cancer	Durvalumab	I/II	SLD	–	OS DO	Parametric TTE (exponential)	TS (t) and TS rel(t) TS (t), TS rel(t), predicted disease progression status, time since progression	IPP	[99]
UC	Durvalumab	I/II	SLD	–	OS	Parametric TTE (exponential)	TS(t) and TS rel(t)	IPP vs. Joint	[109]
UC	Atezolizumab	II	SLD	–	OS	Parametric TTE (Weibull)	TTG and dTS(t)/dt	Joint	[132]
Section 5.1.2 Organ-specific SLD or individual lesion models									
HER2 − metastatic breast cancer	Docetaxel	III	Individual lesion	Docetaxel C(t)	OS	Parametric TTE (Weibull)	TTG, TS(t) of largest lesion at baseline	IPP	[96]
UC	Atezolizumab, chemotherapies	III	Organ-specific SLD	–	OS	Parametric TTE (Weibull)	SLD(t) of target lesions in liver, locoregional, lymph nodes and lung	Joint	[136]
Bladder cancer	Atezolizumab	III	Individual target lesion SLD	–	OS	Parametric TTE (Weibull)	Model 1: SLD Model 2: organ specific SLD Model 3: difference between the maximum and minimum of the individual lesions at each time	Joint	[137]
Section 5.1.3 Volumetric or functional assessment of tumor based models									
NSCLC	Erlotinib	II	SUV_{peak}	Erlotinib C(t)	OS	Parametric TTE (exponential)	FDG $SUV_{peak,BL}$ and relative change in the FDG SUV_{peak} after 1 week of treatment	IPP	[45]
GIST	Sunitinib	I/II	SUV_{max}, SLD	AUC_{daily}	OS	Parametric TTE (exponential)	SUV_{max} rel at week 1 for the best responding lesion	PPP&D	[142]
GIST	Imatinib	Observational study	Uni-dimensional maximum transaxial diameters, V_{actual}, calculated ellipsoidal volumes, tumor density	–	PFS OS	Parametric TTE model (log-normal)	V_{actual} rel (t) up to 3 months and log ($V_{actual,BL}$) Log ($V_{actual}(t)$)	IPP	[140]
Section 5.2.1 Tumor-specific biomarkers									
Ovarian cancer	Carboplatin with doxorubicin orpaclitaxel	III	CA-125	K-PD	PFS	Cox proportional hazard model	CA-125 elimination rate constant	IPP	[145]
Ovarian cancer	Various first-line regimens	III	CA-125	K-PD	PFS OS	Cox proportional hazard model Parametric TTE (Weibull)	Elimination rate constant KELIM	IPP	[146]
CRPC	Abiraterone Acetate	III	PSA	–	OS	Cox proportional hazard model	PSA doubling time	IPP	[147]
CRPC	Eribulin mesilate	II	PSA	K-PD	OS	Parametric TTE (Weibull)	Time to PSA_{nadir}, k_G, PSA_0	IPP	[148]
CRPC	Docetaxel with prednisone	III	PSA	–	OS	Parametric TTE (Weibull)	PSA(t)	Joint	[149]
CRPC	Docetaxel with prednisone and Aflibercept	III	PSA	–	OS	Parametric TTE (Weibull)	PSA(t)	Joint	[117]
MM	Carfilzomib	II	M−protein	–	OS	Parametric TTE (Log-normal)	Early change in tumor size (ECTS) at week 4	IPP	[151]
MM	Isatuximab with pomalidomide and dexamethasone	III	M−protein	Isatuximab C(t), pomalidomide K-PD, dexamethasone K-PD	PFS	Parametric TTE (Weibull)	dM-protein/dt	Joint	[152]
MM	Pomalidomide with lenalidomide	III	M−protein	–	PFS	Parametric TTE (Weibull)	M-protein change at week 4	Joint	[153]

(*continued on next page*)

Table 1 (*continued*)

Tumor	Treatment	Phase	NLME model		Survival model				Ref.
			Biomarkers	Predictors	Outcome	Model type	Predictors	Method *	
	and dexamethasone								
CPRC	Chemotherapy with or without hormonotherapy	Observational study	CTC, PSA	Latent variable (t) driven by K-PD	–	–	–	–	[156]
EGFR, NSCLC	Erlotinib, gefitinib	Observational study	ctDNA (L858R, exon19del, and T790M mutants)	–	PFS	Parametric TTE (Weibull)	L858R rel(t), exon19 rel(t)	IPP	[158]
EGFR, NSCLC	Osimertinib, gefitinib, erlotinib	III	ctDNA	–	PFS	Parametric TTE (Weibull)	ctDNA(t)	IPP	[159]
CLL	Venetoclax with or without rituximab	I/II	MRD, ALC	Venetoclax C(t), rituximab K-PD	–	–	–	Joint	[164]
LBCL	CAR-T Cell immunotherapy	Observational study	CD19 + metabolic tumor volume	Four CAR-T cell phenotypes, CD19+	OS	Cox proportional hazard model	CCS cut-off value calculated from the chosen CAR-T cell	IPP	[166]
Section 5.2.2 Tumor non-specific biomarkers									
SCLC	Etoposide and cisplatin with carboplatin	Medical records	LDH, NSE	Latent disease variable (t) driven by K-PD	TTP	Parametric TTE (log-logistic)	Latent disease variable (t) driven by K-PD	IPP	[167,168]
GEP-NETs	Lanreotide Autogel®	III	CgA	Lanreotide Autogel C(t)	PFS	Parametric TTE (Weibull)	$CgA(t)/CgA_0$	Joint	[169]
CRC, RCC	Sunitinib	II/ IV	sVEGFR-2, sVEGFR-3	Unbound active concentration (Sunitinib + SU12662)	TTP (mCRC), PFS (mRCC)	Parametric TTE (exponential)	Unbound active concentration (Sunitinib + SU12662)	IPP	[170]
Breast cancer	Palbociclib and letrozole	I	TK1, pRb, Ki67	Palbociclib C(t)	PFS	Cox proportional hazard model	$TK1_{BL}$, $TK1_{nadir}$	IPP	[171]
Section 5.3 Models integrating imaging and circulating biomarkers with survival model									
Ovarian cancer	Carboplatin and doxorubicin or paclitaxel	III	SLD CA-125	K-PD SLD	PFS	Parametric TTE (log-logistic)	Model1: ΔCA-125 from baseline to week 6 Model 2: ΔTS from baseline to week 6	IPP	[173,174]
NSCLC	Atezolizumab	I	SLD IL-18 ITAC	AUC_{cycle} Atezolizumab C(t) –	OS	Parametric TTE (exponential)	SLD rel(t)	PPP&D	[175,176]
CRC	Capecitabine, oxaliplatin, and bevacizumab with or without cetuximab	III	SLD CTC	Total normalized dose SLD(t)	OS	Parametric TTE (log-logistic)	λCTC(t)	IPP	[73]
NSCLC	Durvalumab	III	SLD, NLR	–	OS	Parametric TTE (Weibull)		Joint	[177]
CRC	Panitumumab	II	SLD, ct-DNA	–	–	–	–	–	[178]
NSCLC, MM	UV1 vaccine (and ipilimumab for MM)	I	SLD, Stimulation index	UV1 vaccine peptides (t)	OS	Parametric TTE (Weibull, NSCLC), (exponential, MM)	SLD_{BL}(NSCLC), relative change from nadir (MM)	IPPSE	[179]
Section 5.4 Models integrating safety biomarkers with or without survival model									
Breast cancer	Chemotherapies	Observational study	G-CSF ANC	– G-CSF(t)/ $G\text{-}CSF_0$	–	–	–	–	[181]
Breast cancer	Chemotherapies	Observational study	IL-6 CRP	– IL-6 rel(t)	Time to neutropenia	Parametric TTE (exponential)	CRP(t)	IPP	[90]
Section 5.5 Integrated efficacy and safety models									
GIST	Sunitinib	I/II/III	VEGF, sVEGFR-2, sVEGFR-3, sKIT	AUC_{daily}	OS	Parametric TTE (Weibull)	Model 1: sVEGFR-3 rel(t) Model2: ANC(t), Blood pressure rel(t)	IPP	[78,81,182]
			SLD	AUC_{daily}, sVEGFR-3 rel(t), sKIT rel(t)					
			Grade of HFS and fatigue	sVEGFR-3 rel(t)					
			ANC	sVEGFR-3 rel(t)					
			Blood pressure	AUC_{daily}					
RCC	Axitinib	II	VEGF, sVEGFR-1/2/3	AUC_{daily}	OS	Parametric TTE (log-logistic)	SLD(t)	IPP	[183,184]
			SLD	sVEGFR-3 rel(t)					
			Blood pressure	AUC_{daily}					
AML, MDS	Gua-decitabine	I/II	LINE-1 methylation	Decitabine C(t)	–	–	–	–	[49]

(*continued on next page*)

Table 1 (*continued*)

Tumor	Treatment	Phase	NLME model		Survival model				Ref.
			Biomarkers	Predictors	Outcome	Model type	Predictors	Method *	
			ANC	K-PD					
Primary cutaneous melanoma	Adjuvant high dose IFN-α2b	Observational study	LDH, Melanoma-inhibiting activity, Protein S100B, ANC	K-PD	PFS	Parametric TTE (Gompertz)	–	IPP	[185]
					OS	Parametric TTE (exponential)	LDH rel(t)		
HCC and other solid tumors	Roblitinib	I/II	Circulating proteins FGF19, C4	Roblitinib C(t)	TTP	Kaplan–Meier method and log-rank test	–	IPP	[186,187]
			SLD	Roblitinib C(t), composite predictive risk score derived from 75 patients' baseline characteristics using ML					
			ALT	Roblitinib C(t)					
MM	Lenalidomide and dexamethasone with or without ixazomib	III	M−protein	Ixazomib C(t)	Time to relapse	Parametric TTE (log- logistic)	Ixazomib C(t), growth rate of the drug-sensitive sub-population	IPP	[85]
			Platelet counts	Ixazomib AUC_{weekly}, ixazomib C(t), lenalidomide K-PD	DO	Parametric TTE model	M−protein nadir, M-protein increased above a threshold relative to baseline		
			Grade of diarrhoea	Ixazomib AUC_{weekly},	PFS	Parametric TTE model	Ixazomib AUC_{weekly}, M−protein (t), M−protein nadir, the growth rate of the drug-sensitive sub-population		
			Grade of rash	Ixazomib AUC_{weekly}					
MM	Belantamab mafodotin	I/II	M−protein	Belantamab mafodotin C(t)	–	–	–	–	[87]
			Grade of ocular event	Belantamab mafodotin C(t)					
CLL	Ibrutinib	I/II	SPD, Leukocyte count	Latent pBTK (t) driven by AUC_{daily}	OS	Competing risk model	Past model-predicted SPD	IPP	[77]
			Blood pressure	AUC_{daily}	DO		Past model-predicted leukocyte count		

Abbreviations: ALC, absolute lymphocyte count; AUC, area under the curve; ALP, alkaline phosphatase; ALT, alanine aminotransferase; AML, acute myeloid leukaemia; ANC, absolute neutrophil count; bB2M, baseline β2- microglobulin; CA-125, cancer antigen 125; CCS, clinical composite score; CgA, serum chromogranin A; CRP, C-reactive protein; CRC, colorectal cancer; CRPC, castration-resistant prostate cancer; CTC, circulating tumor cells; ct-DNA, circulating tumor DNA; C(t), time course of concentration; DO, dropout; ECOG, Eastern Cooperative Oncology Group; EGFR, epidermal growth factor receptor; FDG, fluorodeoxyglucose FIGO, Féderation Internationale de Gynécologie et d'Obstétrique stages; G-CSF, granulocyte colony-stimulating factor; GEP-NETs, gastroenteropancreatic neuroendocrine tumors; GIST, gastrointestinal stromal tumors; HFS, hand-foot syndrome; IL-6, interleukin 6; IPP, individual PK parameters; IPPSE, individual PK parameters with standard error; ITAC, interferon-inducible T-cell alpha chemoattractant; K-PD, kinetic-PD; k_G, tumor growth rate constant; k_S, tumor shrinkage rate constant; KRAS, kirsten rat sarcoma virus; LBCL, large B-cell lymphoma; LDH, lactate dehydrogenase; LINE-1, long interspersed nucleotide element-1; M−protein, myeloma protein; MDS, myelodysplastic syndromes; MEDFL, extramedullary disease at screening; MM, malignant melanoma; MRD, minimal residual disease; NLR, neutrophil-to-lymphocyte ratio; NSE, neuron-specific enolase; NSCLC, non-small cell lung cancer; OS, overall survival; PFS, progression-free survival; PPP&D, population PK parameters and data; PSA, prostate-specific antigen; RCC, renal cell carcinoma; rel(t), time course of relative change from baseline; rel, relative change from baseline; SCLC, small cell lung cancer; SLD, sum of the longest diameter; SPD, the sum of the product of perpendicular diameters; sBCMA, soluble B cell maturation antigen; sCR, soluble C-reactive protein; sKIT, soluble stem cell factor receptor; sIL-6R, soluble interleukin-6 receptor; sPD-L1, soluble programmed cell death ligand 1; sTNF-R1, soluble tumor necrosis factor receptor 1; sTNF-R2, soluble tumor necrosis factor receptor 2; sVEGFR, soluble vascular endothelial growth factor receptor; sVEGFR-2, soluble vascular endothelial growth factor receptor 2; sVEGFR-3, soluble vascular endothelial growth factor receptor 3; SUV, standardized uptake value; t, time; TK1, thymidine kinase 1; TNBC, triple negative breast cancer; TSR, tumor size ratio; TS(t), tumor size time-course; TTG, time-to-tumor growth; TTP, time to progression; V_{actual}, software-calculated actual volumes.

* Integration method applied when linking NLME model to survival model.

such as random forest, if given larger datasets, may offer better prediction performance compared to linear ML and traditional methods due to their flexibility in accommodating nonlinear relationships between predictors/covariates and OS events.

A multistate modeling framework for SLD-OS analysis has been proposed to prevent the utilization of future observations for present predictions [40]. Tumor size metrics were prospectively tested as predictors of transition hazards in a 5-state multistate survival model (stable, response, progression, second-line treatment, and death) in patients with breast cancer treated with docetaxel. The individuals' tumor size model parameters were updated continuously as time progressed and more SLD observations became available to inform the model. The relative SLD change from baseline was the best predictor of the transition rate from stable to response, and the change in SLD between the two previous measurements predicted the transition from response to progression. In addition, TTP was identified as a predictor for transitions from progression, as well as second-line treatment, to death. This approach could be extended to assess biomarkers and safety

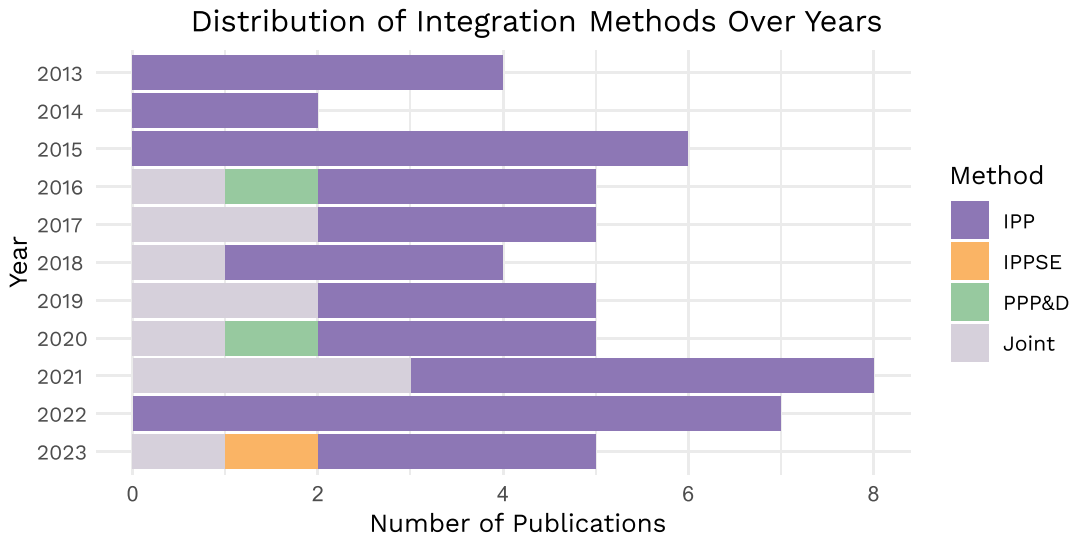

Fig. 5. Distribution of integration methods used to link nonlinear mixed effect models (NLME) with survival models in published integrated models reviewed in Section 5 over the years. The methods include individual PK parameters (IPP), individual PK parameters with standard error (IPPSE), population PK parameters and data (PPP&D), and joint modeling (Joint). This plot highlights the temporal trends in the adoption of these methodologies.

variables.

5.1.2. Organ specific SLD or individual lesion models

The current practice of using SLD measurements based on target lesions ignores the heterogeneity in individual lesions in terms of their individual location, dynamics, response to treatment, and impact on survival. To address this, individual lesion tumor dynamic models have been developed to capture the varying growth rates and treatment responses within the same patient and to assess how each lesion's characteristics influence survival outcomes. Krishnan et al. [96] evaluated the links between the individual lesion tumor dynamics and OS based on a dataset originating from advanced HER2-negative breast cancer patients treated with docetaxel. As the tumor assessment was conducted under RECIST 1.0, data was available for up to 10 target lesions per scan. The IIV, together with inter-lesion variability and inter-organ variability, were quantified using the NLME modeling approach. With this type of model, a 2.6 times higher growth rate could be identified for lesions in the breast and liver, while the estimated docetaxel treatment effect was at least 20 % higher in the breast, liver, and soft tissue compared to other organs. The TTG and time course of the largest lesion at baseline were identified as the best predictors of OS based on parametric TTE models.

Organ-dependent differences were also apparent in urothelial carcinoma patients treated with atezolizumab or chemotherapy [136]. Liver lesions exhibited about five times higher natural growth rate in comparison to other sites, while lymph nodes and lung lesions showed the best response to both treatments. The impact of lesion dynamics on survival also differed across organs: an increase of target lesions SLD in the liver, locoregional, lymph nodes, and lung lesions by 10 mm corresponded to a 12 %, 10 %, 7 %, and 5 % increase in hazard of death, respectively. Compared to using total SLD as a predictor of survival, the organ-specific SLD resulted in a more pronounced improvement in the model fit ($p < 10^{-14}$). The organ-specific SLD-OS joint model was able to discern a significant survival benefit of atezolizumab vs. chemotherapy 3 months earlier than the total SLD-OS joint model and 6 months earlier than the final cut-off date for the OS data.

Furthermore, Kerioui et al. [137] developed a Bayesian multilevel joint individual lesion model in patients with advanced bladder cancer treated with atezolizumab. The model evaluated the time course of each individual target lesion in the lymph nodes, lungs, liver, and bladder, and quantified their impact on survival. The proportion of the total variance in the strength and duration of treatment effect explained by the inter-lesion variability was 21 % and 28 %, respectively. Moreover, individual lesions outperformed SLD in predicting survival, especially at early landmark times, specifically in patients with liver or bladder target lesions.

As evident from the above examples, the opportunity to apply multi-hierarchical models of tumor kinetics at the lesion, organ, and patient levels considered in the integrated approach for the prediction of OS outcomes is an emerging area of research in the discipline of tumor size-survival outcome modeling and simulation. The above examples have highlighted improvements in predictive performance and identification of treatment effects on disease response compared to models developed on SLD data alone. To accurately distinguish between lesion and organ variability, access to dynamics data not limited to the maximum of 5 target lesions and 2 lesions per organ as used in RECIST 1.1 [57] may be needed. Of note, this methodology can be particularly relevant for immunotherapy mechanisms of action, where hyper-progression and dissociated responses with discordant responses between individual lesions have been described. High inter-lesion variability has been quantified in lesion- and organ-level modeling of tumor burden [138]. While the current technical proof-of-principle is encouraging, future research is needed to explore the application of these methods across tumor types and mechanisms of action of investigational and approved anticancer agents, including combination treatments. This is crucial to establish a roadmap and define the right contexts of use for integrating such lesion- and organ-level joint tumor size-survival models as enablers for model-informed oncology drug development.

5.1.3. Volumetric or functional assessment of tumor-based models

RECIST-based tumor size is a measurement of a single dimension and thus susceptible to measurement errors arising from the patient's position during the scan, especially for non-spherical lesions. In addition, tumors may have non-uniform shrinkage or growth during treatment [139]. Therefore, a 3D measurement has been proposed to potentially capture the actual change in tumor burden more accurately, consequently establishing a stronger correlation with long-term clinical outcomes. Schindler et al. [140] developed models for 1D (unidimensional maximum transaxial diameters) and 3D (software-calculated actual volumes V_{actual}, and estimated volumes $V_{ellipsoidal}$ assuming ellipsoidal shape) measurements of liver metastases originating from imatinib-treated patients with gastrointestinal stromal tumor (GIST). In the multivariate analysis, model-derived V_{actual} metrics were found to best predict both PFS (V_{actual} relative change from baseline up to 3 months

and log-transformed V_{actual} baseline) and OS (log-transformed V_{actual} time course). These results advocate for larger clinical trials to evaluate 3D vs. 1D RECIST measurements in predicting clinical outcomes. Tumor density showed a weaker correlation with size-related parameters, indicating that structural changes of a lesion (e.g., reduced vascularization, inflammation, tumor necrosis) may occur independently of, and earlier, than changes in size and thus can provide additional information on tumor response. However, none of the density model-derived metrics was significantly related to PFS or OS.

Besides tumor size and density measurement, tumor metabolic activity reflecting the functional activity can be assessed through imaging via PET using FDG. In a study that included patients with advanced NSCLC treated with erlotinib, the time profile of SUV_{max} from FDG-PET scans was described using a TGI model driven by drug exposure [45]. The presence of epidermal growth factor receptor (EGFR) mutation was associated with a 2.19 higher drug effect. The model-derived baseline FDG SUV_{max} and relative change from baseline at week 1 were significant predictors of OS. Another type of PET, fluorothymidine (FLT)-PET, measures tumor proliferation and DNA synthesis activity. This method was not as significant as FDG-PET for OS prediction in this specific setting of NSCLC treated with erlotinib, which may be attributed to lower uptake and lower specificity of FLT in tumors [141]. Schindler et al. [142] developed an individual lesion FDG-PET SUV_{max} model and an SLD model, linked by the shared effect of drug exposure on the corresponding tumor shrinkage rate parameter, for GIST patients treated with sunitinib. The relative change in model-predicted SUV_{max} for the best-responding lesion at week 1 was identified as a better predictor of OS than SLD. These examples conclude that FDG-PET could be valuable for assessing treatment effects in GIST.

5.2. Models integrating circulating biomarkers with/without a survival model

Identification of predictive circulating biomarkers is crucial in drug development and clinical settings. These biomarkers not only enhance disease monitoring but can also enable early predictions of clinical outcomes. By integrating biomarker data through diverse modeling approaches, their predictive performance for response classification in clinical settings can be thoroughly evaluated and validated, illustrated by integrated models showcased in the green box in Fig. 4. As elaborated in the subsequent subsections, the integration of circulating tumor biomarkers in models encompasses both tumor-specific and non-specific biomarkers.

5.2.1. Tumor-specific biomarkers

One of the tumor markers that evaluate tumor burden and response to therapy in epithelial ovarian cancer is CA 125 [143]. The Gynecologic Cancer Intergroup (GCIG) has defined the CA-125 response to chemotherapy as a 50 % reduction in CA-125 levels maintained for at least 28 days [144]. You et al. developed a semi-mechanistic model quantifying the CA-125 kinetics, in which the estimated CA-125 elimination rate constant was detected as a strong predictor of PFS in ovarian cancer using Cox multivariate analysis [145]. Furthermore, Colomban et al. concluded that the CA-125 elimination rate constant had a higher predictive and prognostic ability for PFS in comparison to the GCIG response criteria using the same model structure on a different dataset [146].

PSA is a protease produced by the prostatic epithelium and released into the bloodstream in cancer cases. Several PSA-survival modeling frameworks have been constructed to explore the relation between PSA kinetics and OS in order to provide a rationale for considering PSA kinetics as surrogate endpoints in prostate cancer patients. Xu et al. revealed a strong association between the individual model-based post-treatment PSA doubling time and OS, using a TGI and a Cox proportional hazard survival model, in metastatic prostate cancer patients following oral administration of abiraterone acetate [147]. Van Hasselt et al. identified the model-predicted PSA time to nadir, PSA growth rate, and baseline PSA as predictors of OS using a TGI and a parametric TTE model in prostate cancer patients treated with eribulin [148]. Desmée et al. quantified the link between the kinetics of PSA, described by a biexponential function, and OS [117]. Desmée et al. also assessed the link between a mechanistic PSA model and OS in such a way that unobserved kinetics of treatment-sensitive and treatment-resistant cells were quantified and evaluated as a predictor of death events in a parametric TTE analysis [149].

Myeloma protein (M−protein) is overproduced by abnormal plasma cells in multiple myeloma (MM) and increases as the tumor burden increases [150]. Jonsson et al. identified an early change in M−protein at week 4 as a predictor of OS using a TGI model in patients treated with carfilzomib [151]. Furthermore, Thai et al. and Cheng et al. described the dynamics of M−protein in patients treated with isatuximab in combination with pomalidomide/dexamethasone and dexamethasone with/without pomalidomide/lenalidomide, respectively, using a similar model [152,153]. The former authors identified the instantaneous change (slope) in serum M−protein as a predictor for PFS using a TTE model, while the latter identified the M−protein change at week 4 as the predictor. Model-based simulations supported the approved dosing schedule of isatuximab (10 mg/kg QW-Q2W) and concluded that changing to monthly dosing after 6 months may have inferior clinical outcomes [152].

The potential impact of novel liquid biopsy-based cancer diagnosis and monitoring approaches is increasing. These approaches enable the detection of cancer biomarkers such as ctDNA and CTC. CTC is a promising prognostic and predictive marker of survival and treatment efficacy, potentially complementing the widely used PSA in metastatic prostate cancer [154,155]. The longitudinal kinetics of PSA and CTC have been linked through a latent variable representing the tumor burden [156]. A non-steady-state indirect model described the latent variable that stimulated the production of both PSA and CTC. PSA and CTC kinetics were described by an indirect model and a cell lifespan model, respectively. Three typical regimens, including chemotherapy and/or hormonal therapy agents, were evaluated using the final framework through simulations. The conclusion was that the CTC count was more sensitive to the variation of the latent variable and indicated an earlier change compared to PSA.

The most commonly reported gene mutations associated with resistance to anti-EGFR treatment in patients with mCRC and NSCLC were kirsten rat sarcoma virus (KRAS) and EGFR mutations, respectively [157]. Janssen et al. [158] described the dynamics of EGFR ctDNA, namely L858R, Exon19del, and T790M mutants, in NSCLC patients treated with erlotinib or gefitinib, using a model consisting of a zero-order input and first-order elimination in addition to time-dependent development of resistance. The most significant predictors of PFS, using a parametric TTE model, were the predicted relative change in L858R and Exon19del concentrations from baseline. In addition, a Bayesian joint model of ctDNA and PFS was developed utilizing data from patients with EGFR-positive NSCLC receiving osimertinib, gefitinib, or erlotinib, demonstrating the value of early ctDNA dynamics in predicting the risk of RECIST-defined disease progression [159].

Minimal residual disease (MRD) is a crucial emerging clinical endpoint in chronic lymphocytic leukemia (CLL) [160]. It is based on measuring the proportion of cancerous cells in the bone marrow or peripheral blood [161]. Studies have shown that MRD status is an independent predictor of long-term survival, providing more precise predictions for PFS and OS in CLL than the International Workshop on CLL response assessment rates [160,162,163]. Gopalakrishnan et al. established an integrated mechanistic model accounting for venetoclax dosing and its PK, rituximab treatment, absolute lymphocyte count (ALC), and MRD data in bone marrow and blood in patients with relapsed or refractory CLL [164]. The model identified a CLL cell subpopulation that is highly susceptible to venetoclax, and another subpopulation that is poorly susceptible to venetoclax. Lymphocytes were

described across three tissues (blood, bone marrow, and other lymphoid tissue), interconnected through blood transfer. Model-based simulations showed that venetoclax in combination with rituximab for two years would maximize the negative status of the MRD in bone marrow ($< 10^{-4}$) rates. While for more than two years, it would be unlikely to achieve further improvements in the negative MRD rate.

Cell therapies, in general, and CAR-T cell therapy, in particular, offer some new MIDD challenges that can be addressed with integrated models. Mc Laughlin et al. listed several actionable variables, including design elements in CAR-T cell discovery, development, and clinical practice, which can be modified to optimize autologous CAR-T cell exposure [165]. Mueller-Schoell et al. developed a population model integrating quantitative systems pharmacology (QSP) knowledge in relapsed/refractory non-Hodgkin lymphoma (NHL) patients treated with CAR-T cell therapy [166]. The model quantified the dynamics of four CAR-T cell phenotypes: 1) naïve CAR-T cells, 2) central memory CAR-T cells, 3) effector memory CAR-T cells, 4) terminally differentiated effector CAR-T cells, and CD19 + metabolic tumor volume, as a PD component and the main driver of CAR-T cell expansion, simultaneously after CAR-T cell infusion. Two subpopulations of patients were identified with different CAR-T cell expansion capacities. Further, the CAR-T expansion capacities were translated into a clinical composite score (CCS) of the 'maximum naïve CAR-T cell concentrations/baseline tumor burden' ratio. A CCS_{TN} value > 0.00136 was proposed as a predictor for survival.

5.2.2. Tumor non-specific biomarkers

Many of the first circulating tumor biomarkers discovered were non-specific indicators of disease burden, such as LDH and other cell death products. Buil-Bruna et al. proposed a population modeling framework quantifying the relationship between LDH and neuron-specific enolase (NSE) concentrations in plasma, and tumor progression levels assessed by imaging scans in small cell lung cancer (SCLC) patients [167]. The two biomarker dynamics were described using turnover models. They were linked together by a latent variable, representing the unobserved tumor size dynamics, which was assumed to be responsible for the production of biomarkers and to be affected by treatment (radiotherapy and chemotherapy) exposure. The model-predicted unobserved disease level strongly correlated with PFS in a parametric TTE model. This framework was later validated using an external dataset supporting its application in model-based personalized medicine [168].

Buil-Bruna et al. have also established a relationship between lanreotide (i.e., a somatostatin analog) concentrations and a surrogate endpoint serum chromogranin A (CgA) in treatment-naive patients with nonfunctioning gastroenteropancreatic neuroendocrine tumors [169]. The CgA dynamics were described by a linear disease progression model where lanreotide concentrations induced a decline in CgA through an inhibitory Emax model. CgA was further linked to PFS through a parametric TTE model to describe the informative dropouts using the simultaneous estimation approach. They concluded that the decline in CgA from baseline decreases the hazard of disease progression.

Tracking the expression levels of vascular endothelial growth factor (VEGF) and soluble VEGF receptors (sVEGFR), is of interest to evaluate the antiangiogenic effects of sunitinib. Despite its high PK variability, which may cause the observed variations in response, sunitinib is administered in a fixed-dose regimen. Diekstra et al. developed a PKPD model characterizing sunitinib PK and its active metabolite SU12662, together with sVEGFR-2 and sVEGFR-3 [170]. sVEGFR-2 levels at baseline were linked to PFS, using the TTE model, in patients with mRCC. In contrast, time-varying unbound active concentration (sunitinib + SU12662) appeared to be more predictive in patients with mCRC.

Yu et al. developed a PKPD model to analyze the serum levels of thymidine kinase 1 (TK1) and the expression of phosphor-retinoblastoma protein (pRb) and Ki67 in skin tissues of advanced breast cancer patients, as influenced by palbociclib's cyclin-dependent kinase (CDK) 4/6 inhibitory action [171]. A precursor-dependent indirect response PD model described the pRb time course, whereas a similar PD model with an additional transit compartment characterized the delayed inhibitory effect on the Ki67 and TK1 response. The influence of palbociclib concentration on these biomarkers was captured using a maximal inhibition model. The exploratory analysis of the biomarker-response relationship indicated that a longer PFS correlated with lower baseline levels of TK1 and the predicted post-treatment minimum TK1 using a Cox proportional hazards model. However, these findings may require further validation through a larger-scale study.

5.3. Models integrating imaging and circulating biomarkers with a survival model

In several integrated modeling frameworks, both longitudinal changes in tumor burden and circulating tumor markers were assessed in response to the therapy and the survival probability, as illustrated in the blue box in Fig. 5.

The surveillance of decreasing CA-125 levels throughout chemotherapy has been thoroughly studied as a potential predictor of therapeutic effectiveness. However, the prognostic significance of various kinetic parameters has yielded variable results across multiple studies, and there is still no consensus on the best approach for describing the kinetics of CA-125 [172]. For this reason, Wilbaux et al. [173,174] evaluated the predictive characteristics of early changes in biomarker CA-125 for clinical benefit in ovarian cancer patients. The dynamics of CA-125 were characterized using an indirect response model that incorporated two separate production rates to represent CA-125 synthesis: one representing the basal production of CA-125 by healthy tissue and one denoting the production rate of CA-125 related to the tumor size variation. Tumor size was described by a k_G influenced by the drug, delayed by an effect compartment, and a first-order reduction denoting the rate at which tumor size diminishes. The final model accurately predicted changes in tumor size induced by chemotherapy using baseline imaging assessment and longitudinal CA-125 values only. Moreover, the model predicted relative change in CA-125 values from baseline at week 6 was a better predictor for PFS than the fractional change in tumor size. Based on the results, the authors proposed that CA-125 can serve as a biomarker for monitoring tumor size dynamics and its changes from the start of treatment can be used as an early predictive marker for PFS.

Netterberg et al. assessed the relationship between atezolizumab exposure, the dynamics of interleukin (IL)-18, interferon-inducible T-cell alpha chemoattractant (ITAC), the time course of SLD and OS in NSCLC patients [175]. Atezolizumab AUC (individual predicted, cycle-specific) was found to be related to initial SLD changes, whereas IL-18 was best associated with the duration of response. Relative change in SLD from baseline was subsequently identified as a better predictor than IL-18 for OS [176].

Netterberg et al. have also presented an integrated modeling framework of SLD, CTC counts, and OS based on data from patients with mCRC [73]. SLD(t) was found to predict the longitudinal observations of mean CTC count in 7.5 ml blood samples denoted as λ_{CTC} (t) based on count models of Poisson type. When tested as a predictor of OS, λ_{CTC} (t) described the data better than SLD(t), and no additional model-derived variable improved the model fit further once λ_{CTC} (t) was incorporated. Predictors of the final OS model also included baseline SLD and age.

For durvalumab, an immune checkpoint inhibitor, Gavrilov et al. characterized the changes in SLD and NIR dynamics under treatment and their relationship to OS in patients with NSCLC [177]. The longitudinal individual model-based predicted SLD and NIR ratio values were both found to significantly improve the prediction of OS, as compared to only baseline covariates.

Yin et al. [178] quantified the dynamics of SLD and ctDNA mutant KRAS levels in patients with mCRC treated with panitumumab to characterize the evolving tumor resistance. The mathematical model

considered various clonal populations and evolving treatment resistance. The model was used to explore new treatment schedules through simulations, such as a continuous schedule, intermittent schedules with treatment holidays, and adaptive schedules guided by ctDNA measurements to improve the treatment outcome. In contrast to the continuous treatment schedule, the simulated intermittent regimen, comprising 8 weeks of treatment followed by a 4-week suspension, extended the median PFS of the simulated population from 36 to 44 weeks. The duration during which the tumor size remained below the baseline level increased from 52 to 60 weeks. However, elongating the treatment break led to suboptimal outcomes.

Therapeutic cancer vaccines represent innovative immunotherapies designed to enhance clinical outcomes when combined with other immunotherapeutic approaches. Nevertheless, challenges persist in their successful clinical development, which could be tackled through MIDD strategies. Ibrahim et al. integrated different clinical responses to UV1, a human telomerase reverse transcriptase-based peptide cancer vaccine candidate, in a single framework to explore different scenarios related to the dosing schedules [179]. The framework characterized SLD measurements and UV1-specific immunological assessments collected from a phase I trial on NSCLC patients and a phase I/IIa trial on malignant melanoma patients. The final structure included a mechanistic tumor growth dynamics model considering the interaction between the vaccine peptides, the immune system, and the tumor, a model describing the likelihood of observing a UV1-specific immune response, and a TTE model for OS. The model-predicted UV1-specific CD4 + T cells increased the probability of observing an immune response in the peripheral blood. The high baseline SLD and relative change from nadir reduced OS in NSCLC and malignant melanoma patients, respectively. The model's forecasts indicated that extending UV1 administration for longer durations, with additional maintenance doses, could lead to a more sustainable reduction in tumor size. This case exemplifies the convergence of QSP and pharmacometrics. This type of synergy will become increasingly crucial in the innovation and advancement of intricate therapeutic approaches and novel mechanisms within cancer immunotherapy.

5.4. Models integrating safety biomarkers with/without a survival model

The sections above have mainly focused on models designed to capture drug efficacy through endpoints such as tumor size changes, PFS, and OS. However, drug safety is another important application of model-based analyses. Myelosuppression is one of the most common side effects of chemotherapy, characterized by a reduction in the production of blood cells. Quartino et al. [180] characterized the time courses of the leukocytes and the neutrophils simultaneously to improve the predictive ability of the myelosuppression model previously developed by Friberg et al. [88]. The final structure comprised a neutrophil model and a non-neutrophil model. Both were structured similarly to the original semi-mechanistic myelosuppression model with refinements such as an optimized number of transit compartments for the two cell types. The leukocytes were derived as the sum of the predicted neutrophils and non-neutrophils. The model provided more accurate forecasts regarding the trajectory of neutrophil counts. Integrating both cell types could help elucidate distinctions between them and enable the prediction of neutrophil counts solely from leukocyte measurements.

As granulocyte colony-stimulating factor (G-CSF) is the main regulating factor of neutrophils, an integrated model was developed to describe the inverse correlation between the dynamics of endogenous G-CSF and ANC following adjuvant chemotherapy [181]. The integrated model identified two effects of elevated G-CSF levels on ANC: enhancing ANC proliferation rate and decreasing the ANC average bone marrow maturation time. G-CSF was described by a turnover model in which the elimination rate was induced by the level of ANC in the blood circulation. The model supported the self-regulatory mechanism of the system.

Netterberg et al. evaluated the ability of IL-6 and C-reactive protein (CRP) to predict the development of febrile neutropenia following adjuvant chemotherapy of breast cancer [90]. The biomarkers were described by turn-over models, while the occurrence of febrile neutropenia was quantified using a parametric TTE model. The time course of IL-6 was the best predictor for forecasting febrile neutropenia events, while the time course of CRP was most closely related to febrile neutropenia. However, because the CRP peak typically occurs at the time of diagnosis of febrile neutropenia, it will be of limited use in determining the need for preventive treatment.

5.5. Integrated efficacy and safety models

Drug safety is a main driver of tolerance and compliance in oncology, where adverse effects often lead to treatment pause or dose reduction, as such, it needs to be integrated with efficacy analysis via model-based analyses. Nevertheless, safety and efficacy evaluations have traditionally been treated as separate entities. The integration of these endpoints in modeling offers a comprehensive method for dose-exposure–response analysis. Integrated frameworks containing both safety and efficacy endpoints, illustrated in the gray box in Fig. 5, can facilitate dose optimization through a quantitative benefit-risk assessment, particularly vital in oncology, to balance treatment advantages against risks, significantly affecting patient outcomes and quality of life.

Hansson *et al.* published two companion articles where a modeling framework was established linking sunitinib exposure, tumor growth over time, longitudinal PD biomarkers (i.e., VEGF, sVEGFR-2, sVEGFR-3, soluble stem cell factor receptor (sKIT)), safety endpoints (fatigue, hand-foot syndrome, neutropenia, and hypertension) and OS [78,81]. The longitudinal PD biomarkers and the changes in diastolic blood pressure over time were described by indirect response models where drug dose or individual model predicted sunitinib AUCs were driving the effect. Discrete-time Markov models described the time course of hand-foot syndrome and fatigue, whereas a semi-physiological myelosuppression model captured changes in ANC. The analysis found that neutropenia, hand-foot syndrome, and fatigue were best predicted by relative changes in sVEGFR-3 from baseline, whereas blood pressure was most closely related to sunitinib daily AUC. OS was predicted equally well by relative changes in sVEGFR-3 from baseline with baseline tumor size, and the time course of ANC in combination with the relative increase of diastolic blood pressure from baseline. The framework was utilized in a simulation study by Centanni et al., evaluating the effect of various dose regimens and dose individualization methods on treatment safety and efficacy [182]. The results suggested that initial dosing at 37.5 mg daily in combination with dose individualization based on ANC or changes in sVEGFR-3 would result in the best gain in terms of efficacy whilst maintaining an appropriate safety level. When the cost-effectiveness of dose adjustments based on therapeutic drug monitoring, ANC(t) or changes in sVEGFR-3 were compared, sVEGFR-3 was found to require the lowest costs per quality of life adjusted life years gained [183].

Schindler et al presented a PKPD modeling framework linking axitinib exposure, longitudinal PD biomarkers (i.e., sVEGFR-1, −2, −3, sKIT), SLD, diastolic blood pressure and OS in mRCC [184]. Through indirect response models, the axitinib AUC stimulated blood pressure production, inhibited sVEGFR-1–3 production, and inhibited VEGF degradation, while no drug effect was found for sKIT. Model-predicted individual relative change of sVEGFR-3 from baseline was found to be a predictor of SLD response, and in turn, the SLD time course was a significant predictor of OS. A subsequent simulation study explored the impact of different dosing strategies and individualization methods [183]. The results indicated that individual model-based biomarker estimations based on clinical biomarker measurements generally could predict dose adjustments with equal or greater accuracy than single clinical biomarker measurements, suggesting the potential usefulness of these biomarkers in guiding dose modifications.

Xu *et al.* [49] evaluated the relationship between guadecitabine

treatment and several clinical outcomes using either guadecitabine dose, summary exposure metrics, and concentration–time profiles. Guadecitabine dose was connected to a myelosuppression dynamic model through a K-PD model with an inhibitory sigmoid Emax relationship. The concentration–time profile of the active metabolite decitabine was linked to the time course of the mechanism-related PD biomarker LINE-1 demethylation in an indirect response model through an Emax relationship. Using logistic regression, the ability to use the individual systemic exposure metrics of decitabine or LINE-1 dynamics in predicting clinical response (yes/no) was explored. While exposure–response relationships for efficacy were not discernible with the explored metrics of decitabine exposure, relationships between the maximum LINE-1 demethylation effect and probability of clinical response could be characterized. Using the final models for simulations, the effects of different dosing regimens on LINE-1 demethylation and ANCs were evaluated. Based on the results, the 5-day regimen of 60 mg/m2 was selected due to less severe neutropenia and more complete recovery compared to the other evaluated regimens.

Irurzun-Arana et al. built a semi-mechanistic model to explore the relationship between LDH, the melanoma-inhibiting activity, and the calcium-binding protein S100B levels and their relation to PFS and OS in advanced melanoma patients treated with adjuvant high dose interferon-α2b [185]. Their framework additionally involved characterizing the dynamics of the ANC to analyze the benefits and toxic effects simultaneously. A K-PD modeling approach was used to quantify the relationship between the dosing rate of interferon and the biomarkers dynamics. They identified the relative change from the baseline of LDH as the only predictor of OS.

Wilbaux *et al.* [186,187] quantified the relationships between roblitinib C(t) and longitudinal changes in the efficacy biomarkers 7α-hydroxy-4-cholesten-3-one (C4), fibroblast growth factor (FGF19) and the safety biomarker alanine transaminase (ALT) using indirect response models, and SLD dynamics with TGI model. A composite predictive risk score, derived from a set of 75 baseline patient characteristics based on ML techniques, was included as a covariate of the TGI model. C_{trough} was identified as a predictor for TTP in K–M and log-rank analyses. Through simulations, the modeling framework was used to compare different dose levels (50, 80, 120, and 150 mg) under fasted and fed conditions. The results supported a dosage selection of 120 mg once daily, either while fasting or with a low-fat meal, achieving a C_{trough} greater than the concentration resulting in 90 % inhibition for most participants. Consequently, the expansion cohort of the First-in-human study of roblitinib was initiated with the selected dosage.

Srimani et al. [85] developed a modeling framework integrating individual patient ixazomib exposure, the occurrence and grades of rash and diarrhea, platelet counts over time, changes in M−protein over time, time to relapse and PFS in patients with MM receiving ixazomib in combination with lenalidomide and dexamethasone. Longitudinal observations of diarrhea and rash grades were described by discrete-time Markov Models, in which the transition rates from grade 0 were driven by ixazomib weekly AUC. A semi-mechanistic hematopoietic model described the time course of platelets, where the combined effect of ixazomib C(t) and weekly AUC, in addition to the effect of a hypothetical effect site lenalidomide concentration $C_{eff}(t)$, drove the changes in the maturation rate of platelets through a linear function describing the effects on depletion of the platelet precursor pool. A two-population indirect response model with sensitive and resistant subpopulations at baseline described total M−protein. Herein, ixazomib C(t) inhibited the zero-order production rate of sensitive M−protein, but did not affect the growth rate of the resistant subpopulation. The time to disease relapse was predicted by ixazombib C(t) and the growth rate of the drug-sensitive subpopulation (k_R) of the M−protein model. The PFS was predicted by ixazomib weekly AUC, M−protein (t), M−protein nadir, and k_R. Potential applications of the model were suggested to be trial simulations and exploration of alternative dosing regimens.

An integrated NLME analysis of belantamab mafodotin, a monoclonal ADC targeting B-cell maturation antigen, has been performed by Collins et al. [87]. Individual C(t) profiles were linked to changes in M−protein concentration and grades of ocular ADs described by discrete-time Markov Models. The models were used for simulations of efficacy and safety endpoints under various doses and intervals, where dose reductions during toxicity were allowed, and dropout from M−protein assessments was assumed to be solely due to disease progression. Simulations predicted a lower probability and overall time with grade 3 + and 2 + ocular events for lower doses and longer dosing intervals, compared with the approved regimen (2.5 mg/kg Q3W), with a less than proportional reduction in efficacy.

The relationship between ibrutinib exposure (daily $AUC_{0\text{-}24}$) and the sum of the product of perpendicular diameters (SPD) of lymph nodes, leukocytes, and blood pressure changes in CLL patients has been assessed by Ibrahim et al. [77]. The ultimate framework (Fig. 6) comprised (i) an integrated model for SPD and leukocytes, encompassing four CLL cell subpopulations with ibrutinib inhibiting phosphorylated BTK production included as a latent variable, (ii) a turnover model wherein ibrutinib triggers an elevation in blood pressure, and (iii) a competing risk model for dropout and mortality. The past model-predicted individual leukocyte count and SPD of lymph nodes were predictors in the multistate model describing competing risks between dropout and death. Simulations showed that in comparison to the approved dosing schedule (420 mg/day), the de-escalation schedules (420 mg/day for cycle 1, then 280 mg/day and 420 mg/day for cycle 1, 280 mg/day for cycle 2, and then 140 mg/ day) exhibit a slightly lower PFS (defined as $\geq$ 50 % increase from nadir in SPD with or without leukocytosis), with an average reduction of approximately 20 % in the proportion of patients experiencing hypertension.

6. Integrated modeling frameworks in oncology drug development: Dosage optimization

Recognizing the drawbacks of the MTD approach, the FDA launched Project Optimus in 2021 to reform the dose selection and optimization paradigm in oncology [188]. This initiative emphasizes a comprehensive understanding of dose-exposure–response dynamics, shifting the emphasis from treating at or near the MTD to selecting a dose level and schedule that optimizes the long-term benefit-to-risk ratio while ensuring adequate multi-cycle tolerability to maintain patient quality of life [12,189]. Consequently, we anticipate an increased role for models that integrate efficacy, safety, and tolerability through drug exposure in supporting the selection of dose levels and schedules that maximize long-term benefits, as highlighted in the FDA's most recent guidance on optimizing oncology drug dosage (published August 2024) [190].

Under the evolving paradigm in oncology clinical development, evidence supporting the optimal dose selection is iteratively generated based on the totality of supporting preclinical data and data from phase I to II studies (e.g., dose expansion cohorts in a randomized dose optimization assessment) [191]. This evidence informs dosage selection in pivotal clinical development. A totality-of-evidence approach builds confidence throughout the development lifecycle by ensuring consistency across multiple methods and relevant data sources. These elements are proactively integrated and used to guide decision-making through iterative modeling and simulation [192]. Alternative trial design and analysis methodologies may also be required for improved dose optimization during clinical development.

It is expected that through Project Optimus, dose-finding will continue in phase II trials or in prospectively designed dose optimization expansion cohorts towards the end of the escalation in phase I trials, comparing at least two dose levels, preferably in a randomized, parallel design within a specific indication. Integration of data generated from phase I and II studies will further increase confidence in the benefit and risk profiles, helping to define an optimal dosage regimen for phase III that can subsequently be recommended for approval. In this context, pharmacometric methods can play a crucial role through integrated

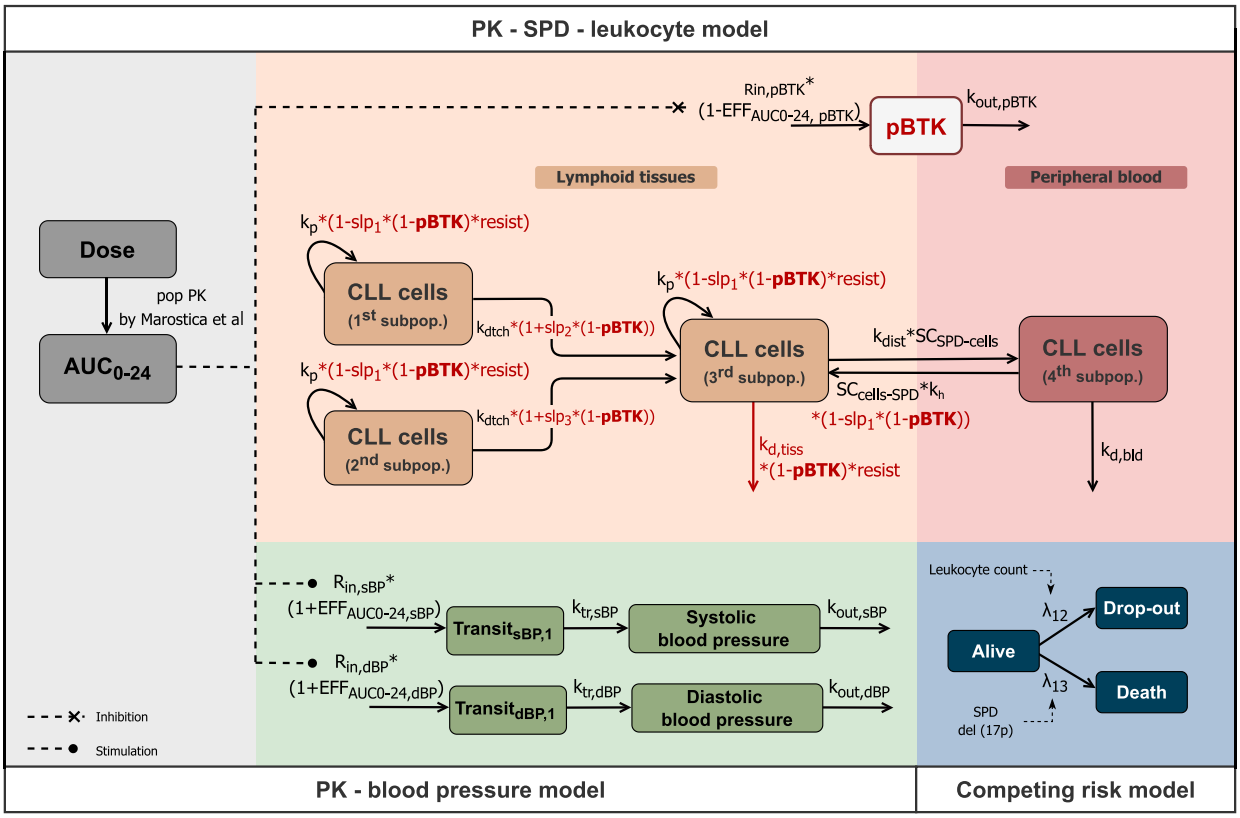

Fig. 6. Schematic representation of the semi-mechanistic PKPD modeling framework for ibrutinib in CLL patients, integrating two efficacy measurements (leukocyte count and sum of product of perpendicular diameters of lymph nodes (SPD)), hypertension toxicity measurements (systolic and diastolic blood pressures) in addition to the competing risk of drop-out and death. Leukocyte count was calculated as the sum of the CLL cells in peripheral blood (4^{th} subpopulation) and the estimated normal leukocyte number in peripheral blood divided by blood volume, while SPD was calculated as the sum of the three subpopulations of CLL cells in lymphoid tissues and the estimated normal lymph node size. Abbreviations: pBTK, phosphorylated Btk; sBP, systolic blood pressure; dBP, diastolic blood pressure; R_{in}, zero-order production rate; k_{out}, turn-over rate constant; k_{tr}, transition rate constant; $EFF_{AUC0-24}$, AUC_{0-24} effect; resist, resistance development; k_p, proliferation rate constant; k_h, homing rate constant; k_{dtch}, detachment rate constant; k_{dist}, re-distribution rate constant; $SC_{cells-SPD}$ and $SC_{SPD-cells}$, scaling factors for translating from CLL cell count to SPD and vice versa, respectively; $k_{d,bld}$, natural death rate constant; $k_{d,tiss}$, ibrutinib-induced death rate constant; slp_1, slope of ibrutinib-induced inhibitory effect on k_p and k_h; slp_2 and slp_3, slopes of ibrutinib-induced stimulatory effect on k_{dtch} of 1^{st} and 2^{nd} subpopulations of CLL cells, respectively, from stroma; λ_{12}, transition rate constant from alive to drop-out state; λ_{13}, transition rate constant from alive to death state. Reprinted from [77].

benefit-risk longitudinal models [193,194], given their capacity to generate evidence for dose and dosing schedule optimization as early as within the First In Human study. One example of such an application is detailed in section 5.5, where the integration of PK, efficacy, and safety data supported the selection of the recommended phase II dose (RP2D) of roblitinib in hepatocellular carcinoma patients [186].

As described in this review, the longitudinal measurements of tumor burden can be characterized using tumor kinetic population PKPD modeling methods. We advocate for the model building to initially be based on dose escalation data (e.g., longitudinal SLD) and associated systemic exposures as well as data from the backfill and/ or expansion cohorts. Model-informed decision-making during early clinical phases is particularly valuable when dose escalation is performed in a relatively homogeneous patient population, expected to show dose/exposure-related antitumor effects due to the pharmacological properties of the investigational drug [195]. Examples of such cases include targeted therapies such as receptor tyrosine kinase inhibitors, studied in patients whose cancers are identified as being driven by specific oncogenes [75,77], or ADCs in patients with cancers with known high expression of the target antigen and an expected sensitivity to the payload's mechanism of action [196]. Depending on the tumor type and measurement methods employed, more than one biomarker can be used to inform the model development, including tumor size (e.g., SLD), molecular measurements (e.g., variant allele fraction in ctDNA), or tumor-specific markers. As the dataset grows, the precision in model parameters will improve with iterative model updates. By the end of phase I, it will be possible to begin simulating from the models to project performance characteristics of a range of candidate doses and dosing schedules to inform further dose optimization/ selection strategies. Indeed, proactive integration of population PK/tumor kinetic models has been valuable in dose selection decisions for several recently approved anticancer agents, including asciminib in chronic myeloid leukemia [75], isatuximab in MM [152,195], and selpercatinib in RET fusion-positive NSCLC [189].

Integrated models that include the most relevant safety endpoints can facilitate the selection of an appropriate dose range to maximize efficacy while ensuring the right level of multi-cycle tolerability for the intended patient population. There exists a range of mechanism-based models tailored for hematological toxicities like neutropenia, thrombocytopenia, anemia, and lymphopenia. The strength of such models lies in their ability to predict the performance of alternative dosing regimens, especially over extended treatment periods, as well as to generate hypotheses for feedback individualization of dosing [197]. In particular, for toxicities such as anemia, hemoglobin measurements in Cycle 1 may not accurately reflect the severity of anemia that could develop with continued dosing, given the lifespan of red blood cells. Simulations using semi-mechanistic models, integrating intermediate compartments (e.g., reticulocyte measurements) [198,199], are valuable for predicting safety across multiple treatment cycles. They can also guide dose optimization planning in early clinical development based on a short duration of dosing while considering the long-term maturation process

of the blood cells [199]. For graded categorical toxicities (e.g., rash, diarrhea, mucositis), longitudinal models characterizing the underlying exposure–response relationships can also be very valuable, even though the level of mechanistic resolution in models for such toxicities is often lower than that for hematological toxicities.

Simulations from models describing multiple variables over time can be used to interrogate non-traditional dosing approaches that are not static but involve titration dosing, as evaluated with ixazomib for the maintenance therapy of transplant-ineligible MM [200], or response-adaptive dosing, as evaluated with ponatinib for the treatment of chronic myeloid leukemia [201], to maximize patient-focused benefit-risk ratio. Integrated models of efficacy and safety endpoints enable simulations of dose interruption and reduction due to safety concerns, resulting in a reduction in efficacy. This approach was applied to belantamab mafodotin, an ADC used to treat MM, as detailed in Section 5.5 [87]. Clinical Utility Index approaches can be applied to maximize the benefit-risk balance, as demonstrated in dose optimization analyses conducted for copanlisib in NHL [202], ipatasertib in prostate cancer [203], and venetoclax in MM [204].

Developing models for combination therapies presents significant challenges due to limited clinical data that evaluate different dosing schedules of the component drugs both as single agents and in combination [205]. Indeed, for defining combination therapies, there may be an even greater gain from integrating data from various sources, including preclinical studies, early-phase trials, and real-world evidence, to build a comprehensive modeling framework where PK and PD interactions between multiple drugs are quantified. For instance, a PKPD modeling framework supported the selection of the isatuximab dosing regimen in relapsed/refractory MM patients [195]. The framework was built in steps as more data became available from phase I clinical trials on single-agent and combination therapy. Model-based simulations for evaluating efficacy supported the use of isatuximab at a dosing regimen of 10 mg/kg QW4-Q2W in combination with pomalidomide and dexamethasone in the phase III trial. Ensuring the accuracy and reliability of models developed for combination therapies is however challenging and the individual patient variability in drug response can become more pronounced in the context of multiple interacting agents. Model-based adaptive optimal design emerges as a promising tool for dose-finding studies involving combination treatments. In this approach, prior information is updated based on interim analyses as more data become available, allowing adjustments to doses and dosing schedules to be made in an informative way throughout the trial [206]. The developed modeling frameworks enable the identification of the optimal dosage for each component drug in the combination therapy to achieve the desired therapeutic effect while minimizing side effects. In an interim analysis, the integrated modeling frameworks could support decisions on halting a trial due to toxicity if the probability of toxicity is high.

7. Integrated modeling frameworks in oncology drug development: Patient-focused development strategies

Although the reviewed examples of integrated modeling have not yet incorporated models for patient-focused variables, integrating these models could greatly enhance the evaluation of treatments from the patient's perspective. Patient-reported outcomes (PROs) are increasingly measured to assess the symptomatic and functional impacts of disease and treatment on patients' quality of life, especially over prolonged treatment durations. [207]. We anticipate increased modeling and integration of PROs in the future, as suggested by the FDA's guidance on oncology dose optimization, which encourages the inclusion of PROs to improve the assessment of tolerability in early-phase dose-finding trials [190].

PROs, such as the PRO-Common Terminology Criteria for Adverse Events (PRO-CTCAE), can provide an early understanding of the impact of adverse effects of an investigational agent on overall tolerability from the patient's perspective [208]. Their utilization in dose optimization trials, as part of the totality of evidence for informing dose selection, is an emerging area with ongoing research in oncology drug development [193]. Early experience with these tools is encouraging. For example, PRO-CTCAE measurements may be useful for describing exposure–response relationships for patient-reported assessments of the impact of AEs, such as diarrhea, on overall quality of life. This complements CTCAE-based investigator-assessed measurements of AE severity in dose optimization evaluations [209].

When AEs that directly impact a patient's well-being and quality of life are observed or expected with long-term administration, based on early investigator-assessed data from the dose escalation phase of a first-in-human study, subsequent randomized dose optimization studies should focus on collecting PRO-CTCAE data for specific AE items/domains for exposure–response analyses. Examples of such AEs include anemia (potentially resulting in fatigue), diarrhea (impacting daily activities), and mucositis (affecting nutrition and overall quality of life). Exposure-response analyses of such targeted PRO-CTCAE domain data, together with efficacy and safety analyses, should enable a comprehensive approach to dose selection for pivotal trials. This ensures that considerations regarding long-term tolerability from a patient perspective are integrated, minimizing unexpected issues at the end of phase III regarding the overall tolerability of the selected starting dosage.

While PRO-CTCAE focuses on assessing treatment tolerability, other tools are designed to evaluate overall health-related quality of life (HRQoL). For example, the Functional Assessment of Cancer Therapy-General (FACT-G) examines four key domains: physical, social/family, emotional, and functional well-being, offering a comprehensive view of how cancer and its treatment affect patients' daily lives. Integrating HRQoL data into modeling frameworks facilitates the identification of patient subgroups with differential treatment outcomes and supports personalized medicine approaches. As an initial attempt, a PKPD framework based on item response theory has been developed to support the evaluation of covariate and exposure effects on FACT-Breast in patients with breast cancer [210]. Moreover, as healthcare decision-makers increasingly consider patient-centered outcomes and cost-effectiveness in their evaluation of treatment value and affordability, models that integrate HRQoL would have the potential to enhance informed decision-making in healthcare.

Another opportunity for quantitative methods to enable patient-focused oncology drug development lies in making clinical trials more inclusive. The American Society of Clinical Oncology, Friends of Cancer Research, and the FDA have actively discussed the rational expansion of eligibility criteria in oncology trials, resulting in position papers and regulatory guidelines to support this effort [211–213]. It is widely acknowledged that the rationale for exclusion criteria in oncology trials may often be poorly conceived. For instance, Liu et al. observed significant inter-trial variability in inclusion criteria in an analysis of clinical trials of immune checkpoint inhibitors for advanced non-small cell lung cancer based on analyzing Real World Data in the Flatiron Health Electronic Health Records database [214]. The authors conducted clinical trial simulations to evaluate more inclusive trial designs, demonstrating *in silico* that broadening eligibility criteria (i.e., including more women and patients over 75 years of age) could be feasible without negatively affecting the hazard ratio for survival benefit or increasing AE-related treatment discontinuations.

8. Integrated modeling frameworks in oncology drug development: Enabling emerging biomarkers

Oncology research has experienced a profound transformation driven by breakthroughs in biomarker discovery, especially with the growing understanding of the hallmarks of cancer [5]. Accordingly, a substantial proportion of the reviewed articles demonstrated a systematic approach to incorporating retrospective longitudinal biomarkers with survival data to identify early predictors of OS, thereby supporting future study design and data analysis [78,81]. As an example, Bruno

et al., through integrating the dynamic of tumor burden (i.e., SLD) dynamics with OS, demonstrated that model-based estimates of TGI metrics are more effective than ORR or PFS in differentiating successful from unsuccessful outcomes in phase III trials [215]. This finding supports the usage of TGI metrics as exploratory endpoints to inform early clinical decision-making. We anticipate that as new biomarkers emerge, the growth and application of integrated models will continue to expand, shaping future research and development strategies in oncology.

As the field continues to evolve, advances in molecular measurements of disease burden are becoming increasingly important in enhancing the predictability of survival. For example, ctDNA measurement has emerged as a powerful, minimally invasive tool that can detect residual disease after definitive treatment or surgery, monitor the effectiveness of ongoing therapy, and identify molecular relapse during post-treatment surveillance across a wide range of cancers [216]. ctDNA can be measured both quantitatively and qualitatively (i.e., genetic characteristics) in "liquid biopsies". It is a valuable biomarker for molecular diagnosis and treatment selection. The FDA Draft Guidance on the use of ctDNA highlights the potential for leveraging the on-treatment dynamics of ctDNA to detect drug activity signals in early-stage drug development for solid tumors [217]. By integrating ctDNA into tumor dynamic models, researchers can gain a deeper understanding of the evolution of drug resistance, paving the way for more effective treatment strategies and improved outcomes [178,218]. MIDD based on integrated models incorporating ctDNA presents three key opportunities. First, baseline ctDNA biomarker data (e.g., mutational profile) can be used as a covariate to describe tumor size changes, guiding precision medicine [218]. Subsequent simulations can enable in-silico assessment of patient selection or enrichment hypotheses with greater precision. The second opportunity is for signal-finding in early-stage trials. A significant treatment effect observed in a model for longitudinal ctDNA may serve as a proof-of-principle [158]. Simulations from such models can inform dose and schedule optimization plans for later phase studies [178]. The third opportunity is to leverage pharmacometric models linking ctDNA dynamics to long-term survival outcomes (e.g., PFS, OS), aiming to assess ctDNA-based measurements of antitumor activity as predictors of clinical outcomes. While much research has focused on the statistical association, as seen in cross-study analyses of NSCLC patients receiving immune checkpoint inhibitor therapy [219], opportunities exist for pharmacometric disease progression modeling (e.g., joint modeling of ctDNA and survival outcomes) [159].

While the landscape of immunotherapies continues to develop, there is a growing need for integrated systems pharmacology and population PKPD models, known as population QSP models. These models can account for dynamic immune events throughout the cancer immune cycle [220]. Examples of population QSP models detailed in section 5 include models for CAR-T cell therapy for NHL [166] and for human telomerase reverse transcriptase-based peptide cancer vaccine for patients with NSCLC and malignant melanoma [179]. Understanding these dynamics helps to identify the biological and treatment-related factors responsible for the observed variability in antitumor effects. This modeling approach can help select optimal combinations and sequences of various anticancer immunotherapies to maximize antitumor responses [221].

Generally, (semi-) mechanistic integrated modeling frameworks aim to provide drug- and mechanism-independent mathematical formulations of disease trajectory that quantify the disease-specific linkage between the dynamics of tumor burden (e.g., tumor size) and survival outcomes (e.g., OS). However, it should be noted that today's cancer biology, influenced by molecular diagnostics, targeted therapies, and immunotherapy, may differ significantly from the past (e.g., the pre-immunotherapy era). To this end, it is important to include contemporaneous data, ideally from treatments with related mechanisms of action, in the development and maintenance of these frameworks during the model development lifecycle. This is necessary for confidence in the fidelity of model-based predictions of survival outcomes and probability of success in phase III trials. For example, a recent analysis [222] evaluated the ability of two previously published NSCLC disease models to predict OS outcomes in a randomized clinical trial of the PD-L1 antibody sugemalimab added to chemotherapy versus placebo plus chemotherapy. This analysis demonstrated superior performance characteristics of a recently developed tumor kinetics-OS model built on data collected in clinical trials of another PD-L1 antibody atezolizumab [127], compared to a seminal NSCLC tumor kinetics-OS model that was built on a diverse and comprehensive dataset of cytotoxic and targeted agents collected from trials that were completed in the pre-immunotherapy era [66]. These considerations can be particularly relevant in global drug development, as there can be regional variations in drug- and disease-related intrinsic and extrinsic factors. Simulations from frameworks built on comprehensive contemporaneous global clinical trial data and real-world data can be valuable in optimizing the design of pivotal multi-regional clinical trials by applying ICH E17 principles [223]. Such model-informed designs can enable efficiency in evidence generation while adequately mitigating the impact of regional heterogeneity (i.e., through covariate analyses in disease models based on multiregional clinical trials) [224].

Integrating multi-dimensional covariate information to address variability at molecular (e.g., genomic, transcriptomic) and imaging (e.g., radiomic) levels can benefit from methodologies beyond traditional methods, introducing a new era of machine intelligence-assisted pharmacometrics [225–228]. For biomarker data such as next-generation sequencing-based ctDNA analysis, transcriptomic assessments, digital pathology readouts, or radiomics signatures of heterogeneity, the number of covariates can often exceed the practical limits of standard covariate modeling methods in the classical NLME software. As such, ML-assisted covariate analyses can complement traditional methods or act as a "filter" to prioritize covariates for formal evaluation in population PKPD models. ML-enabled pharmacometrics is rapidly emerging, with recent examples in tumor kinetic and survival models providing a proof-of-principle for methodology at the intersection of ML and pharmacometrics [135,187,229–231]. The seamless integration of these methods into pharmacometrics workflows is foreseen as a key enabler for precision medicine, fully exploiting advances in multi-modal biomarker technologies. These models demonstrate superior performance in capturing nonlinear relationships between predictors and hazard functions compared to Cox regression models [232]. While this review focuses on clinical applications of integrated pharmacometric models, it is important to note that oncology drug development relies on preclinical tumor growth inhibition studies of patient-derived tumor xenografts for hypothesis generation regarding patient selection and combination therapies. In these studies, extensive molecular characterization can correlate multi-dimensional predictive biomarker profiles to tumor growth inhibition efficacy, identifying biological pathways associated with IIV in treatment response or resistance development. Integrating ML methods for covariate analyses in translational pharmacometrics models represents another promising application to advance precision medicine hypothesis generation and for identifying predictive gene expression profiling-based signatures for efficacy and toxicity outcomes, thereby enhancing the mechanistic value of these models [226,233].

9. Concluding remarks

In summary, this review offers a comprehensive overview of integrated modeling approaches in oncology. It emphasizes frameworks that integrate longitudinal data from diverse PD variables, including biomarkers, safety outcomes, and survival. We anticipate this review to be a valuable resource for the future application of integrated models in the rapidly evolving field of MIDD in oncology, providing insights into current methodologies and emerging opportunities for applying these advanced techniques.

We are in the initial stages of applying integrated models in oncology drug development, and some obstacles remain in creating an accurate

timeline for MIDD deliverables based on this approach due to the difficulties associated with developing and validating mathematical models and the need for adequate computational resources, especially as datasets grow iteratively. Additionally, the complexity of integrated analyses necessitates that pharmacometricians possess the skills to communicate modeling and simulation results, including the sub-models' limitations and assumptions. Ensuring data quality is also a critical concern, with potential issues stemming from study design and data collection practices.

Nevertheless, the use of integrated modeling approaches in oncology MIDD is expected to increase as a consequence of factors including (1) rapidly advancing new anticancer modalities and mechanisms of action with inherent complexity necessitating multi-dimensional therapeutic optimization, (2) need for increased efficiency and success rates in drug development, (3) increased regulatory attention to treatment optimization before approval, (4) emergence of various informative biomarkers, with different dynamics, requiring advanced analyses, (5) advances in ML approaches [234], automated model building tools [235], and extensive computing power and, (6) growing number of trained quantitative scientists across diverse disciplines, including QSP, pharmacometrics, and biostatistics, who can contribute to MIDD analyses. These approaches can anticipate the therapeutic outcomes and patterns that real-world data might exhibit, such as toxicity variations with dosage alterations. They can also offer insights into treatment effects on patients' well-being and quality of life. Ultimately, they can facilitate a deeper understanding of complex biological relationships, potentially enhancing the extrapolation of short-term trial findings to long-term patient outcomes.

Funding

This work was supported by the Swedish Cancer Society [grant number 20 1226 PjF and 23 2921 Pj].

Declaration of competing interest

The authors declare that they have no known competing financial interests or personal relationships that could have appeared to influence the work reported in this paper.

Acknowledgments

We would like to acknowledge Martin Bergstrand, Pharmetheus AB, for input on a draft version of the manuscript, and Tamara Ray, Uppsala University, for proofreading the final version of the manuscript.

Data availability

No data was used for the research described in the article.

References

[1] F. Bray, M. Laversanne, H. Sung, J. Ferlay, R.L. Siegel, I. Soerjomataram, A. Jemal, Global cancer statistics 2022: GLOBOCAN estimates of incidence and mortality worldwide for 36 cancers in 185 countries, CA Cancer J. Clin. 74 (2024) 229–263. Doi: 10.3322/caac.21834.

[2] J.A. DiMasi, H.G. Grabowski, R.W. Hansen, Innovation in the pharmaceutical industry: New estimates of R&D costs, J. Health Econ. 47 (2016) 20–33, https://doi.org/10.1016/j.jhealeco.2016.01.012.

[3] J. Rotow, T.G. Bivona, Understanding and targeting resistance mechanisms in NSCLC, Nat. Rev. Cancer 17 (2017) 637–658, https://doi.org/10.1038/nrc.2017.84.

[4] I. Dagogo-Jack, A.T. Shaw, Tumour heterogeneity and resistance to cancer therapies, Nat. Rev. Clin. Oncol. 15 (2018) 81–94, https://doi.org/10.1038/nrclinonc.2017.166.

[5] D. Hanahan, Hallmarks of cancer: New dimensions, Cancer Discov. 12 (2022) 31–46, https://doi.org/10.1158/2159-8290.CD-21-1059.

[6] B. Seruga, A. Ocana, E. Amir, I.F. Tannock, Failures in phase III: Causes and consequences, Clin. Cancer Res. 21 (2015) 4552–4560, https://doi.org/10.1158/1078-0432.CCR-15-0124.

[7] M. Schlander, K. Hernandez-Villafuerte, C.-Y. Cheng, J. Mestre-Ferrandiz, M. Baumann, How much does it cost to research and develop a new drug? A systematic review and assessment, Pharmacoeconomics 39 (2021) 1243–1269, https://doi.org/10.1007/s40273-021-01065-y.

[8] K. Venkatakrishnan, P. Jayachandran, S.K. Seo, P.H. van der Graaf, J.A. Wagner, N. Gupta, Moving the needle for oncology dose optimization: A call for action, CPT Pharmacometrics Syst. Pharmacol. (2024), https://doi.org/10.1002/psp4.13157.

[9] P. Soltantabar, H.-K. Lon, K. Parivar, D.D. Wang, M. Elmeliegy, Optimizing benefit/risk in oncology: Review of post-marketing dose optimization and reflections on the road ahead, Crit. Rev. Oncol. Hematol. 182 (2023) 103913, https://doi.org/10.1016/j.critrevonc.2023.103913.

[10] W.M. Hryniuk, More is better, J. Clin. Oncol. 6 (1988) 1365–1367, https://doi.org/10.1200/JCO.1988.6.9.1365.

[11] A. Papachristos, J. Patel, M. Vasileiou, G.P. Patrinos, Dose optimization in oncology drug development: the emerging role of pharmacogenomics, pharmacokinetics, and pharmacodynamics, Cancers 15 (2023), https://doi.org/10.3390/cancers15123233.

[12] M. Shah, A. Rahman, M.R. Theoret, R. Pazdur, The drug-dosing conundrum in oncology - When less is more, N. Engl. J. Med. 385 (2021) 1445–1447, https://doi.org/10.1056/NEJMp2109826.

[13] C.J. Peer, B.L. Heiss, D.A. Goldstein, J.C. Goodell, W.D. Figg, M.J. Ratain, Pharmacokinetic simulation analysis of less frequent nivolumab and pembrolizumab dosing: Pharmacoeconomic rationale for dose deescalation, J. Clin. Pharmacol. 62 (2022) 532–540, https://doi.org/10.1002/jcph.1984.

[14] V.M. Patil, V. Noronha, N. Menon, R. Rai, A. Bhattacharjee, A. Singh, K. Nawale, S. Jogdhankar, R. Tambe, S. Dhumal, R. Sawant, M. Alone, D. Karla, Z. Peelay, S. Pathak, A. Balaji, S. Kumar, N. Purandare, A. Agarwal, A. Puranik, A. Mahajan, A. Janu, G. Kumar Singh, N. Mittal, S. Yadav, S. Banavali, K. Prabhash, Low-dose immunotherapy in head and neck cancer: A randomized study, J. Clin. Oncol. 41 (2023) 222–232, https://doi.org/10.1200/JCO.22.01015.

[15] S. Marolleau, A. Mogenet, C. Boeri, M. Hamimed, J. Ciccolini, L. Greillier, Standard atezolizumab leads to severe overexposure in real-world patients with lung cancer: How far could we go in extending dosing intervals and saving money? J. Clin. Oncol. 42 (2024) 3085, https://doi.org/10.1200/jco.2024.42.16_suppl.3085.

[16] Y. Ji, J.Y. Jin, D.M. Hyman, G. Kim, A. Suri, Challenges and opportunities in dose finding in oncology and immuno-oncology, Clin. Transl. Sci. 11 (2018) 345–351, https://doi.org/10.1111/cts.12540.

[17] R. Gieschke, J.L. Steimer, Pharmacometrics: Modelling and simulation tools to improve decision making in clinical drug development, Eur. J. Drug Metab. Pharmacokinet. 25 (2000) 49–58, https://doi.org/10.1007/bf03190058.

[18] R.L. Lalonde, K.G. Kowalski, M.M. Hutmacher, W. Ewy, D.J. Nichols, P. A. Milligan, B.W. Corrigan, P.A. Lockwood, S.A. Marshall, L.J. Benincosa, T. G. Tensfeldt, K. Parivar, M. Amantea, P. Glue, H. Koide, R. Miller, Model-based drug development, Clin. Pharmacol. Ther. 82 (2007) 21–32, https://doi.org/10.1038/sj.clpt.6100235.

[19] P.A. Milligan, M.J. Brown, B. Marchant, S.W. Martin, P.H. van der Graaf, N. Benson, G. Nucci, D.J. Nichols, R.A. Boyd, J.W. Mandema, S. Krishnaswami, S. Zwillich, D. Gruben, R.J. Anziano, T.C. Stock, R.L. Lalonde, Model-based drug development: A rational approach to efficiently accelerate drug development, Clin. Pharmacol. Ther. 93 (2013) 502–514, https://doi.org/10.1038/clpt.2013.54.

[20] Y. Wang, H. Zhu, R. Madabushi, Q. Liu, S.-M. Huang, I. Zineh, Model-informed drug development: Current US regulatory practice and future considerations, Clin. Pharmacol. Ther. 105 (2019) 899–911, https://doi.org/10.1002/cpt.1363.

[21] ICH, E4 Dose-Response Information to Support Drug Registration. U.S. Food and Drug Administration, (1994). https://database.ich.org/sites/default/files/E4_Guideline.pdf (accessed 2024).

[22] L.J. Lesko, Perspective on model-informed drug development, CPT Pharmacometrics Syst. Pharmacol. 10 (2021) 1127–1129, https://doi.org/10.1002/psp4.12699.

[23] Y. Ryeznik, O. Sverdlov, E.M. Svensson, G. Montepiedra, A.C. Hooker, W. K. Wong, Pharmacometrics meets statistics-A synergy for modern drug development, CPT Pharmacometrics Syst. Pharmacol. 10 (2021) 1134–1149, https://doi.org/10.1002/psp4.12696.

[24] J.S. Barrett, M.J. Fossler, K.D. Cadieu, M.R. Gastonguay, Pharmacometrics: a multidisciplinary field to facilitate critical thinking in drug development and translational research settings, J. Clin. Pharmacol. 48 (2008) 632–649, https://doi.org/10.1177/0091270008315318.

[25] Bhavatharini, Deepalakshmi, Arun, Pharmacometrics: The science applied from bench to bedside, J. Appl. Pharm. Sci. (2022). Doi: 10.7324/japs.2021.120104.

[26] A. Ruiz-Garcia, P. Baverel, D. Bottino, M. Dolton, Y. Feng, I. González-García, J. Kim, S. Robey, I. Singh, D. Turner, S.-P. Wu, D. Yin, D. Zhou, H. Zhu, P. Bonate, A comprehensive regulatory and industry review of modeling and simulation practices in oncology clinical drug development, J. Pharmacokinet. Pharmacodyn. (2023), https://doi.org/10.1007/s10928-023-09850-2.

[27] V.D. Sharma, V.A. Bhattaram, K. Krudys, Z. Li, A. Marathe, N. Mehrotra, X. Wang, J. Liu, E. Stier, J. Florian, R. Madabushi, H. Zhu, Driving efficiency: Leveraging model-informed approaches in 505(b)(2) regulatory actions, J. Clin. Pharmacol. (2024), https://doi.org/10.1002/jcph.6109.

[28] D.R. Mould, R.N. Upton, Basic concepts in population modeling, simulation, and model-based drug development-part 2: introduction to pharmacokinetic modeling methods, CPT Pharmacometrics Syst. Pharmacol. 2 (2013) e38, https://doi.org/10.1038/psp.2013.14.

[29] B.C. Bender, E. Schindler, L.E. Friberg, Population pharmacokinetic-pharmacodynamic modelling in oncology: a tool for predicting clinical response, Br. J. Clin. Pharmacol. 79 (2015) 56–71, https://doi.org/10.1111/bcp.12258.
[30] N. Holford, A time to event tutorial for pharmacometricians, CPT Pharmacometrics Syst. Pharmacol. 2 (2013) e43, https://doi.org/10.1038/psp.2013.18.
[31] N. Holford, S.C. Ma, B.A. Ploeger, Clinical trial simulation: A review, Clin. Pharmacol. Ther. 88 (2010) 166–182, https://doi.org/10.1038/clpt.2010.114.
[32] P. Girard, Clinical trial simulation: A tool for understanding study failures and preventing them, Basic Clin. Pharmacol. Toxicol. 96 (2005) 228–234, https://doi.org/10.1111/j.1742-7843.2005.pto960313.x.
[33] K. Venkatakrishnan, P.H. van der Graaf, Model-informed drug development: Connecting the dots with a totality of evidence mindset to advance therapeutics, Clin. Pharmacol. Ther. 110 (2021) 1147–1154, https://doi.org/10.1002/cpt.2422.
[34] L.B. Sheiner, B. Rosenberg, V.V. Marathe, Estimation of population characteristics of pharmacokinetic parameters from routine clinical data, J. Pharmacokinet. Biopharm. 5 (1977) 445–479, https://doi.org/10.1007/BF01061728.
[35] D.R. Mould, R.N. Upton, Basic concepts in population modeling, simulation, and model-based drug development, CPT Pharmacometrics Syst. Pharmacol. 1 (2012) e6.
[36] Y. Li, W.-T. Hwang, S.L. Maude, D.T. Teachey, N.V. Frey, R.M. Myers, A. Barz Leahy, H. Liu, D.L. Porter, S.A. Grupp, P.A. Shaw, Statistical considerations for analyses of time-to-event endpoints in oncology clinical trials: Illustrations with CAR-T immunotherapy studies, Clin. Cancer Res. 28 (2022) 3940–3949, https://doi.org/10.1158/1078-0432.CCR-22-0560.
[37] C. Schmoor, M. Schumacher, J. Finke, J. Beyersmann, Competing risks and multistate models, Clin. Cancer Res. 19 (2013) 12–21, https://doi.org/10.1158/1078-0432.CCR-12-1619.
[38] U. Beyer, D. Dejardin, M. Meller, K. Rufibach, H.U. Burger, A multistate model for early decision-making in oncology, Biom. J. 62 (2020) 550–567, https://doi.org/10.1002/bimj.201800250.
[39] C.-W. Lin, M. Nagase, S. Doshi, S. Dutta, A multistate platform model for time-to-event endpoints in oncology clinical trials, CPT Pharmacometrics Syst. Pharmacol. (2023), https://doi.org/10.1002/psp4.13069.
[40] S.M. Krishnan, L.E. Friberg, R. Bruno, U. Beyer, J.Y. Jin, M.O. Karlsson, Multistate model for pharmacometric analyses of overall survival in HER2-negative breast cancer patients treated with docetaxel, CPT Pharmacometrics Syst. Pharmacol. (2021), https://doi.org/10.1002/psp4.12693.
[41] S.M. Krishnan, L.E. Friberg, F. Mercier, R. Zhang, B. Wu, J.Y. Jin, T. Hoang, M. Ballinger, R. Bruno, M.O. Karlsson, Multistate pharmacometric model to define the impact of second-line immuno-therapies on the survival outcome of IMpower131 study, Clin. Pharmacol. Ther. (2023), https://doi.org/10.1002/cpt.2838.
[42] H. Liu, A.-M. Milenković-Grišić, S.M. Krishnan, S. Jönsson, L.E. Friberg, P. Girard, K. Venkatakrishnan, Y. Vugmeyster, A. Khandelwal, M.O. Karlsson, A multistate modeling and simulation framework to learn dose-response of oncology drugs: Application to bintrafusp alfa in non-small cell lung cancer, CPT Pharmacometrics Syst. Pharmacol. (2023), https://doi.org/10.1002/psp4.12976.
[43] B.P. Solans, M.J. Garrido, I.F. Trocóniz, Drug exposure to establish pharmacokinetic–response relationships in oncology, Clin. Pharmacokinet. 59 (2020) 123–135, https://doi.org/10.1007/s40262-019-00828-3.
[44] J.-F. Lu, L. Claret, L. Sutjandra, M. Kuchimanchi, R. Melara, R. Bruno, Y.-N. Sun, Population pharmacokinetic/pharmacodynamic modeling for the time course of tumor shrinkage by motesanib in thyroid cancer patients, Cancer Chemother. Pharmacol. 66 (2010) 1151–1158, https://doi.org/10.1007/s00280-010-1456-0.
[45] A.A. Suleiman, S. Frechen, M. Scheffler, T. Zander, D. Kahraman, C. Kobe, J. Wolf, L. Nogova, U. Fuhr, Modeling tumor dynamics and overall survival in advanced non–small-cell lung cancer treated with erlotinib, J. Thorac. Oncol. 10 (2015) 84–92, https://doi.org/10.1097/JTO.0000000000000330.
[46] P. Jacqmin, E. Snoeck, E.A. van Schaick, R. Gieschke, P. Pillai, J.-L. Steimer, P. Girard, Modelling response time profiles in the absence of drug concentrations: Definition and performance evaluation of the K–PD model, J. Pharmacokinet. Pharmacodyn. 34 (2007) 57–85, https://doi.org/10.1007/s10928-006-9035-z.
[47] A. Stein, W. Wang, A.A. Carter, O. Chiparus, N. Hollaender, H. Kim, R.J. Motzer, C. Sarr, Dynamic tumor modeling of the dose-response relationship for everolimus in metastatic renal cell carcinoma using data from the phase 3 RECORD-1 trial, BMC Cancer 12 (2012) 311, https://doi.org/10.1186/1471-2407-12-311.
[48] Q.X. Ooi, C. Hasegawa, S.B. Duffull, D.F.B. Wright, Kinetic-pharmacodynamic model for drugs with non-linear elimination: Parameterisation matters, Br. J. Clin. Pharmacol. 86 (2020) 196–198, https://doi.org/10.1111/bcp.14154.
[49] C. Xu, T.K. Goggin, X.-Y. Su, P. Taverna, A. Oganesian, J.N. Lowder, M. Azab, H. Kantarjian, Simultaneous modeling of biomarker and toxicity response predicted optimal regimen of guadecitabine (SGI-110) in myeloid malignancies, CPT Pharmacometrics Syst. Pharmacol. 6 (2017) 712–718, https://doi.org/10.1002/psp4.12248.
[50] D. Vera-Yunca, Z.P. Parra-Guillen, P. Girard, I.F. Trocóniz, N. Terranova, Relevance of primary lesion location, tumour heterogeneity and genetic mutation demonstrated through tumour growth inhibition and overall survival modelling in metastatic colorectal cancer, Br. J. Clin. Pharmacol. 88 (2022) 166–177, https://doi.org/10.1111/bcp.14937.
[51] J.R. Proctor, H. Wong, Time-dependent clearance can confound exposure-response analysis of therapeutic antibodies: A comprehensive review of the current literature, Clin. Transl. Sci. 17 (2024) e13676.
[52] H.I. Dai, Y. Vugmeyster, N. Mangal, Characterizing exposure-response relationship for therapeutic monoclonal antibodies in immuno-oncology and beyond: Challenges, perspectives, and prospects, Clin. Pharmacol. Ther. 108 (2020) 1156–1170, https://doi.org/10.1002/cpt.1953.
[53] A.-M. Grisic, W. Xiong, L. Tanneau, S. Jönsson, L.E. Friberg, M.O. Karlsson, H. Dai, J. Zheng, P. Girard, A. Khandelwal, Model-based characterization of the bidirectional interaction between pharmacokinetics and tumor growth dynamics in patients with metastatic merkel cell carcinoma treated with avelumab, Clin. Cancer Res. 28 (2022) 1363–1371, https://doi.org/10.1158/1078-0432.ccr-21-2662.
[54] FDA-NIH Biomarker Working Group, BEST (Biomarkers, EndpointS, and other Tools) Resource, Food and Drug Administration (US), Silver Spring (MD), n.d. https://www.ncbi.nlm.nih.gov/pubmed/27010052.
[55] M. Danhof, G. Alvan, S.G. Dahl, J. Kuhlmann, G. Paintaud, Mechanism-based pharmacokinetic-pharmacodynamic modeling-a new classification of biomarkers, Pharm. Res. 22 (2005) 1432–1437, https://doi.org/10.1007/s11095-005-5882-3.
[56] C.-C. Ko, L.-R. Yeh, Y.-T. Kuo, J.-H. Chen, Imaging biomarkers for evaluating tumor response: RECIST and beyond, Biomark. Res. 9 (2021) 52, https://doi.org/10.1186/s40364-021-00306-8.
[57] E.A. Eisenhauer, P. Therasse, J. Bogaerts, L.H. Schwartz, D. Sargent, R. Ford, J. Dancey, S. Arbuck, S. Gwyther, M. Mooney, L. Rubinstein, L. Shankar, L. Dodd, R. Kaplan, D. Lacombe, J. Verweij, New response evaluation criteria in solid tumours: Revised RECIST guideline (version 1.1), Eur. J. Cancer 45 (2009) 228–247, https://doi.org/10.1016/j.ejca.2008.10.026.
[58] M. Vogsen, F. Harbo, N.M. Jakobsen, H.J. Nissen, S.E. Dahlsgaard-Wallenius, O. Gerke, J.D. Jensen, J.T. Asmussen, A.M.B. Jylling, P.-E. Braad, W. Vach, M. Ewertz, M.G. Hildebrandt, Response monitoring in metastatic breast cancer: A prospective study comparing 18F-FDG PET/CT with conventional CT, J. Nucl. Med. 64 (2023) 355–361, https://doi.org/10.2967/jnumed.121.263358.
[59] M. Vanderhoek, S.B. Perlman, R. Jeraj, Impact of different standardized uptake value measures on PET-based quantification of treatment response, J. Nucl. Med. 54 (2013) 1188–1194, https://doi.org/10.2967/jnumed.112.113332.
[60] R.L. Wahl, H. Jacene, Y. Kasamon, M.A. Lodge, From RECIST to PERCIST: Evolving considerations for PET response criteria in solid tumors, J. Nucl. Med. 50 (Suppl 1) (2009) 122S–S150, https://doi.org/10.2967/jnumed.108.057307.
[61] K. Pinker, C. Riedl, W.A. Weber, Evaluating tumor response with FDG PET: updates on PERCIST, comparison with EORTC criteria and clues to future developments, Eur. J. Nucl. Med. Mol. Imaging 44 (2017) 55–66, https://doi.org/10.1007/s00259-017-3687-3.
[62] H.J. Janse van Rensburg, P. Spiliopoulou, L.L. Siu, Circulating biomarkers for therapeutic monitoring of anti-cancer agents, Oncologist 27 (2022) 352–362, https://doi.org/10.1093/oncolo/oyac047.
[63] R.N. Upton, D.R. Mould, Basic concepts in population modeling, simulation, and model-based drug development: part 3-introduction to pharmacodynamic modeling methods, CPT Pharmacometrics Syst. Pharmacol. 3 (2014) e88, https://doi.org/10.1038/psp.2013.71.
[64] Y.N. Sun, W.J. Jusko, Transit compartments versus gamma distribution function to model signal transduction processes in pharmacodynamics, J. Pharm. Sci. 87 (1998) 732–737, https://doi.org/10.1021/js970414z.
[65] L.-S. Tham, L. Wang, R.A. Soo, S.-C. Lee, H.-S. Lee, W.-P. Yong, B.-C. Goh, N.H. G. Holford, A pharmacodynamic model for the time course of tumor shrinkage by gemcitabine + carboplatin in non-small cell lung cancer patients, Clin. Cancer Res. 14 (2008) 4213–4218, https://doi.org/10.1158/1078-0432.CCR-07-4754.
[66] Y. Wang, C. Sung, C. Dartois, R. Ramchandani, B.P. Booth, E. Rock, J. Gobburu, Elucidation of relationship between tumor size and survival in non-small-cell lung cancer patients can aid early decision making in clinical drug development, Clin. Pharmacol. Ther. 86 (2009) 167–174, https://doi.org/10.1038/clpt.2009.64.
[67] R. Bruno, D. Bottino, D.P. de Alwis, A.T. Fojo, J. Guedj, C. Liu, K.R. Swanson, J. Zheng, Y. Zheng, J.Y. Jin, Progress and opportunities to advance clinical cancer therapeutics using tumor dynamic models, Clin. Cancer Res. 26 (2020) 1787–1795, https://doi.org/10.1158/1078-0432.CCR-19-0287.
[68] N. Al-Huniti, Y. Feng, J.J. Yu, Z. Lu, M. Nagase, D. Zhou, J. Sheng, Tumor growth dynamic modeling in oncology drug development and regulatory approval: Past, present, and future opportunities, CPT Pharmacometrics Syst. Pharmacol. 9 (2020) 419–427, https://doi.org/10.1002/psp4.12542.
[69] B. Ribba, N.H. Holford, P. Magni, I. Trocóniz, I. Gueorguieva, P. Girard, C. Sarr, M. Elishmereni, C. Kloft, L.E. Friberg, A review of mixed-effects models of tumor growth and effects of anticancer drug treatment used in population analysis, CPT: Pharmacometrics Syst. Pharmacol. 3 (2014) 113, https://doi.org/10.1038/psp.2014.12.
[70] A. Yin, D.J.A.R. Moes, J.G.C. van Hasselt, J.J. Swen, H.-J. Guchelaar, A review of mathematical models for tumor dynamics and treatment resistance evolution of solid tumors, CPT Pharmacometrics Syst. Pharmacol. 8 (2019) 720–737, https://doi.org/10.1002/psp4.12450.
[71] L. Claret, P. Girard, P.M. Hoff, E. Van Cutsem, K.P. Zuideveld, K. Jorga, J. Fagerberg, R. Bruno, Model-based prediction of phase III overall survival in colorectal cancer on the basis of phase II tumor dynamics, J. Clin. Oncol. 27 (2009) 4103–4108, https://doi.org/10.1200/JCO.2008.21.0807.
[72] B. Bender, J. Jin, L. Friberg, A Mechanism-Based Model of Tumor Quiescence and Resistance in HER2-Negative Metastatic Breast Cancer in Patients Receiving Docetaxel or Paclitaxel, Population Approach Group Europe (PAGE) Conference (2017). https://www.page-meeting.org/?abstract=7344 (accessed 2024).
[73] I. Netterberg, M.O. Karlsson, L.W.M.M. Terstappen, M. Koopman, C.J.A. Punt, L. E. Friberg, Comparing circulating tumor cell counts with dynamic tumor size changes as predictor of overall survival: A quantitative modeling framework,

Clin. Cancer Res. 26 (2020) 4892–4900, https://doi.org/10.1158/1078-0432.CCR-19-2570.
[74] Population Pharmacokinetic/Pharmacodynamic Modelingof Tumor Size Dynamics in Pembrolizumab-TreatedAdvanced Melanoma, n.d.
[75] F.P. Combes, Y.F. Li, M. Hoch, S. Lorenzo, Y.-Y. Ho, S.K.B. Sy, Exposure-efficacy analysis of asciminib in philadelphia chromosome-positive chronic myeloid leukemia in chronic phase, Clin. Pharmacol. Ther. 112 (2022) 1040–1050, https://doi.org/10.1002/cpt.2699.
[76] W.D. Stein, J.L. Gulley, J. Schlom, R.A. Madan, W. Dahut, W.D. Figg, Y.-M. Ning, P.M. Arlen, D. Price, S.E. Bates, T. Fojo, Tumor regression and growth rates determined in five intramural NCI prostate cancer trials: the growth rate constant as an indicator of therapeutic efficacy, Clin. Cancer Res. 17 (2011) 907–917, https://doi.org/10.1158/1078-0432.CCR-10-1762.
[77] E.I.K. Ibrahim, M.O. Karlsson, L.E. Friberg, Assessment of ibrutinib scheduling on leukocyte, lymph node size and blood pressure dynamics in chronic lymphocytic leukemia through pharmacokinetic-pharmacodynamic models, CPT Pharmacometrics Syst. Pharmacol. (2023), https://doi.org/10.1002/psp4.13010.
[78] E.K. Hansson, M.A. Amantea, P. Westwood, P.A. Milligan, B.E. Houk, J. French, M.O. Karlsson, L.E. Friberg, PKPD modeling of VEGF, sVEGFR-2, sVEGFR-3, and sKIT as predictors of tumor dynamics and overall survival following sunitinib treatment in GIST, CPT Pharmacometrics Syst. Pharmacol. 2 (2013) e84, https://doi.org/10.1038/psp.2013.61.
[79] E. Hénin, B. You, E. VanCutsem, P.M. Hoff, J. Cassidy, C. Twelves, K.P. Zuideveld, F. Sirzen, C. Dartois, G. Freyer, M. Tod, P. Girard, A dynamic model of hand-and-foot syndrome in patients receiving capecitabine, Clin. Pharmacol. Ther. 85 (2009) 418–425, https://doi.org/10.1038/clpt.2008.220.
[80] R.J. Keizer, A. Gupta, M.R. Mac Gillavry, M. Jansen, J. Wanders, J.H. Beijnen, J. H.M. Schellens, M.O. Karlsson, A.D.R. Huitema, A model of hypertension and proteinuria in cancer patients treated with the anti-angiogenic drug E7080, J. Pharmacokinet. Pharmacodyn. 37 (2010) 347–363, https://doi.org/10.1007/s10928-010-9164-2.
[81] E.K. Hansson, G. Ma, M.A. Amantea, J. French, P.A. Milligan, L.E. Friberg, M. O. Karlsson, PKPD modeling of predictors for adverse effects and overall survival in sunitinib-treated patients with GIST, CPT: Pharmacometrics & Syst.Pharmacol. 2 (2013) 85, https://doi.org/10.1038/psp.2013.62.
[82] E. Schindler, M.O. Karlsson, A minimal continuous-time markov pharmacometric model, AAPS J. 19 (2017) 1424–1435, https://doi.org/10.1208/s12248-017-0109-1.
[83] C. Xu, P. Ravva, J.S. Dang, J. Laurent, C. Adessi, C. McIntyre, G. Meneses-Lorente, F. Mercier, A continuous-time multistate Markov model to describe the occurrence and severity of diarrhea events in metastatic breast cancer patients treated with lumretuzumab in combination with pertuzumab and paclitaxel, Cancer Chemother. Pharmacol. 82 (2018) 395–406, https://doi.org/10.1007/s00280-018-3621-9.
[84] E. Schmulenson, L. Krolop, S. Simons, S. Ringsdorf, Y.-D. Ko, U. Jaehde, Evaluation of patient-reported severity of hand-foot syndrome under capecitabine using a Markov modeling approach, Cancer Chemother. Pharmacol. 86 (2020) 435–444, https://doi.org/10.1007/s00280-020-04128-7.
[85] J.K. Srimani, P.M. Diderichsen, M.J. Hanley, K. Venkatakrishnan, R. Labotka, N. Gupta, Population pharmacokinetic/pharmacodynamic joint modeling of ixazomib efficacy and safety using data from the pivotal phase III TOURMALINE-MM1 study in multiple myeloma patients, CPT Pharmacometrics Syst. Pharmacol. 11 (2022) 1085–1099, https://doi.org/10.1002/psp4.12815.
[86] T. Lu, Y. Yang, J.Y. Jin, M. Kågedal, Analysis of longitudinal-ordered categorical data for muscle spasm adverse event of vismodegib: Comparison between different pharmacometric models, CPT Pharmacometrics Syst. Pharmacol. 9 (2020) 96–105, https://doi.org/10.1002/psp4.12487.
[87] J. Collins, M. van Noort, C. Rathi, T.M. Post, H. Struemper, R.C. Jewell, G. Ferron-Brady, Longitudinal efficacy and safety modeling and simulation framework to aid dose selection of belantamab mafodotin for patients with multiple myeloma, CPT Pharmacometrics Syst. Pharmacol. (2023), https://doi.org/10.1002/psp4.13016.
[88] L.E. Friberg, A. Henningsson, H. Maas, L. Nguyen, M.O. Karlsson, Model of chemotherapy-induced myelosuppression with parameter consistency across drugs, J. Clin. Oncol. 20 (2002) 4713–4721, https://doi.org/10.1200/JCO.2002.02.140.
[89] G.J. Fetterly, J.S. Owen, K. Stuyckens, J.A. Passarell, P. Zannikos, A. Soto-Matos, M.A. Izquierdo, J.J. Perez-Ruixo, Semimechanistic pharmacokinetic/pharmacodynamic model for hepatoprotective effect of dexamethasone on transient transaminitis after trabectedin (ET-743) treatment, Cancer Chemother. Pharmacol. 62 (2008) 135–147, https://doi.org/10.1007/s00280-007-0583-8.
[90] I. Netterberg, M.O. Karlsson, E.I. Nielsen, A.L. Quartino, H. Lindman, L.E. Friberg, The risk of febrile neutropenia in breast cancer patients following adjuvant chemotherapy is predicted by the time course of interleukin-6 and C-reactive protein by modelling, Br. J. Clin. Pharmacol. 84 (2018) 490–500, https://doi.org/10.1111/bcp.13477.
[91] C. Zecchin, I. Gueorguieva, N.H. Enas, L.E. Friberg, Models for change in tumour size, appearance of new lesions and survival probability in patients with advanced epithelial ovarian cancer, Br. J. Clin. Pharmacol. 82 (2016) 717–727, https://doi.org/10.1111/bcp.12994.
[92] J. Yu, N. Wang, M. Kågedal, A new method to model and predict progression free survival based on tumor growth dynamics, CPT Pharmacometrics Syst. Pharmacol. 9 (2020) 177–184, https://doi.org/10.1002/psp4.12499.
[93] M. Baaz, T. Cardilin, M. Jirstrand, Model-based prediction of progression-free survival for combination therapies in oncology, CPT Pharmacometrics Syst. Pharmacol. (2023), https://doi.org/10.1002/psp4.13003.
[94] C. Hu, M.E. Sale, A joint model for nonlinear longitudinal data with informative dropout, J. Pharmacokinet. Pharmacodyn. 30 (2003) 83–103, https://doi.org/10.1023/a:1023249510224.
[95] M.R. Gastonguay, J.L. French, D.F. Heitjan, J.A. Rogers, J.E. Ahn, P. Ravva, Missing data in model-based pharmacometric applications: points to consider, J. Clin. Pharmacol. 50 (2010) 63S–74S, https://doi.org/10.1177/0091270010378409.
[96] S.M. Krishnan, S.S. Laarif, B.C. Bender, A.L. Quartino, L.E. Friberg, Tumor growth inhibition modeling of individual lesion dynamics and interorgan variability in HER2-negative breast cancer patients treated with docetaxel, CPT Pharmacometrics Syst. Pharmacol. 10 (2021) 511–521, https://doi.org/10.1002/psp4.12629.
[97] L.E. Friberg, R. de Greef, T. Kerbusch, M.O. Karlsson, Modeling and simulation of the time course of asenapine exposure response and dropout patterns in acute schizophrenia, Clin. Pharmacol. Ther. 86 (2009) 84–91, https://doi.org/10.1038/clpt.2009.44.
[98] M.A. Björnsson, L.E. Friberg, U.S.H. Simonsson, Performance of nonlinear mixed effects models in the presence of informative dropout, AAPS J. 17 (2015) 245–255, https://doi.org/10.1208/s12248-014-9700-x.
[99] Y. Zheng, R. Narwal, C. Jin, P.G. Baverel, X. Jin, A. Gupta, Y. Ben, B. Wang, P. Mukhopadhyay, B.W. Higgs, L. Roskos, Population modeling of tumor kinetics and overall survival to identify prognostic and predictive biomarkers of efficacy for durvalumab in patients with urothelial carcinoma, Clin. Pharmacol. Ther. 103 (2018) 643–652, https://doi.org/10.1002/cpt.986.
[100] K. Sanghavi, J. Ribbing, J.A. Rogers, M.A. Ahmed, M.O. Karlsson, N. Holford, E. Chasseloup, M. Ahamadi, K.G. Kowalski, S. Cole, E. Kerwash, J.R. Wade, C. Liu, Y. Wang, M.N. Trame, H. Zhu, J.J. Wilkins, ISoP standards & best practices committee, covariate modeling in pharmacometrics: General points for consideration, CPT Pharmacometrics Syst. Pharmacol. (2024), https://doi.org/10.1002/psp4.13115.
[101] U. Wählby, A.H. Thomson, P.A. Milligan, M.O. Karlsson, Models for time-varying covariates in population pharmacokinetic-pharmacodynamic analysis, Br. J. Clin. Pharmacol. 58 (2004) 367–377, https://doi.org/10.1111/j.1365-2125.2004.02170.x.
[102] B.D. Lacroix, L.E. Friberg, M.O. Karlsson, Evaluation of IPPSE, an alternative method for sequential population PKPD analysis, J. Pharmacokinet. Pharmacodyn. 39 (2012) 177–193, https://doi.org/10.1007/s10928-012-9240-x.
[103] K. Zhudenkov, S. Gavrilov, A. Sofronova, O. Stepanov, N. Kudryashova, G. Helmlinger, K. Peskov, A workflow for the joint modeling of longitudinal and event data in the development of therapeutics: Tools, statistical methods, and diagnostics, CPT Pharmacometrics Syst. Pharmacol. 11 (2022) 425–437, https://doi.org/10.1002/psp4.12763.
[104] M. Kerioui, J. Bertrand, R. Bruno, F. Mercier, J. Guedj, S. Desmée, Modelling the association between biomarkers and clinical outcome: An introduction to nonlinear joint models, Br. J. Clin. Pharmacol. 88 (2022) 1452–1463, https://doi.org/10.1111/bcp.15200.
[105] L. Zhang, S.L. Beal, L.B. Sheiner, Simultaneous vs. sequential analysis for population PK/PD data I: best-case performance, J. Pharmacokinet. Pharmacodyn. 30 (2003) 387–404, https://doi.org/10.1023/b:jopa.0000012998.04442.1f.
[106] R.M. Savic, M.O. Karlsson, Importance of shrinkage in empirical bayes estimates for diagnostics: Problems and solutions, AAPS J. 11 (2009) 558–569, https://doi.org/10.1208/s12248-009-9133-0.
[107] X.S. Xu, M. Yuan, M.O. Karlsson, A. Dunne, P. Nandy, A. Vermeulen, Shrinkage in nonlinear mixed-effects population models: Quantification, influencing factors, and impact, AAPS J. 14 (2012) 927–936, https://doi.org/10.1208/s12248-012-9407-9.
[108] S.M. Krishnan, L.E. Friberg, Bayesian forecasting of tumor size metrics and overall survival, CPT Pharmacometrics Syst. Pharmacol. 11 (2022) 1604–1613, https://doi.org/10.1002/psp4.12869.
[109] T. Chen, Y. Zheng, L. Roskos, D.E. Mager, Comparison of sequential and joint nonlinear mixed effects modeling of tumor kinetics and survival following Durvalumab treatment in patients with metastatic urothelial carcinoma, J. Pharmacokinet. Pharmacodyn. 50 (2023) 251–265, https://doi.org/10.1007/s10928-023-09848-w.
[110] A. Gonçalves, M. Marchand, P. Chan, J.Y. Jin, J. Guedj, R. Bruno, Comparison of two-stage and joint TGI-OS modeling using data from six atezolizumab clinical studies in patients with metastatic non-small cell lung cancer, CPT Pharmacometrics Syst. Pharmacol. (2023), https://doi.org/10.1002/psp4.13057.
[111] B. Ribba, N. Holford, F. Mentré, The use of model-based tumor-size metrics to predict survival, Clin. Pharmacol. Ther. 96 (2014) 133–135, https://doi.org/10.1038/clpt.2014.111.
[112] H.B. Mistry, Time-dependent bias of tumor growth rate and time to tumor regrowth, CPT Pharmacometrics Syst. Pharmacol. 5 (2016) 587, https://doi.org/10.1002/psp4.12145.
[113] A. Khandelwal, A.-M. Grisic, J. French, K. Venkatakrishnan, Pharmacometrics golems: Exposure-response models in oncology, Clin. Pharmacol. Ther. 112 (2022) 941–945, https://doi.org/10.1002/cpt.2564.
[114] X. Mi, B.G. Hammill, L.H. Curtis, E.-C.-C. Lai, S. Setoguchi, Use of the landmark method to address immortal person-time bias in comparative effectiveness research: A simulation study, Stat. Med. 35 (2016) 4824–4836, https://doi.org/10.1002/sim.7019.
[115] K. Brendel, C. Dartois, E. Comets, A. Lemenuel-Diot, C. Laveille, B. Tranchand, P. Girard, C.M. Laffont, F. Mentré, Are population pharmacokinetic and/or pharmacodynamic models adequately evaluated? A survey of the literature from

2002 to 2004, Clin. Pharmacokinet. 46 (2007) 221–234. Doi: 10.2165/00003088-200746030-00003.
[116] T.H.T. Nguyen, M.-S. Mouksassi, N. Holford, N. Al-Huniti, I. Freedman, A. C. Hooker, J. John, M.O. Karlsson, D.R. Mould, J.J. Pérez Ruixo, E.L. Plan, R. Savic, J.G.C. van Hasselt, B. Weber, C. Zhou, E. Comets, F. Mentré, Model evaluation group of the International Society of Pharmacometrics (ISoP) best practice committee, model evaluation of continuous data pharmacometric models: Metrics and graphics, CPT Pharmacometrics Syst. Pharmacol. 6 (2017) 87–109, https://doi.org/10.1002/psp4.12161.
[117] S. Desmée, F. Mentré, C. Veyrat-Follet, B. Sébastien, J. Guedj, Nonlinear joint models for individual dynamic prediction of risk of death using Hamiltonian Monte Carlo: Application to metastatic prostate cancer, BMC Med. Res. Methodol. 17 (2017) 105, https://doi.org/10.1186/s12874-017-0382-9.
[118] G.W. Brier, Verification of forecasts expressed in terms of probability, Mon. Weather Rev. 78 (1950) 1–3, https://doi.org/10.1175/1520-0493(1950)078<0001:vofeit>2.0.co;2.
[119] L. Claret, J.Y. Jin, C. Ferté, H. Winter, S. Girish, M. Stroh, P. He, M. Ballinger, A. Sandler, A. Joshi, A. Rittmeyer, D. Gandara, J.-C. Soria, R. Bruno, A model of overall survival predicts treatment outcomes with atezolizumab versus chemotherapy in non–small cell lung cancer based on early tumor kinetics, Clin. Cancer Res. 24 (2018) 3292–3298, https://doi.org/10.1158/1078-0432.ccr-17-3662.
[120] L.P. Balant, M. Rowland, L. Aarons, F. Mentré, P.L. Morselli, J.L. Steimer, S. Vozeh, New strategies in drug development and clinical evaluation: the population approach. Commentary on an action for co-operative research, Eur. J. Clin. Pharmacol. 45 (1993) 93–94, https://doi.org/10.1007/BF00315486.
[121] L. Claret, F. Mercier, B.E. Houk, P.A. Milligan, R. Bruno, Modeling and simulations relating overall survival to tumor growth inhibition in renal cell carcinoma patients, Cancer Chemother. Pharmacol. 76 (2015) 567–573, https://doi.org/10.1007/s00280-015-2820-x.
[122] A. Sostelly, F. Mercier, Tumor size and overall survival in patients with platinum-resistant ovarian cancer treated with chemotherapy and bevacizumab, Clin. Med. Insights Oncol. 13 (2019) 1179554919852071, https://doi.org/10.1177/1179554919852071.
[123] L. Claret, M. Gupta, K. Han, A. Joshi, N. Sarapa, J. He, B. Powell, R. Bruno, Evaluation of tumor-size response metrics to predict overall survival in Western and Chinese patients with first-line metastatic colorectal cancer, J. Clin. Oncol. 31 (2013) 2110–2114, https://doi.org/10.1200/JCO.2012.45.0973.
[124] L. Claret, R. Bruno, J.-F. Lu, Y.-N. Sun, C.-P. Hsu, Exploratory modeling and simulation to support development of motesanib in Asian patients with non–small cell lung cancer based on MONET1 study results, Clin. Pharmacol. Ther. 95 (2014) 446–451, https://doi.org/10.1038/clpt.2014.11.
[125] K. Han, L. Claret, A. Sandler, A. Das, J. Jin, R. Bruno, Modeling and simulation of maintenance treatment in first-line non-small cell lung cancer with external validation, BMC Cancer 16 (2016) 473, https://doi.org/10.1186/s12885-016-2455-2.
[126] K. Han, L. Claret, Y. Piao, P. Hegde, A. Joshi, J.R. Powell, J. Jin, R. Bruno, Simulations to predict clinical trial outcome of bevacizumab plus chemotherapy vs. chemotherapy alone in patients with first-line gastric cancer and elevated plasma VEGF-A, CPT Pharmacometrics Syst. Pharmacol. 5 (2016) 352–358, https://doi.org/10.1002/psp4.12064.
[127] P. Chan, M. Marchand, K. Yoshida, S. Vadhavkar, N. Wang, A. Lin, B. Wu, M. Ballinger, N. Sternheim, J.Y. Jin, R. Bruno, Prediction of overall survival in patients across solid tumors following atezolizumab treatments: A tumor growth inhibition-overall survival modeling framework, CPT Pharmacometrics Syst. Pharmacol. 10 (2021) 1171–1182, https://doi.org/10.1002/psp4.12686.
[128] E. Chigutsa, A.J. Long, J.E. Wallin, Exposure-response analysis of necitumumab efficacy in squamous non-small cell lung cancer patients, CPT Pharmacometrics Syst. Pharmacol. 6 (2017) 560–568, https://doi.org/10.1002/psp4.12209.
[129] M. Garcia-Cremades, C. Pitou, P.W. Iversen, I.F. Troconiz, Predicting tumour growth and its impact on survival in gemcitabine-treated patients with advanced pancreatic cancer, Eur. J. Pharm. Sci. 115 (2018) 296–303, https://doi.org/10.1016/j.ejps.2018.01.033.
[130] Y. Feng, X. Wang, S. Suryawanshi, A. Bello, A. Roy, Linking tumor growth dynamics to survival in ipilimumab-treated patients with advanced melanoma using mixture tumor growth dynamic modeling, CPT Pharmacometrics Syst. Pharmacol. 8 (2019) 825–834, https://doi.org/10.1002/psp4.12454.
[131] M. Kerioui, F. Mercier, J. Bertrand, C. Tardivon, R. Bruno, J. Guedj, S. Desmée, Bayesian inference using Hamiltonian Monte-Carlo algorithm for nonlinear joint modeling in the context of cancer immunotherapy, Stat. Med. 39 (2020) 4853–4868, https://doi.org/10.1002/sim.8756.
[132] C. Tardivon, S. Desmée, M. Kerioui, R. Bruno, B. Wu, F. Mentré, F. Mercier, J. Guedj, Association between tumor size kinetics and survival in patients with urothelial carcinoma treated with atezolizumab: Implication for patient follow-up, Clin. Pharmacol. Ther. 106 (2019) 810–820, https://doi.org/10.1002/cpt.1450.
[133] N. Terranova, P. Girard, U. Klinkhardt, A. Munafo, Resistance development: A major piece in the jigsaw puzzle of tumor size modeling, CPT Pharmacometrics Syst. Pharmacol. 4 (2015) 320–323, https://doi.org/10.1002/psp4.45.
[134] J. Zhou, Y. Liu, Y. Zhang, Q. Li, Y. Cao, Modeling tumor evolutionary dynamics to predict clinical outcomes for patients with metastatic colorectal cancer: A retrospective analysis, Cancer Res. 80 (2020) 591–601, https://doi.org/10.1158/0008-5472.CAN-19-1940.
[135] P. Chan, X. Zhou, N. Wang, Q. Liu, R. Bruno, J.Y. Jin, Application of machine learning for tumor growth inhibition – Overall survival modeling platform, CPT Pharmacometrics Syst. Pharmacol. 10 (2021) 59–66, https://doi.org/10.1002/psp4.12576.
[136] M. Kerioui, S. Desmée, F. Mercier, A. Lin, B. Wu, J.Y. Jin, X. Shen, C. Le Tourneau, R. Bruno, J. Guedj, Assessing the impact of organ-specific lesion dynamics on survival in patients with recurrent urothelial carcinoma treated with atezolizumab or chemotherapy, ESMO Open 7 (2022) 100346, https://doi.org/10.1016/j.esmoop.2021.100346.
[137] M. Kerioui, M. Beaulieu, S. Desmée, J. Bertrand, F. Mercier, J.Y. Jin, R. Bruno, J. Guedj, Nonlinear multilevel joint model for individual lesion kinetics and survival to characterize intra-individual heterogeneity in patients with advanced cancer, Biometrics (2023), https://doi.org/10.1111/biom.13912.
[138] M. Kerioui, J. Bertrand, S. Desmée, C. Le Tourneau, F. Mercier, R. Bruno, J. Guedj, Assessing the increased variability in individual lesion kinetics during immunotherapy: Does it exist, and does it matter? JCO Precis Oncol 7 (2023) e2200368, https://doi.org/10.1200/PO.22.00368.
[139] M. Khoury, G.C. Sim, M. Harao, L. Radvanyi, B. Amini, R.S. Benjamin, P.W. T. Pisters, R.E. Pollock, W.W. Tseng, Multicystic dedifferentiated retroperitoneal liposarcoma: Tumour cyst fluid analysis and implications for management, BMJ Case Rep. 2015 (2015), https://doi.org/10.1136/bcr-2015-211218.
[140] E. Schindler, S.M. Krishnan, R.H.J. Mathijssen, A. Ruggiero, G. Schiavon, L. E. Friberg, Pharmacometric modeling of liver metastases' diameter, volume, and density and their relation to clinical outcome in imatinib-treated patients with gastrointestinal stromal tumors, CPT Pharmacometrics Syst. Pharmacol. 6 (2017) 449–457, https://doi.org/10.1002/psp4.12195.
[141] C.C. Zhang, Z. Yan, W. Li, K. Kuszpit, C.L. Painter, Q. Zhang, P.B. Lappin, T. Nichols, M.E. Lira, T. Affolter, N.R. Fahey, C. Cullinane, M. Spilker, K. Zasadny, P. O'Brien, D. Buckman, A. Wong, J.G. Christensen, [18F]FLT–PET imaging does not always "Light Up" proliferating tumor cells, Clin. Cancer Res. 18 (2012) 1303–1312, https://doi.org/10.1158/1078-0432.CCR-11-1433.
[142] E. Schindler, M.A. Amantea, M.O. Karlsson, L.E. Friberg, PK-PD modeling of individual lesion FDG-PET response to predict overall survival in patients with sunitinib-treated gastrointestinal stromal tumor, CPT Pharmacometrics Syst. Pharmacol. 5 (2016) 173–181, https://doi.org/10.1002/psp4.12057.
[143] R.C. Bast Jr, T.L. Klug, E. St John, E. Jenison, J.M. Niloff, H. Lazarus, R. S. Berkowitz, T. Leavitt, C.T. Griffiths, L. Parker, V.R. Zurawski Jr, R.C. Knapp, A radioimmunoassay using a monoclonal antibody to monitor the course of epithelial ovarian cancer, N. Engl. J. Med. 309 (1983) 883–887, https://doi.org/10.1056/NEJM198310133091503.
[144] G.J.S. Rustin, M. Quinn, T. Thigpen, A. du Bois, E. Pujade-Lauraine, A. Jakobsen, E. Eisenhauer, S. Sagae, K. Greven, I. Vergote, A. Cervantes, J. Vermorken, Re: New guidelines to evaluate the response to treatment in solid tumors (ovarian cancer), J. Natl. Cancer Inst. 96 (2004) 487–488, https://doi.org/10.1093/jnci/djh081.
[145] B. You, O. Colomban, M. Heywood, C. Lee, M. Davy, N. Reed, S. Pignata, N. Varsellona, G. Emons, K. Rehman, K.D. Steffensen, A. Reinthaller, E. Pujade-Lauraine, A. Oza, The strong prognostic value of KELIM, a model-based parameter from CA 125 kinetics in ovarian cancer: data from CALYPSO trial (a GINECO-GCIG study), Gynecol. Oncol. 130 (2013) 289–294, https://doi.org/10.1016/j.ygyno.2013.05.013.
[146] O. Colomban, M. Tod, A. Leary, I. Ray-Coquard, A. Lortholary, A.C. Hardy-Bessard, J. Pfisterer, A. Du Bois, C. Kurzeder, A. Burges, Others, early modeled longitudinal CA-125 kinetics and survival of ovarian cancer patients: A GINECO AGO MRC CTU StudyThe CA-125 kinetic KELIM and survival in ovarian cancer, Clin. Cancer Res. 25 (2019) 5342–5350, https://doi.org/10.1158/1078-0432.CCR-18-3335.
[147] X.S. Xu, C.J. Ryan, K. Stuyckens, M.R. Smith, F. Saad, T.W. Griffin, Y.C. Park, M. K. Yu, A. Vermeulen, I. Poggesi, P. Nandy, Correlation between prostate-specific antigen kinetics and overall survival in abiraterone acetate–treated castration-resistant prostate cancer patients, Clin. Cancer Res. 21 (2015) 3170–3177, https://doi.org/10.1158/1078-0432.CCR-14-1549.
[148] J.G.C. van Hasselt, A. Gupta, Z. Hussein, J.H. Beijnen, J.H.M. Schellens, A.D. R. Huitema, Disease progression/clinical outcome model for castration-resistant prostate cancer in patients treated with eribulin, CPT Pharmacometrics Syst. Pharmacol. 4 (2015) 386–395, https://doi.org/10.1002/psp4.49.
[149] S. Desmée, F. Mentré, C. Veyrat-Follet, B. Sébastien, J. Guedj, Using the SAEM algorithm for mechanistic joint models characterizing the relationship between nonlinear PSA kinetics and survival in prostate cancer patients, Biometrics 73 (2017) 305–312, https://doi.org/10.1111/biom.12537.
[150] B.G.M. Durie, J.-L. Harousseau, J.S. Miguel, J. Bladé, B. Barlogie, K. Anderson, M. Gertz, M. Dimopoulos, J. Westin, P. Sonneveld, H. Ludwig, G. Gahrton, M. Beksac, J. Crowley, A. Belch, M. Boccadaro, M. Cavo, I. Turesson, D. Joshua, D. Vesole, R. Kyle, R. Alexanian, G. Tricot, M. Attal, G. Merlini, R. Powles, P. Richardson, K. Shimizu, P. Tosi, G. Morgan, S.V. Rajkumar, International Myeloma Working Group, International uniform response criteria for multiple myeloma, Leukemia 20 (2006) 1467–1473, https://doi.org/10.1038/sj.leu.2404284.
[151] F. Jonsson, Y. Ou, L. Claret, D. Siegel, S. Jagannath, R. Vij, A. Badros, S. Aggarwal, R. Bruno, A tumor growth inhibition model based on M-protein levels in subjects with relapsed/refractory multiple myeloma following single-agent carfilzomib use, CPT Pharmacometrics Syst. Pharmacol. 4 (2015) 711–719, https://doi.org/10.1002/psp4.12044.
[152] H.-T. Thai, N. Gaudel, M. Cerou, G. Ayral, J.-B. Fau, B. Sebastien, H. van de Velde, D. Semiond, C. Veyrat-Follet, Joint modelling and simulation of M-protein dynamics and progression-free survival for alternative isatuximab dosing with pomalidomide/dexamethasone, Br. J. Clin. Pharmacol. 88 (2022) 2052–2064, https://doi.org/10.1111/bcp.15123.

[153] Y. Cheng, K. Hong, N. Chen, X. Yu, T. Peluso, S. Zhou, Y. Li, Aiding early clinical drug development by elucidation of the relationship between tumor growth inhibition and survival in relapsed/refractory multiple myeloma patients, Ejhaem 3 (2022) 815–827, https://doi.org/10.1002/jha2.494.
[154] J.S. de Bono, H.I. Scher, R.B. Montgomery, C. Parker, M.C. Miller, H. Tissing, G. V. Doyle, L.W.W.M. Terstappen, K.J. Pienta, D. Raghavan, Circulating tumor cells predict survival benefit from treatment in metastatic castration-resistant prostate cancer, Clin. Cancer Res. 14 (2008) 6302–6309, https://doi.org/10.1158/1078-0432.CCR-08-0872.
[155] H.I. Scher, G. Heller, A. Molina, T.S. Kheoh, G. Attard, J. Moreira, S.K. Sandhu, C. Parker, C. Logothetis, R.T. McCormack, K. Fizazi, A. Anand, D.C. Danila, M. Fleisher, D. Olmos, C.M. Haqq, J.S. De Bono, Evaluation of circulating tumor cell (CTC) enumeration as an efficacy response biomarker of overall survival (OS) in metastatic castration-resistant prostate cancer (mCRPC): Planned final analysis (FA) of COU-AA-301, a randomized, double-blind, placebo-controlled, phase III study of abiraterone acetate (AA) plus low-dose prednisone (P) post docetaxel, J. Clin. Orthod. 29 (2011) LBA4517, https://doi.org/10.1200/jco.2011.29.18_suppl.lba4517.
[156] M. Wilbaux, M. Tod, J. De Bono, D. Lorente, J. Mateo, G. Freyer, B. You, E. Hénin, A joint model for the kinetics of CTC count and PSA concentration during treatment in metastatic castration-resistant prostate cancer, CPT Pharmacometrics Syst. Pharmacol. 4 (2015) 277–285, https://doi.org/10.1002/psp4.34.
[157] K.C.S. Oliveira, I.B. Ramos, J.M.C. Silva, W.F. Barra, G.J. Riggins, V. Palande, C. T. Pinho, M. Frenkel-Morgenstern, S.E.B. Santos, P.P. Assumpcao, R.R. Burbano, D.Q. Calcagno, Current perspectives on circulating tumor DNA, precision medicine, and personalized clinical management of cancer, Mol. Cancer Res. 18 (2020) 517–528, https://doi.org/10.1158/1541-7786.MCR-19-0768.
[158] J.M. Janssen, R.B. Verheijen, T.T. van Duijl, L. Lin, M.M. van den Heuvel, J. H. Beijnen, N. Steeghs, D. van den Broek, A.D.R. Huitema, T.P.C. Dorlo, Longitudinal nonlinear mixed effects modeling of EGFR mutations in ctDNA as predictor of disease progression in treatment of EGFR-mutant non-small cell lung cancer, Clin. Transl. Sci. 15 (2022) 1916–1925, https://doi.org/10.1111/cts.13300.
[159] M. Johnson, C. Serra Traynor, K. Vishwanathan, P. Overend, R. Hartmaier, A. Markovets, J. Chmielecki, G.M. Mugundu, J.C. Barrett, H. Tomkinson, S. S. Ramalingam, Longitudinal circulating tumor DNA modeling to predict disease progression in first-line mutant epidermal growth factor receptor non-small cell lung cancer, Clin. Pharmacol. Ther. 115 (2024) 349–360, https://doi.org/10.1002/cpt.3113.
[160] P.A. Thompson, W.G. Wierda, Eliminating minimal residual disease as a therapeutic end point: working toward cure for patients with CLL, Blood 127 (2016) 279–286, https://doi.org/10.1182/blood-2015-08-634816.
[161] M. Hallek, B.D. Cheson, D. Catovsky, F. Caligaris-Cappio, G. Dighiero, H. Döhner, P. Hillmen, M. Keating, E. Montserrat, N. Chiorazzi, S. Stilgenbauer, K.R. Rai, J. C. Byrd, B. Eichhorst, S. O'Brien, T. Robak, J.F. Seymour, T.J. Kipps, iwCLL guidelines for diagnosis, indications for treatment, response assessment, and supportive management of CLL, Blood 131 (2018) 2745–2760, https://doi.org/10.1182/blood-2017-09-806398.
[162] S. Böttcher, M. Ritgen, K. Fischer, S. Stilgenbauer, R.M. Busch, G. Fingerle-Rowson, A.M. Fink, A. Bühler, T. Zenz, M.K. Wenger, M. Mendila, C.-M. Wendtner, B.F. Eichhorst, H. Döhner, M.J. Hallek, M. Kneba, Minimal residual disease quantification is an independent predictor of progression-free and overall survival in chronic lymphocytic leukemia: a multivariate analysis from the randomized GCLLSG CLL8 trial, J. Clin. Oncol. 30 (2012) 980–988, https://doi.org/10.1200/JCO.2011.36.9348.
[163] G. Kovacs, S. Robrecht, A.M. Fink, J. Bahlo, P. Cramer, J. von Tresckow, C. Maurer, P. Langerbeins, G. Fingerle-Rowson, M. Ritgen, M. Kneba, H. Döhner, S. Stilgenbauer, W. Klapper, C.-M. Wendtner, K. Fischer, M. Hallek, B. Eichhorst, S. Böttcher, Minimal residual disease assessment improves prediction of outcome in patients with Chronic Lymphocytic Leukemia (CLL) who achieve partial response: Comprehensive analysis of two phase III studies of the German CLL study group, J. Clin. Oncol. 34 (2016) 3758–3765, https://doi.org/10.1200/JCO.2016.67.1305.
[164] S. Gopalakrishnan, W. Wierda, B. Chyla, R. Menon, D. Miles, R. Humerickhouse, W. Awni, A.H. Salem, S. Mensing, K.J. Freise, Integrated mechanistic model of minimal residual disease kinetics with venetoclax therapy in chronic lymphocytic leukemia, Clin. Pharmacol. Ther. 109 (2021) 424–432, https://doi.org/10.1002/cpt.2005.
[165] A.M. Mc Laughlin, P.A. Milligan, C. Yee, M. Bergstrand, Model-informed drug development of autologous CAR-T cell therapy: Strategies to optimize CAR-T cell exposure leveraging cell kinetic/dynamic modeling, CPT Pharmacometrics Syst. Pharmacol. (2023), https://doi.org/10.1002/psp4.13011.
[166] A. Mueller-Schoell, N. Puebla-Osorio, R. Michelet, M.R. Green, A. Künkele, W. Huisinga, P. Strati, B. Chasen, S.S. Neelapu, C. Yee, C. Kloft, Early survival prediction framework in CD19-specific CAR-T cell immunotherapy using a quantitative systems pharmacology model, Cancers 13 (2021), https://doi.org/10.3390/cancers13112782.
[167] N. Buil-Bruna, J.-M. López-Picazo, M. Moreno-Jiménez, S. Martín-Algarra, B. Ribba, I.F. Trocóniz, A population pharmacodynamic model for lactate dehydrogenase and neuron specific enolase to predict tumor progression in small cell lung cancer patients, AAPS J. 16 (2014) 609–619, https://doi.org/10.1208/s12248-014-9600-0.
[168] N. Buil-Bruna, T. Sahota, J.-M. López-Picazo, M. Moreno-Jiménez, S. Martín-Algarra, B. Ribba, I.F. Trocóniz, Early prediction of disease progression in small cell lung cancer: Toward model-based personalized medicine in oncology, Cancer Res. 75 (2015) 2416–2425, https://doi.org/10.1158/0008-5472.CAN-14-2584.
[169] N. Buil-Bruna, M. Dehez, A. Manon, T.X.Q. Nguyen, I.F. Trocóniz, Establishing the quantitative relationship between lanreotide Autogel®, Chromogranin A, and progression-free survival in patients with nonfunctioning gastroenteropancreatic neuroendocrine tumors, AAPS J. 18 (2016) 703–712, https://doi.org/10.1208/s12248-016-9884-3.
[170] M.H. Diekstra, A. Fritsch, F. Kanefendt, J.J. Swen, D. Moes, F. Sörgel, M. Kinzig, C. Stelzer, D. Schindele, T. Gauler, S. Hauser, D. Houtsma, M. Roessler, B. Moritz, K. Mross, L. Bergmann, E. Oosterwijk, L.A. Kiemeney, H.J. Guchelaar, U. Jaehde, Population modeling integrating pharmacokinetics, pharmacodynamics, pharmacogenetics, and clinical outcome in patients with sunitinib-treated cancer, CPT Pharmacometrics Syst. Pharmacol. 6 (2017) 604–613, https://doi.org/10.1002/psp4.12210.
[171] Y. Yu, W. Sun, Y. Liu, D. Wang, Pharmacodynamic modeling of CDK4/6 inhibition-related biomarkers and the characterization of the relationship between biomarker response and progression-free survival in patients with advanced breast cancer, J. Clin. Pharmacol. 62 (2022) 376–384, https://doi.org/10.1002/jcph.1971.
[172] C.K. Lee, M. Friedlander, C. Brown, V.J. Gebski, A. Georgoulopoulos, I. Vergote, S. Pignata, N. Donadello, B. Schmalfeldt, R. Delva, M.R. Mirza, P. Sauthier, E. Pujade-Lauraine, S.J. Lord, R.J. Simes, Early decline in cancer antigen 125 as a surrogate for progression-free survival in recurrent ovarian cancer, J. Natl. Cancer Inst. 103 (2011) 1338–1342, https://doi.org/10.1093/jnci/djr282.
[173] M. Wilbaux, E. Hénin, A. Oza, O. Colomban, E. Pujade-Lauraine, G. Freyer, M. Tod, B. You, Dynamic modeling in ovarian cancer: An original approach linking early changes in modeled longitudinal CA-125 kinetics and survival to help decisions in early drug development, Gynecol. Oncol. 133 (2014) 460–466, https://doi.org/10.1016/j.ygyno.2014.04.003.
[174] M. Wilbaux, E. Hénin, A. Oza, O. Colomban, E. Pujade-Lauraine, G. Freyer, M. Tod, B. You, Prediction of tumour response induced by chemotherapy using modelling of CA-125 kinetics in recurrent ovarian cancer patients, Br. J. Cancer 110 (2014) 1517–1524, https://doi.org/10.1038/bjc.2014.75.
[175] I. Netterberg, C.-C. Li, L. Molinero, N. Budha, S. Sukumaran, M. Stroh, E. N. Jonsson, L.E. Friberg, A PK/PD analysis of circulating biomarkers and their relationship to tumor response in atezolizumab-treated non-small cell lung cancer patients, Clin. Pharmacol. Ther. 105 (2019) 486–495, https://doi.org/10.1002/cpt.1198.
[176] I. Netterberg, R. Bruno, Y.-C. Chen, H. Winter, C.-C. Li, J.Y. Jin, L.E. Friberg, Tumor time-course predicts overall survival in non-small cell lung cancer patients treated with atezolizumab: Dependency on follow-up time, CPT Pharmacometrics Syst. Pharmacol. 9 (2020) 115–123, https://doi.org/10.1002/psp4.12489.
[177] S. Gavrilov, K. Zhudenkov, G. Helmlinger, J. Dunyak, K. Peskov, S. Aksenov, Longitudinal tumor size and neutrophil-to-lymphocyte ratio are prognostic biomarkers for overall survival in patients with advanced non-small cell lung cancer treated with durvalumab, CPT Pharmacometrics Syst. Pharmacol. 10 (2021) 67–74, https://doi.org/10.1002/psp4.12578.
[178] A. Yin, J.G.C. van Hasselt, H.-J. Guchelaar, L.E. Friberg, D.J.A.R. Moes, Anti-cancer treatment schedule optimization based on tumor dynamics modelling incorporating evolving resistance, Sci. Rep. 12 (2022) 4206, https://doi.org/10.1038/s41598-022-08012-7.
[179] E.I.K. Ibrahim, E.B. Ellingsen, S.M. Mangsbo, L.E. Friberg, Bridging responses to a human telomerase reverse transcriptase-based peptide cancer vaccine candidate in a mechanism-based model, Int. Immunopharmacol. 126 (2024) 111225, https://doi.org/10.1016/j.intimp.2023.111225.
[180] A.L. Quartino, L.E. Friberg, M.O. Karlsson, A simultaneous analysis of the time-course of leukocytes and neutrophils following docetaxel administration using a semi-mechanistic myelosuppression model, Invest. New Drugs 30 (2012) 833–845, https://doi.org/10.1007/s10637-010-9603-3.
[181] A.L. Quartino, M.O. Karlsson, H. Lindman, L.E. Friberg, Characterization of endogenous G-CSF and the inverse correlation to chemotherapy-induced neutropenia in patients with breast cancer using population modeling, Pharm. Res. 31 (2014) 3390–3403, https://doi.org/10.1007/s11095-014-1429-9.
[182] M. Centanni, S.M. Krishnan, L.E. Friberg, Model-based dose individualization of sunitinib in gastrointestinal stromal tumorsmodel-based individualization of sunitinib in GIST, Clin. Cancer Res. 26 (2020) 4590–4598. https://aacrjournals.org/clincancerres/article-abstract/26/17/4590/82846.
[183] M. Centanni, L.E. Friberg, Model-based biomarker selection for dose individualization of tyrosine-kinase inhibitors, Front. Pharmacol. 11 (2020) 316, https://doi.org/10.3389/fphar.2020.00316.
[184] E. Schindler, M.A. Amantea, M.O. Karlsson, L.E. Friberg, A pharmacometric framework for axitinib exposure, efficacy, and safety in metastatic renal cell carcinoma patients, CPT Pharmacometrics Syst. Pharmacol. 6 (2017) 373–382, https://doi.org/10.1002/psp4.12193.
[185] I. Irurzun-Arana, E. Asín-Prieto, S. Martín-Algarra, I.F. Trocóniz, Predicting circulating biomarker response and its impact on the survival of advanced melanoma patients treated with adjuvant therapy, Sci. Rep. 10 (2020) 7478, https://doi.org/10.1038/s41598-020-63441-6.
[186] M. Wilbaux, S. Yang, A. Jullion, D. Demanse, D.G. Porta, A. Myers, C. Meille, Y. Gu, Integration of pharmacokinetics, pharmacodynamics, safety, and efficacy into model-informed dose selection in oncology first-in-human study: A case of roblitinib (FGF401), Clin. Pharmacol. Ther. 112 (2022) 1329–1339, https://doi.org/10.1002/cpt.2752.
[187] M. Wilbaux, D. Demanse, Y. Gu, A. Jullion, A. Myers, V. Katsanou, C. Meille, Contribution of machine learning to tumor growth inhibition modeling for hepatocellular carcinoma patients under Roblitinib (FGF401) drug treatment,

CPT Pharmacometrics Syst. Pharmacol. 11 (2022) 1122–1134, https://doi.org/10.1002/psp4.12831.
[188] Project Optimus: reforming the dose optimization and dose selection paradigm in oncology, FDA, Oncology Center of Excellence (2024). https://www.fda.gov/about-fda/oncology-center-excellence/project-optimus (accessed August 13, 2024).
[189] J. Fourie Zirkelbach, M. Shah, J. Vallejo, J. Cheng, A. Ayyoub, J. Liu, R. Hudson, R. Sridhara, G. Ison, L. Amiri-Kordestani, S. Tang, T. Gwise, A. Rahman, R. Pazdur, M.R. Theoret, Improving dose-optimization processes used in oncology drug development to minimize toxicity and maximize benefit to patients, J. Clin. Oncol. 40 (2022) 3489–3500, https://doi.org/10.1200/JCO.22.00371.
[190] Optimizing the Dosage of Human Prescription Drugs and Biological Products for the Treatment of Oncologic Diseases, Draft Guidance for Industry, U.S. Food & Drug Administration (2024). https://www.fda.gov/media/164555/download (accessed September 9, 2024).
[191] D. Samineni, K. Venkatakrishnan, A.A. Othman, Y.K. Pithavala, S. Poondru, C. Patel, P. Vaddady, W. Ankrom, S. Ramanujan, N. Budha, M. Wu, N. Haddish-Berhane, H. Fritsch, A. Hussain, J. Kanodia, M. Li, M. Li, M. Melhem, A. Parikh, V. V. Upreti, N. Gupta, Dose optimization in oncology drug development: An international consortium for innovation and quality in pharmaceutical development white paper, Clin. Pharmacol. Ther. 116 (2024) 531–545, https://doi.org/10.1002/cpt.3298.
[192] K. Venkatakrishnan, J. Cook, Driving access to medicines with a totality of evidence mindset: An opportunity for clinical pharmacology, Clin. Pharmacol. Ther. 103 (2018) 373–375, https://doi.org/10.1002/cpt.926.
[193] W. Gao, J. Liu, B. Shtylla, K. Venkatakrishnan, D. Yin, M. Shah, T. Nicholas, Y. Cao, Realizing the promise of project optimus: Challenges and emerging opportunities for dose optimization in oncology drug development, CPT Pharmacometrics Syst. Pharmacol. (2023), https://doi.org/10.1002/psp4.13079.
[194] K. Venkatakrishnan, P.H. van der Graaf, Toward project optimus for oncology precision medicine: Multi-dimensional dose optimization enabled by quantitative clinical pharmacology, Clin. Pharmacol. Ther. 112 (2022) 927–932, https://doi.org/10.1002/cpt.2742.
[195] K. Koiwai, R. El-Cheikh, H.-T. Thai, C. Brillac, J.-B. Fau, C. Veyrat-Follet, M.-L. Risse, H. van de Velde, D. Semiond, L. Nguyen, PK/PD modeling analysis for dosing regimen selection of isatuximab as single agent and in combination therapy in patients with multiple myeloma, CPT Pharmacometrics Syst. Pharmacol. 10 (2021) 928–940, https://doi.org/10.1002/psp4.12666.
[196] O. Yin, H. Iwata, C.-C. Lin, K. Tamura, J. Watanabe, R. Wada, H. Kastrissios, M. AbuTarif, T. Garimella, C. Lee, L. Zhang, J. Shahidi, F. LaCreta, Exposure-response relationships in patients with HER2-positive metastatic breast cancer and other solid tumors treated with trastuzumab deruxtecan, Clin. Pharmacol. Ther. 110 (2021) 986–996, https://doi.org/10.1002/cpt.2291.
[197] M.O. Karlsson, T. Anehall, L.E. Friberg, A. Henningsson, C. Kloft, M. Sandström, R. Xie, Pharmacokinetic/pharmacodynamic modelling in oncological drug development, Basic Clin. Pharmacol. Toxicol. 96 (2005) 206–211, https://doi.org/10.1111/j.1742-7843.2005.pto960310.x.
[198] C. Fornari, L. Oplustil O'Connor, C. Pin, A. Smith, J.W.T. Yates, S.Y.A. Cheung, D. I. Jodrell, J.T. Mettetal, T.A. Collins, Quantifying drug-induced bone marrow toxicity using a novel haematopoiesis systems pharmacology model, CPT Pharmacometrics Syst. Pharmacol. 8 (2019) 858–868, https://doi.org/10.1002/psp4.12459.
[199] A. Thorsted, C. Zecchin, A. Berges, M.O. Karlsson, L.E. Friberg, Predicting the long-term effects of therapeutic neutralization of Oncostatin M on human hematopoiesis, Clin. Pharmacol. Ther. (2024), https://doi.org/10.1002/cpt.3246.
[200] J.K. Srimani, P.M. Diderichsen, M.J. Hanley, R. Labotka, N. Gupta, Dose titration of ixazomib maintenance therapy in transplant-ineligible multiple myeloma: Exposure-response analysis of the TOURMALINE-MM4 study, Clin. Pharmacol. Ther. 114 (2023) 220–229, https://doi.org/10.1002/cpt.2917.
[201] M.J. Hanley, P. Diderichsen, B. Rich, A. Largajolli, E. Schindler, A. Vorog, K. Venkatakrishnan, N. Gupta, Response-based dosing for ponatinib: Model-based analyses of the dose-ranging OPTIC study, Clin. Pharmacol. Ther. 114 (2023) 413–422, https://doi.org/10.1002/cpt.2956.
[202] P.N. Morcos, J. Moss, J. Veasy, F. Hiemeyer, B.H. Childs, D. Garmann, Model-based benefit/risk analysis for the copanlisib intermittent dosing regimen, Clin. Pharmacol. Ther. 115 (2024) 1092–1104, https://doi.org/10.1002/cpt.3173.
[203] R. Zhu, B. Poland, R. Wada, Q. Liu, L. Musib, D. Maslyar, E. Cho, W. Yu, H. Ma, J. Y. Jin, N. Budha, Exposure-response-based product profile-driven clinical utility index for ipatasertib dose selection in prostate cancer, CPT Pharmacometrics Syst. Pharmacol. 8 (2019) 240–248, https://doi.org/10.1002/psp4.12394.
[204] K.J. Freise, A.K. Jones, M.E. Verdugo, R.M. Menon, P.C. Maciag, A.H. Salem, Moving beyond maximum tolerated dose for targeted oncology drugs: Use of clinical utility index to optimize venetoclax dosage in multiple myeloma patients, Clin. Pharmacol. Ther. 102 (2017) 970–976, https://doi.org/10.1002/cpt.712.
[205] H. Hwangbo, S.C. Patterson, A. Dai, D. Plana, A.C. Palmer, Additivity predicts the efficacy of most approved combination therapies for advanced cancer, Nat Cancer (2023), https://doi.org/10.1038/s43018-023-00667-z.
[206] P.B. Pierrillas, S. Fouliard, M. Chenel, A.C. Hooker, L.F. Friberg, M.O. Karlsson, Model-Based Adaptive Optimal Design (MBAOD) improves combination dose finding designs: An example in oncology, AAPS J. 20 (2018) 39, https://doi.org/10.1208/s12248-018-0206-9.
[207] J. Lai-Kwon, Z. Yin, A. Minchom, C. Yap, Trends in patient-reported outcome use in early phase dose-finding oncology trials - An analysis of Clinicaltrials.gov, Cancer Med. 10 (2021) 7943–7957, https://doi.org/10.1002/cam4.4307.
[208] A. Regnault, A. Loubert, B. Gorsh, R. Davis, A. Cardellino, K. Creel, S. Quéré, S. Sapra, L. Nelsen, L. Eliason, A toolbox of different approaches to analyze and present PRO-CTCAE data in oncology studies, J. Natl. Cancer Inst. 115 (2023) 586–596, https://doi.org/10.1093/jnci/djad018.
[209] Getting the Dose Right: Optimizing Dose Selection Strategies in Oncology – An FDA-ASCO Virtual Workshop, (2022). https://www.fda.gov/news-events/fda-meetings-conferences-and-workshops/getting-dose-right-optimizing-dose-selection-strategies-oncology-fda-asco-virtual-workshop-05032022#event-materials (accessed 2024).
[210] E. Schindler, L.E. Friberg, B.L. Lum, B. Wang, A. Quartino, C. Li, S. Girish, J.Y. Jin, M.O. Karlsson, A pharmacometric analysis of patient-reported outcomes in breast cancer patients through item response theory, Pharm. Res. 35 (2018), https://doi.org/10.1007/s11095-018-2403-8.
[211] L. Fashoyin-Aje, J.A. Beaver, R. Pazdur, Promoting inclusion of members of racial and ethnic minority groups in cancer drug development, JAMA Oncol. 7 (2021) 1445–1446, https://doi.org/10.1001/jamaoncol.2021.2137.
[212] E.S. Kim, T.S. Uldrick, C. Schenkel, S.S. Bruinooge, R.D. Harvey, A. Magnuson, A. Spira, J.L. Wade, M.D. Stewart, D.M. Vega, J.A. Beaver, A.M. Denicoff, G. Ison, S.P. Ivy, S. George, R.P. Perez, P.A. Spears, W.D. Tap, R.L. Schilsky, Continuing to broaden eligibility criteria to make clinical trials more representative and inclusive: ASCO-friends of cancer research joint research statement, Clin. Cancer Res. 27 (2021) 2394–2399, https://doi.org/10.1158/1078-0432.CCR-20-3852.
[213] Friends of Cancer Research (Friends), Clinical Trial Eligibility Criteria. Broadening Eligibility Criteria to Make Clinical Trials More Representative, (2024). https://friendsofcancerresearch.org/clinical-trial-eligibility-criteria/ (accessed 2024).
[214] R. Liu, S. Rizzo, S. Whipple, N. Pal, A.L. Pineda, M. Lu, B. Arnieri, Y. Lu, W. Capra, R. Copping, J. Zou, Evaluating eligibility criteria of oncology trials using real-world data and AI, Nature 592 (2021) 629–633, https://doi.org/10.1038/s41586-021-03430-5.
[215] R. Bruno, M. Marchand, K. Yoshida, P. Chan, H. Li, W. Zou, F. Mercier, P. Chanu, B. Wu, A. Lee, C. Li, J.Y. Jin, M.L. Maitland, M. Reck, M.A. Socinski, Tumor dynamic model-based decision support for phase Ib/II combination studies: A retrospective assessment based on resampling of the phase III study IMpower150, Clin. Cancer Res. 29 (2023) 1047–1055, https://doi.org/10.1158/1078-0432.CCR-22-2323.
[216] Y.R. Murciano-Goroff, S.P. Suehnholz, A. Drilon, D. Chakravarty, Precision Oncology: 2023 in Review, Cancer Discov. 13 (2023) 2525–2531. Doi: 10.1158/2159-8290.CD-23-1194.
[217] FDA, Use of Circulating Tumor Deoxyribonucleic Acid for Early-Stage Solid Tumor Drug Development. Draft Guidance for Industry, (2022). https://www.fda.gov/regulatory-information/search-fda-guidance-documents/use-circulating-tumor-deoxyribonucleic-acid-early-stage-solid-tumor-drug-development-draft-guidance (accessed 2024).
[218] A. Yin, G.D.M. Veerman, J.G.C. van Hasselt, C.M.J. Steendam, H.J. Dubbink, H.-J. Guchelaar, L.E. Friberg, A.-M.-C. Dingemans, R.H.J. Mathijssen, D.J.A.R. Moes, Quantitative modeling of tumor dynamics and development of drug resistance in non-small cell lung cancer patients treated with erlotinib, CPT Pharmacometrics Syst. Pharmacol. 13 (2024) 612–623, https://doi.org/10.1002/psp4.13105.
[219] D.M. Vega, K.K. Nishimura, N. Zariffa, J.C. Thompson, A. Hoering, V. Cilento, A. Rosenthal, V. Anagnostou, J. Baden, J.A. Beaver, A.A. Chaudhuri, D. Chudova, A.D. Fine, J. Fiore, R. Hodge, D. Hodgson, N. Hunkapiller, D.M. Klass, J. Kobie, C. Peña, G. Pennello, N. Peterman, R. Philip, K.J. Quinn, D. Raben, G.L. Rosner, M. Sausen, A. Tezcan, Q. Xia, J. Yi, A.G. Young, M.D. Stewart, E.L. Carpenter, C. Aggarwal, J. Allen, Changes in circulating tumor DNA reflect clinical benefit across multiple studies of patients with non-small-cell lung cancer treated with immune checkpoint inhibitors, JCO Precis. Oncol. 6 (2022) e2100372, https://doi.org/10.1200/PO.21.00372.
[220] I. Mellman, D.S. Chen, T. Powles, S.J. Turley, The cancer-immunity cycle: Indication, genotype, and immunotype, Immunity 56 (2023) 2188–2205, https://doi.org/10.1016/j.immuni.2023.09.011.
[221] G. Helmlinger, V. Sokolov, K. Peskov, K.M. Hallow, Y. Kosinsky, V. Voronova, L. Chu, T. Yakovleva, I. Azarov, D. Kaschek, A. Dolgun, H. Schmidt, D.W. Boulton, R.C. Penland, Quantitative systems pharmacology: An exemplar model-building workflow with applications in cardiovascular, metabolic, and oncology drug development, CPT Pharmacometrics Syst. Pharmacol. 8 (2019) 380–395, https://doi.org/10.1002/psp4.12426.
[222] Y. Sheng, S.-W. Teng, J. Wang, H. Wang, A.N. Tse, Tumor growth inhibition-overall survival modeling in non-small cell lung cancer: A case study from GEMSTONE-302, CPT Pharmacometrics Syst. Pharmacol. 13 (2024) 437–448, https://doi.org/10.1002/psp4.13094.
[223] U.S. Food and Drug Administration, E17 General Principles for Planning and Design of Multi-Regional Clinical Trials, (2018). https://www.fda.gov/regulatory-information/search-fda-guidance-documents/e17-general-principles-planning-and-design-multi-regional-clinical-trials (accessed August 19, 2024).
[224] K. Venkatakrishnan, N. Gupta, P.F. Smith, T. Lin, N. Lineberry, T. Ishida, L. Wang, M. Rogge, Asia-inclusive clinical research and development enabled by translational science and quantitative clinical pharmacology: Toward a culture that challenges the status quo, Clin. Pharmacol. Ther. 113 (2023) 298–309, https://doi.org/10.1002/cpt.2591.
[225] L. Hutchinson, B. Steiert, A. Soubret, J. Wagg, A. Phipps, R. Peck, J.-E. Charoin, B. Ribba, Models and machines: How deep learning will take clinical pharmacology to the next level, CPT Pharmacometrics Syst. Pharmacol. 8 (2019) 131–134, https://doi.org/10.1002/psp4.12377.
[226] L.B. Zwep, K.L.W. Duisters, M. Jansen, T. Guo, J.J. Meulman, P.J. Upadhyay, J.G. C. van Hasselt, Identification of high-dimensional omics-derived predictors for tumor growth dynamics using machine learning and pharmacometric modeling,

CPT Pharmacometrics Syst. Pharmacol. 10 (2021) 350–361, https://doi.org/10.1002/psp4.12603.
[227] N. Terranova, K. Venkatakrishnan, L.J. Benincosa, Application of machine learning in translational medicine: Current status and future opportunities, AAPS J. 23 (2021) 74, https://doi.org/10.1208/s12248-021-00593-x.
[228] N. Terranova, K. Venkatakrishnan, Machine learning in modeling disease trajectory and treatment outcomes: An emerging enabler for model-informed precision medicine, Clin. Pharmacol. Ther. (2023), https://doi.org/10.1002/cpt.3153.
[229] N. Terranova, J. French, H. Dai, M. Wiens, A. Khandelwal, A. Ruiz-Garcia, J. Manitz, A. von Heydebreck, M. Ruisi, K. Chin, P. Girard, K. Venkatakrishnan, Pharmacometric modeling and machine learning analyses of prognostic and predictive factors in the JAVELIN Gastric 100 phase III trial of avelumab, CPT Pharmacometrics Syst. Pharmacol. 11 (2022) 333–347, https://doi.org/10.1002/psp4.12754.
[230] P. Courlet, D. Abler, M. Guidi, P. Girard, F. Amato, N. Vietti Violi, M. Dietz, N. Guignard, A. Wicky, S. Latifyan, R. De Micheli, M. Jreige, C. Dromain, C. Csajka, J.O. Prior, K. Venkatakrishnan, O. Michielin, M.A. Cuendet, N. Terranova, Modeling tumor size dynamics based on real-world electronic health records and image data in advanced melanoma patients receiving immunotherapy, CPT Pharmacometrics Syst. Pharmacol. 12 (2023) 1170–1181, https://doi.org/10.1002/psp4.12983.
[231] A.-M. Milenković-Grišić, N. Terranova, D.R. Mould, Y. Vugmeyster, T. Mrowiec, A. Machl, P. Girard, K. Venkatakrishnan, A. Khandelwal, Tumor growth inhibition modeling in patients with second line biliary tract cancer and first line non-small cell lung cancer based on bintrafusp alfa trials, CPT Pharmacometrics Syst. Pharmacol. 13 (2024) 143–153, https://doi.org/10.1002/psp4.13068.
[232] X. Gong, M. Hu, L. Zhao, Big data toolsets to pharmacometrics: Application of machine learning for time-to-event analysis, Clin. Transl. Sci. 11 (2018) 305–311, https://doi.org/10.1111/cts.12541.
[233] J.G.C. van Hasselt, P.H. van der Graaf, Towards integrative systems pharmacology models in oncology drug development, Drug Discov. Today Technol. 15 (2015) 1–8, https://doi.org/10.1016/j.ddtec.2015.06.004.
[234] Z. Huang, P. Denti, H. Mistry, F. Kloprogge, Machine Learning and Artificial Intelligence in PK-PD Modeling: Fad, Friend, or Foe? Clin, Clin. Pharmacol. Ther 115 (2024) 652–654.
[235] X. Chen, R. Nordgren, S. Belin, et al., A fully automatic tool for development of population pharmacokinetic models, CPT Pharmacometrics Syst Pharmacol. 00 (2024) 1–14.